2009

Permeation of organic compounds through ductile iron pipe gaskets

Chu-lin Cheng
Iowa State University

Permeation of organic compounds through ductile iron pipe gaskets

by

Chu-Lin Cheng

A dissertation submitted to the graduate faculty

in partial fulfillment of the requirements for the degree of

DOCTOR OF PHILOSOPHY

Major: Environmental Science

Program of Study Committee:
Say Kee Ong, Major Professor
Roy Gu
Chris Rehmann
Lee Burras
Jiasong Fang

Iowa State University

Ames, Iowa

2009

TABLE OF CONTENTS

LIST OF TABLES

LIST OF FIGURES

CHAPTER 3

CHAPTER 4

CHAPTER 5

ACKNOWLEDGEMENTS

I would like to express my appreciation to a number of people who have assisted and supported me in the process of completing this dissertation. First and foremost, I am deeply indebted to my major advisor, Professor Say Kee Ong, for his guidance, support, constructive criticisms, and encouragement throughout the course of this research. Without his direction, this work would not be accomplished. I would also like to extend profound gratitude to Professor Chris Rehmann for his enthusiastic guidance with technical and mathematical challenges that I encountered during this study. I would also like to acknowledge Professor Roy Gu, Professor Lee Burras, and Professor Jiasong Fang for serving on my committee as well as providing invaluable discussions and insights.

Special thanks to Mr. James Gaunt's invaluable assistance and advice throughout the course of this research. I would like to thank Dr. Warren Straszheim's assistance in operating the instruments in Materials Analysis Research Laboratory and Mr. David Schoeller of Environmental Engineering Research Laboratory for his tremendous work in volatile organic compound sample analysis.

This research was financially supported by Awwa Research Foundation through the grant of # 2946. I would like to acknowledge the following organizations and individuals for their contributions of expertise and materials to this research: Endot Industries, Inc.; Cresline Plastic Pipe Co., Inc.; Chevron Phillips Chemical Company LP; Griffin Pipe; Hultec S&B Technical Products; Iplex Pipelines Australia Pty Ltd; Specified Fittings; and Uni-Bell PVC Pipe Association.

I am extremely thankful to Kathy Petersen and all staff at Civil, Construction, and Environmental Engineering Department for their administrative supports. I would also like to extend many thanks to my colleagues and friends at Iowa State, especially Dr. Feng Mao, Dr. Warisara Lertpaitoonpan, Dr. Tsung-Pin Yeh, and Dr. Wen-Hsing Chen who have helped me stay through these years. I am also grateful to Dr. Chien-Tsung Lu of Purdue University, Professor Shihwu Sung, and Dr. Bjorn Brooks for their continuous support and encouragement throughout these years. Their support and care helped me overcome setbacks and stay focused on my graduate study. I greatly value their friendship.

Last but most importantly, none of this would have been possible without the love and patience of my wife and kids. I would like to express my heart-felt gratitude to my parents for supporting me for these years. Without them, this dissertation would not be possible.

ABSTRACT

Ductile iron (DI) pipes have been used for the conveyance of drinking water in drinking water distribution systems over the past several decades. It has been estimated that almost half of all new water mains installed in North America are DI pipes. Although DI pipe itself is resistant to chemical permeation, the polymeric gaskets that join and seal the pipe segments are reported to be susceptible to permeation by organic contaminants. Pipe-drum, diffusion cell experiments, and numerical simulations were conducted in this research to obtain a faster mean to evaluate possible permeations through DI gaskets.

Of the five types of gasket materials tested using the gravimetric sorption test, ethylene-propylene-diene monomer (EPDM) had the highest sorption of gasoline, while fluoroelastomer rubber (FKM) exhibited very low sorption of gasoline. The sorption test results suggested that the least to most resistance to permeation of premium gasoline for the five gasket materials were EPDM, styrene-butadiene rubber (SBR), chloroprene rubber (CR; neoprene), acrylonitrile butadiene rubber (NBR), and FKM. A typical gasket was found to be made of two portions, the heel and the bulb, of the same polymer but different formulation. Gravimetric sorption tests suggested that the heel portion of all gaskets may be more resistant to permeation than the bulb making it the limiting step for permeation of organic compounds in gasoline.

Pipe-drum experiments showed that SBR gasket had the highest permeation rates of benzene, toluene, ethylbenzene, and xylenes (BTEX), followed by CR, EPDM, and NBR. With regards to threats to drinking water under water stagnation conditions in the pipe, the 5 μg/L maximum contaminant level (MCL) for benzene will likely be exceeded during an 8-

hour stagnation period for SBR gaskets in contact with free-product premium gasoline. NBR gaskets were found to be sufficiently resistant to permeation by benzene or other BTEX compounds in gasoline and the benzene concentration is unlikely to exceed EPA MCLs. Assessment based on data from the pipe-drum experiments suggested that when there is flow of water in the pipe, benzene and other BTEX compounds in gasoline will not exceed EPA MCLs.

A diffusion cell device was developed to obtain diffusion coefficients of BTEX compounds for various gasket materials under controlled conditions. Using curve fitting of the permeation data by numerical modeling, the diffusion coefficients of BTEX compounds through SBR and NBR gasket materials was found to range from 10^{-7} to 10^{-8} cm^2/s. The steady-state permeation rates were found to correlate in a linear relationship with thickness while the diffusion coefficients were found to be invariable to the thickness of the polymer tested (2 mm to 5 mm). The diffusion cell provided a rapid, inexpensive, and relatively well-controlled means to study permeation of polymeric gasket materials for DI pipes and the data obtained were used to model benzene permeation of the pipe-drum experiments.

The permeation of benzene through a 4-inch SBR gasket of a pipe joint was modeled using Multiphysics diffusion module. The simulations showed that the heel portions as well as part of the bulb portions of a gasket were likely to be in contact with the contaminants. Model simulation predicted that a 4-inch SBR gasket under hydrostatic pressure would permeate more organic chemicals than a pipe without hydrostatic pressure, posing greater risk to organic chemical permeations. Increase in the length/size of the bulb portion of a 4-inch

SBR gasket by compression or swelling from 10% to 30%, reduced the permeated mass of benzene by about 29% to 71% within 150 days of exposure to gasoline.

In summary, SBR and NBR gaskets are compatible with any level of gasoline contamination in groundwater. NBR gasket is the most effective choice when a gasket material resistant to gasoline is desired. Diffusion cell experiments in combination with numerical simulations can be used in evaluating possible BTEX permeations effectively. Gasket exposure area and its orientation in the socket after pipe joint assembly are likely to affect permeation path and permeated mass of contaminants. Results from this study can be used as a basis for crisis management for DI pipes exposed to gasoline and for development of a better gasket to improve the reliability of infrastructure of development of water distribution system.

CHAPTER 1. INTRODUCTION

1.1 General introduction

Over the past several decades, ductile iron (DI) pipes have been used for the conveyance of drinking water in drinking water distribution systems. Rajani and Kleiner (2003) estimated that almost half of all new water mains installed in North America are DI pipes. In comparison with other metal pipes such as cast iron, cement, and cement-lined pipes, DI iron pipes exhibit better resistance to corrosion and therefore have lower maintenance expenses. Plastic pipes have been marketed as an alternative to steel pipes, are lighter, more easily installed, and more durable than metal pipes in environment with acidic soils. However, plastic pipes are limited in their usages by the total loadings on the ground surface such as traffic and buildings. On the other hand, DI pipe has long been recognized as the superior pipe material due to its strength and durability (Bonds, 2000; DIPRA, 2003). Although DI pipe itself is resistant to chemical permeation, the polymeric materials that join and seal the pipe segments are reported to be susceptible to permeation by organic contaminants (Holsen et al., 1991; Park et al., 1991; Selleck and Marinas, 1991; Glaza and Park, 1992; DWI0772, 1997; DIPRA, 2003).

According to a recent survey, permeation incidents for DI pipes were reported due to gross soil contamination with highly volatile hydrocarbons and chlorinated organic solvents in the area surrounding the pipe (Ong et al., 2008). Permeation of organic contaminants through the polymer materials adversely affects the quality of drinking water in distribution system and poses a health risk to consumers. The chemical permeations for drinking water

pipe gaskets are sparse, qualitative and incomplete. There is a need to conduct laboratory experiments under controlled conditions to understand further the permeation of organic contaminants though gasket materials.

1.2 Motivation and Objectives

Previous studies have greatly improved the level of understanding of chemical permeation through polymers and their associated risks. However, there are some significant issues that remain unresolved especially for chemical permeation through an intact gasket within a DI pipe joint. There are very few studies conducting permeation of chemicals through an intact gasket and virtually no studies on the modeling of chemical permeation through an intact gasket. Pipe-drum experiment where a pipe joint is submerged in the target chemical in a drum is one of conventional techniques for studying permeation of chemicals. Pipe-drum experiments provide permeation rate data but require a long time before breakthrough is obtained. Because of the shape and the irregular geometries of the gaskets, permeation pathways of organic compounds may be complex. In addition, the influence of thickness on permeation properties of the polymer is unclear and debatable. Furthermore, it is unclear how a gasket would orientate within the bell and spigot of the pipe and which surfaces of the gasket would be exposed to external contaminants and internal drinking water, especially when the gasket is in service. Testing of the different sizes of gaskets for the different pipe sizes with pipe-drum experiments would be time consuming and costly.

The overall goal of this research was to examine the permeation of gasoline through a commonly used gasket for DI pipes. The research involves lab experiments and numerical simulations. The specific objectives of this study were to:

1) Study the permeation of gasoline through DI pipe joints with various gasket materials using pipe-drum experiments under simulated environmental conditions
2) Develop a low cost testing device to evaluate gasoline permeation through gasket materials for controlled boundary conditions and to investigate the thickness effect on diffusion coefficients
3) Obtain diffusion coefficients and possible contact/exposure areas (boundary conditions) of chemical permeations through different gaskets with numerical modeling.

1.3 Dissertation Organization

This dissertation is organized with Chapter 2 introducing the fundamentals of chemical permeability and diffusion through polymers and a comprehensive review of previous research on the permeation of organic contaminants through polymeric materials. In Chapter 3, permeation experiments using various gasket polymeric materials in pipe-drum apparatuses were conducted to assess the permeation of gasoline (in particular, benzene, toluene, ethylbenzene, and xylenes, or BTEX) through the gaskets of DI pipe joints. In Chapter 4, a low cost diffusion cell device is presented and used to examine the permeation of organic solvents through various gasket materials and thicknesses under controlled boundary conditions along with numerical modeling of the permeation results. In Chapter 5,

the results of the modeling efforts in Chapter 4 were incorporated in a model to simulate the permeation of BTEX for pipe-drum experiments of Chapter 3 and for various contamination scenarios. The general conclusions and future work for the dissertation are presented in Chapter 6.

1.4 References

Bonds, R.W. 2000. Ductile iron pipe versus HDPE pipe. Ductile Iron Pipe Research Association, Birmingham, AL.

Ductile Iron Pipe Research Association (DIPRA). 2003. Ductile iron pipe versus PVC. Ductile Iron Pipe Research Association, Birmingham, AL.

DWI0772. 1997. Permeation of benzene, trichloroethene and tetrachloroethene through plastic pipes. Drinking Water Inspectorate, London, UK.

Glaza E.C. and J.K. Park. 1992. Permeation of organic contaminants through gasketed pipe joints. *Journal AWWA*, 84(7): 92-100.

Holsen, T.M., J.K. Park, D. Jenkins, and R.E. Selleck. 1991. Contamination of potable water by permeation of plastic pipe. *Journal AWWA*, 83(8): 53-56.

Ong, S.K., J.A. Gaunt, F. Mao, C.L. Cheng, L. Esteve-Agelet, and C.R. Hurburgh. 2008. Impact of petroleum-based hydrocarbons on PE/PVC pipes and pipe gaskets. *Awwa Research Foundation Report No. 91204*. Awwa Research Foundation, Denver, CO.

Rajani, B and Y. Kleiner. 2003. Protection of ductile iron water mains against external corrosion: review of methods and case histories. *Journal AWWA*, 95(11): 110-125.

Selleck R.E. and B.J. Marinas. 1991. Analyzing the permeation of organic chemicals through plastic pipe. *Journal AWWA*, 83(7): 92-97.

Park, J.K., L. Bontoux, T.M. Holsen, D. Jenkins, and R.E. Selleck 1991. Permeation of polybutylene pipe and gasket material by organic chemicals. *Journal AWWA*, 83(10): 71-78.

CHAPTER 2. LITERATURE REVIEW

2.1 Background

Organic polymeric materials are extensively used in every day products, such as food packaging film, protective clothes, disposable gloves, geomembranes in landfills, and pipe gaskets. They are one of the most widely used materials due to their superior physical-chemical properties and low cost (Massey, 2003). These materials have water-proof capabilities and are used to contain various gaseous and organic liquids. However, polymeric materials are not completely resistant to permeation, and for critical application such as containing hazardous materials or wastes or use of protective clothing, it is important to understand the extent of chemical permeation. Over the past several decades, engineers and scientists have examined the permeation of hazardous compounds through polymeric materials used in every day products which may result in human health risk (Crank and Park, 1968; Crank, 1975; Comyn, 1985; Neogi, 1996).

Plastic pipes are increasingly being used for drinking water mains and service lines due to their ease of installation and light weight property. Polymeric gaskets are used in ductile iron pipes and plastic pipes of water mains to secure sections of pipes and to prevent leakage. Drinking water in both plastic pipes and ductile iron pipes are threatened by hazardous chemicals and petroleum products in contaminated soils due to gasoline spills or leakages from underground storage tanks (Park et al., 1991; Holsen et al., 1991a; Glaza and Park, 1992). Almost half of all new water mains installed in North America are ductile iron (Rajani and Kleiner, 2003). Although DI pipe itself is resistant to permeation, the gaskets

between pipe sections are susceptible to permeation by organic contaminants (Holsen et al., 1991a; Park et al., 1991; Selleck et al., 1991; Glaza and Park, 1992; DWI0772, 1997; Ong et al., 2008). In the case of a water main, the odor and smell of the chemical in drinking water may not be noticeable even though the maximum contaminant level (MCL) has been exceeded. Contamination of drinking water due to possible permeation of chemicals through plastic pipes has been investigated by several researchers (Holsen et al., 1991a, 1991b; Park et al., 1991; Selleck et al., 1991; Glaza and Park, 1992; Hopman et al., 1992; Ong, et al., 2008), but studies on the permeation of organic chemicals through polymeric gaskets of ductile iron pipes and plastic pipes are limited.

2.2 Permeation Definition and Mechanism

The permeability of penetrants through any polymeric material is dependent on two main factors: the solubility of a penetrant in the polymeric material and the rate of diffusion through the material. The solubility of a penetrant is dependent on the chemical interaction between the permeant molecule and the polymer; and the rate of diffusion is dependent on the size of the permeant molecule and the physical texture (amorphous or crystalline) of the polymer. The permeability coefficient measures the relative permeation behavior and is used to compare the permeability of the penetrants through different polymers. Penetrants in general could be liquid or gases. The most often studied gases and vapors are water vapor, oxygen, carbon dioxide, and nitrogen (Massey, 2003; Duncan et al., 2005).

Permeation is assumed to occur over a three-step physico-chemical process: (1) adsorption: penetrants partition from surrounding medium (soil or solution) to the surface of

the polymeric material, (2) diffusion: penetrants diffuse through the polymeric materials, and (3) desorption: penetrants partition from polymeric material into the receiving medium (Holsen et al., 1991a; Duncan et al., 2005; Rowe, 2005).

2.2.1 Sorption

Sorption is a generalized term used to describe the penetration and dispersal of penetrant molecules into a polymeric matrix. It may include absorption, adsorption, incorporation into micro-voids, cluster formation, and solvation-shell formation (Rogers, 1985). Due to the interaction of the penetrant with the polymer, the distribution of penetrant at the surface of the polymeric material may be different due to the penetrant concentration, and can be affected by temperature, and the swelling-induced structural states of the polymer. The activity of the penetrant within the polymer would be dependent on the mode of sorption in a polymer and the extent to which penetrant molecules are sorbed.

If there is no solvency of the polymer or swelling of the polymer, the partitioning of the penetrant into the polymeric materials may be described by Henry's Law.

$$C_{p1} = S_1 C_e \qquad [1]$$

where C_{p1} is the concentration of penetrant on the polymer surface in contact with the medium; C_e is the concentration of penetrant in the medium; and S_1 is the partitioning coefficient for a given penetrant-polymer pair at a given temperature.

2.2.2 Diffusion

Once the penetrant has partitioned into the material, the penetrant diffuses and moves within the polymeric matrix by Brownian molecular motion and by the difference in concentration gradient.

Fickian Law of Diffusion

Diffusion of the penentrant can be described using Fick's First Law. The law states that the rate of transfer of the diffusing penetrants through unit area of a section in the x-direction is assumed to be proportional to the concentration gradient measured normal to the section $(\frac{\partial C}{\partial x})$.

$$F = -D\frac{\partial C}{\partial x} \qquad [2]$$

where F is the rate of transfer of penetrants per unit area of the section (μg/cm^2/s), C is the concentration of penetrants (μg/cm^3), x is the space coordinate measured normal to the section (cm), and D is the diffusion coefficient (cm^2/s). The first law is for diffusion under steady state condition where the concentration throughout the section is not varying with time.

By considering the mass balance of penetrants diffusing through a representative element volume in Cartesian coordinates, the governing equation describing non-steady state diffusion is as follows:

$$\frac{\partial C}{\partial t} = \frac{\partial}{\partial x}(D_x \frac{\partial C}{\partial x}) + \frac{\partial}{\partial y}(D_y \frac{\partial C}{\partial y}) + \frac{\partial}{\partial z}(D_z \frac{\partial C}{\partial z}) \qquad [3]$$

where D_x, D_y, and D_z are the diffusion coefficients in the x, y, and z directions. It can be simplified to one-dimensional diffusion as shown below, which is known as Fick's Second Law (assuming $D = D_x = D_y = D_z$).

$$\frac{\partial C}{\partial t} = \frac{\partial}{\partial x}(D\frac{\partial C}{\partial x}) \quad [4]$$

If the diffusion coefficient is a constant, then the equation becomes

$$\frac{\partial C}{\partial t} = D\frac{\partial^2 C}{\partial x^2} \quad [5]$$

Note that the above equation assumes that the polymeric material remain intact and does not change in size due to swelling.

Classification of Diffusion

Alfrey et al. (1966) proposed a useful classification for diffusion behavior based on the relative rates of diffusion and polymer relaxation. The authors proposed:

- Case I or Fickian diffusion, in which diffusion is much less than that of polymer relaxation rate;
- Case II diffusion, the other extreme in which diffusion is very rapid compared with polymer relaxation rate; and
- Non-Fickian, or anomalous diffusion, which occurs when diffusion and polymer relaxation rates are comparable.

Polymer relaxation is the phenomenon of stretching or reorientation of polymer structure which provides free volume for absorption and diffusion (Crank, 1975; Duncan et al., 2005; Rowe, 2005). Different polymers have different polymer relaxation rates. Free

volume itself is an intrinsic property of the polymer matrix and can be thought of as extremely small-scale porosity (molecular scale) arising from the gaps left between entangled polymer chains and is dependant on the vibrations and translations of the surrounding polymer chains. Free volume pores are dynamic and transient in nature. Absorption and diffusion of molecules in plastics will depend to a considerable extent on the available free volume within the polymer (Duncan et al., 2005).

Diffusion Coefficients

For many penetrant-polymer systems, D is a function of the sorbed penetrant concentration (Crank, 1975; Comyn, 1985; Rogers, 1985; Park and Nibras, 1993; Park et al., 1996a, 1996b; Sangam and Rowe, 2001; Vahdat and Sullivan, 2001; Vesely, 1991; Neogi, 1996; Duncan et al., 2005). The concentration dependence of the diffusion coefficient is a reflection of the plasticizing action of sorbed penetrant (Rogers, 1985). In this case, the governing equation of Fick's becomes

$$\frac{\partial C}{\partial t} = \frac{\partial}{\partial x}(D(C)\frac{\partial C}{\partial x}) \qquad [6]$$

There are relatively few rigorous solutions for the diffusion equation for a concentration-dependent D. One procedure to estimate $D(C)$ is to utilize a solution for a constant D for a given concentration and then extracting a value of $D(C)$ from those data for various concentrations. In this procedure, Equation [6] is transformed into:

$$\frac{\partial C}{\partial t} = D(C)\frac{\partial^2 C}{\partial x^2} + \frac{\partial D(C)}{\partial C}(\frac{\partial C}{\partial x})^2 \qquad [7]$$

Experiments are then performed over sufficiently small intervals of C such that $\frac{\partial D(C)}{\partial C}$ is small compared with $D(C)$ so that the second term may be neglected. This gives a mean or integral value of the diffusion coefficient $\overline{D}$, over the concentration range, C_1 to C_2, defined as

$$\overline{D} = \frac{1}{C_2 - C_1} \int_{C_1}^{C_2} D(C) dC \qquad [8]$$

$\overline{D}$ may be determined over several ranges of concentration to obtain an estimate of $D(C)$.

2.2.3 Desorption

Desorption is the opposite process of sorption. Net desorption occurs if the concentration of the penetrant in the receiving medium is lower than the concentration required for maintaining the partition equilibrium with the polymer. As in sorption process, Henry's Law can be used to express the relationship between the concentrations in the two phases

$$C_{p2} = S_2 C_r \qquad [9]$$

where C_{p2} is the concentration of penetrant on polymer surface in contact with the receiving medium; C_r is the concentration of penetrant in the receiving medium; and S_2 is the partitioning coefficient between a given penetrant, receiving medium, and polymer at temperature of interest. When the receiving medium is identical to the exposed medium and there is no hysteresis in the sorption/desorption isotherm, S_2 may be assumed to be equal to S_1 in Equation [1] (Rowe, 2005; Mao, 2008). Note that if penentrant molecules are strongly

bound in the polymer, the desorption of the penetrant may exhibit significant hysteresis. Then desorption is not simply the inverse process of sorption.

2.2.4 Permeability

The permeation of small molecules through polymer material involves sorption, diffusion and desorption processes. For a polymer with a fixed thickness, l, with concentrations at the two surfaces equal to C_{p1} and C_{p2}. The flux through the polymer is given by

$$F = D\frac{C_{p1} - C_{p2}}{l} \qquad [10]$$

Substituting Equation [1] and Equation [9] into Equation [10], and assuming the exposed medium and the receiving medium share the same solubility parameter S for the penetrant, Equation [10] becomes

$$F = D\frac{S_1 C_e - S_2 C_r}{l} = DS\frac{C_e - C_r}{l} = P\frac{C_e - C_r}{l} \qquad [11]$$

where P is defined as the permeability or permeation coefficient (cm^2/s). Essentially, P is a mass transfer coefficient that takes account of the sorption, diffusion and desorption processes (Rowe, 2005).

2.2.5 Factors affecting penetrant permeation through polymer

The rate at which an organic chemical penetrates the polymer is dependent on many factors, which can be generalized as physical, chemical and environmental factors. For example, these factors include polymer material type and thickness, the type of penetrating

contaminant, the concentration of the contaminant in the pores of the soil surrounding the materials, the presence of other contaminants, the extent of soil contamination, and the temperature or pressure in the environment (Silkowski et al., 1984; Vahdat, 1987; Selleck et al., 1991; Perkins and You, 1992; Joo et al., 2004, 2005; Park et al., 1996a; 1996b; Anna et al., 1998; Duncan et al., 2005; Chao et al., 2006a, 2006b, 2007).

Polymer Type and Properties

Polymeric materials used for environmental and public health purposes include polyvinyl chloride (PVC), high-density polyethylene (HDPE), nitrile rubber and neoprene (CR) (Jencen and Hardy, 1988, 1989; Park et al., 1996a, 1996b; Papiernik et al., 2001). Polymers can be classified into three groups based on their physical response to heat: thermoplastics, thermosets, and thermoplastic elastomers. Thermoplastics can be formed and reformed to different shapes, while thermosets do not become moldable when heated. Thermoplastic elastomers show both properties of thermoplastics and thermosets. The main difference between thermoset elastomers and thermoplastic elastomers is the type of crosslinking bond in their structures. Crosslinking is a critical structural factor which imparts high elastic properties.

Polymeric materials can be crystalline, amorphous, or semi-crystalline (having both crystalline and amorphous polymers) in structures. Higher crystallinity in general leads to better barrier properties (Massey, 2003). Amorphous, or so-called glassy polymers, exhibit anomalous or non-Fickian behavior (Crank, 1975). PVC is an amorphous glassy polymer with very limited flexibility of the polymer chains while PE is a partially crystalline rubber-

polymer having amorphous areas with high chain mobility. Low molecular weight organic molecules permeate PVC material through the free volumes of the relatively immobile polymer chains, whereas permeation of PE occurs through the amorphous areas of relatively mobile polymer chains. This polymer structural difference accounts for the different performance between PE and PVC to resist the permeation of organic chemicals. The permeation of organic chemicals through glassy PVC pipe is typically classified as a Case II diffusion (Vonk, 1985; Berens, 1985). As such, PVC is regarded as virtually impermeable to certain organic compounds at a low solute activity while permeation does occur in PE at these low solution activities (Vonk, 1985, 1986; Mao, 2008)

For HDPE geomembranes (semi-crystalline polymers), the crystalline zones act as impermeable barriers to permeating molecules in two ways (Naylor, 1989). First, crystalline regions act as excluded volumes for the sorption process and as impermeable barriers for diffusion. Secondly, they act as giant cross-linking regions with respect to those chains where penetrants enter and leave those regions from the surrounding non-crystalline matrix during sorption and diffusion process. The cross-linking strains the mobility of the polymer segments and makes the diffusion process more dependent on the size and shape of the penetrant molecule (Naylor, 1989; Rogers, 1985).

Diffusion is favorable (shown by an increase in value of the permeation coefficient) when the polymer and penetrants are similar in structure. For instance, strong polar molecules have very low transport rates through polyethylene (PE), which is non-polar. Rowe et al. (1996) found that the permeation affinity for PE has the following order: alcohols<acids<ketones<esters<aromatic hydrocarbons<halogenated hydrocarbons which

was also shown by the work done by other researchers (August and Taztky, 1984). Rowe et al. (1996) studied the diffusion of organic pollutants through HDPE geomembranes and observed that some organic compounds (methyl ethyl ketones, acetic acid) migrated at much slower rates than chlorinated solvents (dichloromethanes, 1,1-dichloroethane, and 1,2-dichloroethanes). Work done by Park and Bontoux (1992) showed that a polar compound (methanol) was found to be absorbed less than nonpolar compounds (toluene, 1,2-dichlorobenzene, and 1,1,1-trichloroethane) in nonpolar thermoplastics such as polybutylene (PB) and PE.

Penetrant

Permeation rates are impacted by the type of penetrant, its concentration, and the size and shape of the penetrant molecule (Silkowski et al., 1984; Vahdat, 1987; Park et al., 1991; Selleck et al., 1991; Perkins and You, 1992; Joo et al., 2004, 2005; Park et al., 1996a; 1996b; Anna et al., 1998; Duncan et al., 2005). Contaminations in the field are generally characterized by complex mixtures of organic chemicals. Petroleum products are the most common contaminants, encountered in the field due to the spill or leakage from underground storage tanks. Gasket materials can be in contact with either free product gasoline (non-aqueous phase) or different concentrations of gasoline aqueous solutions (aqueous phase), or even with organic vapor if the pipe is in the unsaturated zone of the contaminated aquifer in field.

Saleem et al. (1989) reported smaller diffusion coefficients through low-density polyethylene (LDPE) for compounds with higher molar volume such as aliphatic aromatic

and chlorinated penetrants than compounds with lower molar volume. In another example, the magnitude of the diffusion coefficients for chlorinated benzene compounds were smaller than methyl substituted benzenes due to the bulky chlorine atoms, which markedly reduce their mobility. The shape of penetrants has been reported to have a profound effect on the diffusion process (Berens and Hopfenberg, 1982; Saleem et al., 1989). Penetrants with linear, flexible and symmetrical molecules have higher mobility than rigid molecules. For instance, Saleem et al. (1989) showed that the diffusion coefficient for o-xylene was lower than for p-xylene. This is attributed to the symmetrical structure of p-xylene compared to the distorted shape of o-xylene with its two adjacent methyl groups. Berens and Hopfenberg (1982) have shown that the diffusion of n-alkane and other elongated or flattened molecules are higher, by a factor of 1000, than the diffusion of spherical molecules with similar molecular weight.

Based on pure-Fickian diffusion within a polymer, the penetrant-polymer partition and diffusion coefficients are usually assumed to be constant and are independent of the bulk concentration of penetrant. However, this assumption is only valid when the bulk concentration is low. In most cases, the diffusion coefficient is a function of the bulk concentration of the penetrant because, in the presence of the penetrant molecules, the polymer will weaken due to the interactions between adjacent polymer chains and the penetrants, which in turn leads to plastization of the polymer. Vonk (1985) reported that the diffusion coefficient of toluene in the softened PVC increased by several orders of magnitude in comparison with that in the original PVC. Muler et al. (1998) also found that the diffusion coefficients in PE geomembranes were approximately one order of magnitude lower for an

aqueous solution than for a pure solvent. In a sorption study of organic chemicals in thermoplastics and elastomers, Park and Bontoux (1992) showed that the partition coefficient increased logarithmically with increasing solvent activity for nonpolar compounds.

Environmental factors

The surrounding environment factors, such as temperature, hydrostatic pressure, and soil characteristics, also play a part in influencing the permeation of organic pollutants. The permeation process is temperature dependent since energy is required for the permeation process. It is expected that for many polymer-penetrant systems, plots of Log D vs. the reciprocal of the absolute temperature are linear over a limited temperature range (Saleem et al., 1989; Aminabhavi and Naik, 1998). It has been established (Naylor, 1989; Chainey, 1990) that over small temperature ranges, temperature dependence of the diffusion, solubility and permeability coefficients can be described by the Arrhenius relationship:

$$D = D_0 e^{(-\frac{E_d}{RT})} \qquad [12]$$

$$P = P_0 e^{(-\frac{Ep}{RT})} \qquad [13]$$

where E_d and E_p are the activation energies of diffusion and permeation, respectively, and D_0 and P_0 are the diffusion coefficients and permeation coefficients at absolute temperature T.

Impact of hydrostatic pressures on organic compound permeation is uncertain. Selleck and Marinas (1991) indicated that hydrostatic pressure within the pipeline may provide resistance to permeation, although this assumption was not based on any clear

thermodynamic theory. An article in Opflow (2006) indicated that contaminants may be drawn into the pipe at each gasket connection due to the hydrostatic pressure differences. This statement was challenged through a communication note by an AWWA committee (Larson, 2006) where the committee claimed that gaskets were designed to withstand both internal and external pressures while providing a seal under pressure. The committee further indicated that there would be widespread evidence of leakage due to the external hydrostatic pressure if the article in Opflow was the case. It is generally believed that an increase in the contaminant pressure may result in two opposing effects: (a) increase the concentration of the contaminant dissolved in the polymer material, and (b) decrease the "free volume" due to an increase in pressure on the polymeric material (Stern, 1972).

The permeation rates are affected by the organic content of the adjacent soils of the pipe (Holsen et al., 1991b). In high humidity or water-saturated conditions, partitioning into the soil organic matter is the dominant mechanism for soil uptake of organic chemcials, which lowers the organic concentration and therefore affects the concentration gradient (Chiou and Shoup, 1985). Mao (2008) showed that the higher organic matter in the organic topsoil had greater soil uptake of BTEX than low organic carbon sand resulting in a significant decrease of BTEX concentrations in the soil pore water which in turn resulted in a lower permeation rate of BTEX through PE pipes than for similar experiments with low organic carbon sand.

2.2.6 Estimation of permeation properties

Gravimetric sorption method

The equilibrium sorption of a contaminant by a polymeric material in the gravimetric sorption test has been used to correlate the permeation properties of polymeric materials (Berens, 1985; Park and Bontoux, 1993). In the gravimetric sorption test, the percent weight gains are typically plotted against the time of the experiment and the diffusion coefficient estimated using the "half-time method" (Crank, 1975; Neogi, 1996). Assuming constant diffusion coefficient and no swelling of the polymer, the mass sorbed for a polymer sheet is given by:

$$\frac{M_t}{M_\infty} = 1 - \frac{8}{\pi^2}\sum_{m=0}^{\infty}\frac{1}{(2m+1)}\exp\left\{\frac{-D(2m+1)^2\pi^2 t}{\ell^2}\right\} \qquad [14]$$

where M_t is the total mass of contaminant absorbed by the sheet at time t, and M_∞ is the equilibrium mass attained theoretically after infinite time. The equation assumes that the concentration on each surface of the sheet immediately attains a value corresponding to the equilibrium uptake when placed in the contaminants, and remains constant afterwards. Using the half-time method, the value of $\frac{t}{\ell^2}$ for which $\frac{M_t}{M_\infty}$ =1/2 is given by:

$$\left(\frac{T_{1/2}}{\ell^2}\right) = -\frac{1}{\pi^2 D}\ln\left\{\frac{\pi^2}{16} - \frac{1}{9}\left(\frac{\pi^2}{16}\right)^9\right\} \qquad [15]$$

Equation can be further simplified with the error of about 0.001% as

$$D_{T_{1/2}} = 0.049\frac{\ell^2}{T_{1/2}} \qquad [16]$$

where $D_{T_{1/2}}$ is the diffusion coefficient (cm^2/s) obtained from half-time method; ℓ is thickness of material (cm); $T_{1/2}$ is the time where the mass sorbed equals to half of the equilibrium mass sorbed (s).

The measurement of mass uptake by the polymer is comparatively simple, but it does not yield information on the time needed for the contaminant to break through a given thickness of polymer. In addition, the sorption behavior is dependent on the geometry of polymer materials and appropriate equations considering the geometry of the test specimen must be used to process the sorption data. Because of the irregular geometry of a pipe gasket, the gasket must be trimmed to regular shapes which in turn raised the question of how the sorption results of the regular shaped specimens can fully represent or be used for evaluating the permeation of an intact gasket.

Time lag method

The plot of cumulative mass permeated with time can be used to estimate the diffusion coefficient by using "the time-lag method" (Crank, 1975). Using Fick's diffusion equation, the total mass of chemical diffusing through a plane sheet Q_t as a function of time t, is given by the following equation based on the simplifying assumptions: (i) the outer concentration of contaminant remains constant (C); and (ii) the initial concentration of the contaminant in the polymer is zero; and (iii) the inner concentration of the contaminant is kept at zero.

$$\frac{Q_t}{\ell C} = \frac{Dt}{\ell^2} - \frac{1}{6} - \frac{2}{\pi^2}\sum_{1}^{\infty}\frac{(-1)^n}{n^2}\exp\left(\frac{-Dn^2\pi^2 t}{\ell^2}\right) \qquad [17]$$

As t approaches infinity, then

$$Q_t = \frac{DC}{\ell}(t - \frac{\ell^2}{6D}) \quad [18]$$

The equation has an intercept on the t axis given by

$$T_L = \frac{\ell^2}{6D} \text{ or } D_{T_L} = \frac{\ell^2}{6T_L} \quad [19]$$

where D_{T_L} is the diffusion coefficient (cm2/s) calculated by time-lag method; ℓ is the thickness of material (cm); and T_L is the lag time (s) at steady-state permeation.

2.3 Permeation of Organic Contaminants through Ductile Iron Gaskets

Permeation of plastic pipes by organic chemicals may result in the degradation of drinking water quality. Since permeation can occur either from the vapor or aqueous phase, both water mains and fittings installed in the vadose zone and saturated zones are susceptible to contamination by permeation (DWI0441, 1992)

2.3.1 Previous studies

In the 1980's, two surveys on the effects of organic chemicals on drinking water pipes were completed in Netherlands (Vonk, 1985) and in the United States (Thompson and Jenkins, 1987). Most pipe permeation incidents were related to petroleum products (98 percent of all incidents), mainly gasoline spills or leaks (Thompson, 1987; Holsen et al., 1991a). The aromatic compounds in gasoline, benzene, toluene, ethyl benzene and o-, m-, p-xylene (BTEX), permeated PB and PE pipes readily and were the compounds of concern in permeation incidents. A small number of incidents (5 percent) involved chlorinated solvents such as trichloroethylene (TCE). Other contaminants that exhibit high rates of permeation

included simple chlorinated aromatics, chlorinated and unchlorinated straight-chain aliphatic hydrocarbons, and phenolic compounds (Holsen et al., 1991a, 1991b). Plastic pipes showed excellent resistance to the permeation by strongly polar pesticides (e.g., paraquat, malathion, and atrazine) and long-chained high molecular weight hydrocarbons (DWI0032, 1990; Vonk, 1985). Park and his colleagues (Park et al., 1991; Glaza and Park, 1992) showed that organic contaminants might be permeating through the gaskets of pipe joints in the water distribution system. Recently, a national survey in the U.S. conducted by Iowa State University showed that the majority of the reported incidents were associated with gross soil contamination in the area surrounding the drinking water pipes. The high risk areas for occurrences of permeation incidents included industrial areas, former sites of fuel stations, and near underground storage tanks, but permeation incidents can also occur in low risk areas such residential areas, mainly due to the disposal and accidental leaking of gasoline, oil, and paint thinner products (Holen et al., 1991a).

The occurrence of contamination was generally identified by the customer as indicated by an unusual taste and odor in the tap water. For many highly toxic substances, including benzene, vinyl chloride, and dichloromethane, the taste and odor thresholds are well above the drinking water maximum contaminant levels (MCLs) (DWI0441, 1992).

2.3.2 Ductile iron (DI) pipe joints and gaskets

In the early 1970s, ductile iron (DI) replaced gray cast iron as the pipe material for most of drinking water pipes. In recent years, almost half of all new water mains installed in North America were estimated to be ductile iron (Ragani and Kleiner, 2003). The most popular and

easiest-to-assemble joint and fitting for DI pipe is the push-on joint (Bonds, 2003). The joint consists of a single rubber gasket placed in a groove inside the socket of the bell end of the pipe. The beveled end of the pipe (or spigot) is pushed past the gasket, compressing the gasket, and forming a pressure-tight and dependable seal.

For DI pipes, permeation through gaskets is the most likely pathway, other than leakage through cracks or holes due to corrosion or physical failure of parts of the iron pipe itself (DIPRA, 2003; Rajani and Kleiner, 2003; Bonds et al., 2005; Rajani, 2008; Rehan, 2008). The most common DI pipe gaskets used are the Tyton® gaskets for diameter ranging from 3 to 24 inches (Bonds, 2003; Griffin, 2006). Gasket materials used in push-on joints are made of ethylene-propylene-diene monomer (EPDM), chloroprene rubber (CR; neoprene), styrene-butadiene rubber (SBR), acrylonitrile butadiene rubber (NBR), or fluoroelastomer rubber (FKM). Different types of gasket are recommended for use under specific circumstances. For instance, SBR and CR are used for water distribution, while NBR and FKM gaskets are used for pipes conveying hydrocarbons and petroleum products. Among these gaskets, SBR is the most commonly used pipe gasket in the drinking water field (more than 90%) due to its low cost (Park et al., 1991; Ong et al., 2008). Previous research has reported that SBR is less resistant to gasoline than NBR (Glaza and Park, 1991), but there are no studies on the susceptibility of contaminant permeation through the other gaskets (Park et al., 1991; Glaza and Park, 1992).

Effect of different portions of a gasket

Close examination of Tyton® gaskets indicates that a typical gasket consists of a hard "heel" and a soft "bulb" portion. The heel portion anchors the gasket in place during the assembly of the joint and the bulb forms the hydrostatic seal. The heel and bulb may have different resilience characteristics and different polymer formulations and possibly different permeation characteristics. No research has investigated the permeation differences of the bulb or heel portion of a gasket. Either portion may be the rate limiting step for the permeation of organic chemicals through the gasket and into the drinking water.

Influence of material thickness

Because of the various sizes and geometries of gaskets and polymeric products available in the market, the permeation pattern of BTEX compounds may be different for different thicknesses and different gasket products. Nelson et al. (1981) examined Neoprene, Latex, PVC and Buna-N gloves against chloroform, pentane, toluene, and trichloroethylene and found that the permeation rate for each material type was inversely proportional to glove thickness. Berardinelli and Hall (1985) studied the permeation of latex neoprene gloves by acetone and reported that the breakthrough time was directly proportional to the square of the material thickness, and that the steady-state permeation rate, or steady-state concentration of penetrant was inversely proportional to thickness. Jencen and Hardy (1988) examined permeation of toluene and 1,1,1-trichloroethane through different thickness of neoprene gloves and acetone through natural rubber gloves, and found that the square root of the breakthrough times were linearly related to the thicknesses of the gloves while the steady-

state permeation rates were inversely proportional to material thicknesses. Schwope et al. (1988) used open-loop and closed-loop mode based on American Society for Testing and Materials (ASTM) Method F739 to test permeation of protective cloth and found that the breakthrough times were not proportional to the square of the material thicknesses. Work done by Vahdat (1987) on the permeation of toluene through butyl nomex, neoprene, polyvinyl alcohol (PVA) and butyl gloves showed that the permeation rates were dependent on the challenge concentration, thickness of material and the area exposed, but the estimated diffusion coefficients were independent of these factors. A study by Park et al. (1991) on the permeation of mixtures of organic chemicals through polybutylene, low-density polyethylene (LDPE) pipes and SBR gaskets showed that the estimated diffusion coefficients for the polymeric materials decreased exponentially as the thickness of the polymer material increased. In other studies, Park et al. (1996a; 1996b) reported that the diffusion coefficients of methylene chloride, toluene, trichloroethylene (TCE), and m-xylene decreased exponentially with material thicknesses for the permeation of mixtures of these chemicals at concentration of 10-100 mg/L through high-density polyethylene (HDPE), very low-density polyethylene (VLDPE), and polyvinyl chloride (PVC) geomembranes. Norenberg et al. (1999a, 1999b) indicated that permeation coefficient decreased with increasing membrane thickness for permeations of nitrogen, oxygen, and argon through polypropylene and polyethylene membranes in gas cell experiments. A study by Tseng et al. (2000), using positron annihilation lifetime spectroscopy (PALS) to measure dye-probe diffusion coefficients in thin films of monodisperse polystyrene, found that the diffusion coefficients decreased exponentially with increase of film thicknesses at temperature below 150 $^{\circ}$C and

diffusion coefficients increased when the film thickness was at about 350 nm. Soles et al. (2003) examined water vapor through poly(tert-butoxycarboxystyrene, PBOCSt) using incoherent neutron scattering measurements and indicated that the diffusion coefficients increase exponentially as film thicknesses increase. Vogt et al. (2004) investigated moisture diffusion through poly(4-ammonium styrenesulfonic acid) films using Fickian and two-stage absorption models and found that water diffusion coefficients into the films increased exponentially as a function of initial film thickness. Studies on the influences of thickness on the diffusion coefficients of a polymeric material exposed to organic chemicals are limited with data showing both linear and exponential correlations, while a study showed no correlations.

Experimental devices for polymeric materials

Testing apparatuses based on ASTM F739 are commonly used for thin materials with thicknesses of less than 1 mm (Berens, 1985; Anna et al., 1998; Phalen and Que Hee, 2003; Xu and Que Hee, 2006; Chao et al., 2006a; 2007) which are suitable for materials used in membranes and gloves. There is no commercial diffusion cell device with capability of testing irregular and thick polymeric samples in the market. In a recent report, a research team from University of South Florida reported the need for the development of a new diffusion cell to evaluate oxygen diffusion through concrete composite systems with the fiber reinforced polymer films of thickness ranging from 0.75 mm to 7.2 mm (Khoe et al., 2009). The pipe-drum or pipe-bottle apparatus where a pipe or a pipe joint is placed in a drum or bottle containing the penetrant is commonly used to study permeation of chemicals (Vonk,

1985; Park et al., 1991; Ong et al., 2008; Mao, 2008). Permeation rates are estimated by measuring the concentrations of the penetrants in the water inside the pipe. The pipe-drum experiment is a time-consuming experiment and for thick polymers or large diameter gaskets, a long time is needed before break through occurs. Efforts are needed to develop various experimental setups which can improve and speed up testing of thick polymeric materials.

Numerical simulation

To author's knowledge, no studies have investigated the permeation of organic contaminants through DI pipe gaskets using numerical models. There were a few studies simulating permeation of organic compounds through plastic pipe materials and geomembranes. Selleck and Marinas (1991) developed analytical solutions for pure-Fickian diffusion of hydrophobic contaminants through plastic pipes. In their modeling work, the driving force for the diffusion process was the difference between the internal activity (in the drinking water) and external activity (in the soil) of organic compounds, with the assumption of equilibrium partitioning of organic compounds between the pipe wall and the pipe water. The analytical solutions were used to calculate the breakthrough times for 3/4-inch polybutylene pipes exposed to a variety of organic contaminants. Chao et al. (2006a; 2007) employed one-dimensional analytical model to evaluate permeation parameters of organic compounds through nitrile and neoprene gloves, and high density polyethylene (HDPE) geomembranes. Predictions of the one-dimensional model fitted well with the experimental results of the ASTM F739 diffusion cell. They found that the diffusion coefficients estimated from the sorption tests and diffusion cell were inappropriate in modeling. Duncan et al.

(2005) indicated that ABAQUS, a modeling package based on the finite element method, was used in simulating the permeations of water moistures in several studies (Hambly et al., 1996; Loh et al., 2005). Numerical models are used to supplement experimental measurements, improving understanding and enabling extrapolation of behaviors over timescales and in large components that are not experimentally convenient. Modeling thus can be undertaken to help analyze experimental data diffusion cells and predict possible performance of a particular polymer material exposed to organic solvent.

While numerous studies have focused on the permeation of contaminants through plastic pipes in the water industry, little is known about the performance of commonly used elastomeric gaskets in DI and PVC pipes in contact with organic contaminants and the chemical permeation of gaskets under contamination conditions commonly encountered in the field.

2.4 Summary

Protection of drinking water supplies and distribution systems from contamination is important to minimize health risks. An understanding of the permeation of contaminants such as gasoline products especially BTEX through polymeric gaskets and pipes will further improve efforts in engineering sustainable and protective water distribution systems. While many studies have focused on the permeation of contaminants through plastic pipes in the water industry, not much is known about the performance of commonly used polymeric gaskets in contact with organic contaminants.

The pertaining issues to chemical permeation of gaskets include the performance of different gasket materials in the field, the impacts of material thickness and different portions of a polymeric gasket on BTEX permeation, the permeation pathways of pentrants within a gasket, and possible exposure surface area of a gasket in the DI pipe joint. Although there is a need to understand the risk of chemical permeations through gaskets, there are sparse studies available to assess the risks. In addition, the techniques to study the chemical permeations through gaskets are limited.

2.5 Reference

Alfrey, T.J., E.F. Gurnee, and W.G. Lloyd. 1966. Diffusion in glassy polymers. *Journal Polymer Science*. Part C, 12(1): 249-261.

Aminabhavi, T.M. and H.G. Naik. 1998. Chemical compatibility testing of geomembranes-Sorption/desorption, diffusion and swelling phenomena: Effect of size and shape of the penetrant molecules. *Geomembranes and Geotextiles*, 16(6): 333-354.

Aminabhavi, T.M. and H.G. Naik. 1999. Molecular migration of low sorbing organic liquids into polymeric geomembranes. *Polymer International*, 48(5): 373-381.

Anna, D.H., E.T. Zellers, and R. Sulewski. 1998. ASTM F739 method for testing the permeation resistance of protective clothing materials: Critical analysis with proposed changes in procedure and test-cell design. *Journal American Industrial Hygiene Association*, 59(8): 547-556.

American Society for Testing and Materials (ASTM). 1999. Resistance of protective clothing materials to permeation by liquids or gases under conditions of continuous contact (F739-99a). *ASTM*, Philadelphia, PA.

August, H. and R. Taztky. 1984. Permeability of commercial available polymeric liners for hazardous landfill leachate organic constituents, *International Conference on Geomembrane*, Denver, USA, pp: 151-156.

Berardinelli, S.P., R.L. Mickelsen, and M.M. Roder. 1983. Chemical protective clothing: A comparison of chemical permeation test cells and direct-reading instruments. *Journal American Industrial Hygiene Association*, 44(12): 886-889.

Berardinelli, S.P. and R. Hall. 1985. Site-specific whole glove chemical permeation. *Journal American Industrial Hygiene Association*, 46(2): 60-64.

Berens, A.R. and H.B. Hopfenberg. 1982. Diffusion of organic vapors at low concentrations in glassy PVC, polystyrene, and PMMA. *Journal Membrane Science*, 10(2-3): 283-303.

Berens, A.R. 1985. Prediction of organic chemical permeation through PVC pipe, *Journal AWWA*, 77(11): 57-64.

Bhanushali, D., S. Kloos, C. Kurth and D. Bhattacharyya. 2001. Performance of solvent-resistant membranes for non-aqueous systems: solvent permeation results and modeling. *Journal Membrane Science*, 189(1): 1-21.

Bonds, R.W. 2003. Ductile iron pipe joints and their uses. DIPRA. Birmingham, AL.

Bonds, R.W., L.M. Barnard, A.M. Horton, and G.L. Oliver. 2005. Corrosion and corrosion control of iron pipe: 75 years of research. *Journal AWWA*, 97(6): 88-98.

Chao, K.P., J.S. Lai, H.C. Lin, and Y.P. Hsu. 2006a. Comparison of permeability determined by permeation cell and immersion methods for organic solvents through protective gloves. *Polymer Testing*, 25(7): 975-984.

Chao, K.P., P. Wang, and C.H. Lin. 2006b. Estimation of diffusion coefficients and solubilities for organic solvents permeation through high-density polyethylene geomembrane. *Journal Environmental Engineering*, 132(5): 519-526.

Chao, K.P., P. Wang, and Y.T. Wang. 2007. Diffusion and solubility coefficients determined by permeation and immersion experiments for organic solvents in HDPE geomembrane. *Journal Hazardous Materials*, 142(1-2): 227-235.

Chiou, C.T. and T.D. Shoup. 1985. Soil sorption of organic vapors and effects of humidity on sorptive mechanism and capacity. *Journal Environmental Science and Technology*, 19(12): 1196-1200.

Chiou, C.T. and D.E. Kile. 2000. Contaminant sorption by soil and bed sediment: Is there a difference? *Fact Sheet-087-00*, June 2000, U.S. Geological Survey, Denver, CO.

Comyn, J. 1985. Polymer Permeability. Elsevier Applied Science Publisher. New York, US.

Crank, J. 1975. The Mathematics of Diffusion. Clarendon Press, Oxdord, UK.

Crum, D.E. and K.E. Carns. 1985. Discussion: prediction of organic chemical permeation through PVC pipe-a water supplier's perspective. *Journal AWWA*, 77(11): 64.

Dillon, I.G. and E. Obasuyi. 1985. Permeation of hexane through butyl nomex. *Journal American Industrial Hygiene Association*, 46(5): 233-235.

DWI0032. 1990. Effect of distribution on organic contaminants in potable water. Foundation for Water Research, London, U.K.

DWI0441. 1992. Effects of organic chemicals in contaminated land on buried services. Foundation for Water Research, London, U.K.

DWI0772. 1997. Effects Permeation of Benzene, Trichloroethene and Tetrachloroethene through Plastic Pipes: An Assessment for Drinking Water Inspectorate. Foundation for Water Research, London, U.K.

Duncan, B., J. Urquhart, and S. Roberts. 2005. Review of measurement and modeling of permeation and diffusion in polymers. *Report of National Physical Laboratory*, Teddington, U.K.

Glaza, E.C. and J.K. Park. 1992. Permeation of organic contaminants through gasketed pipe joints. *Journal AWWA*, 84(7): 92-100.

Griffin Pipe Products Co. 2006. Push-on Joint Pipe. Council Bluffs, IA.

Griffin Pipe Products Co. 2007. Gasket materials used for ductile iron pipe in water and sewage service, Council Bluffs, IA.

Edil, T.B. 2003. A review of aqueous-phase VOC transport in modern landfill liners. *Waste Management*, 23(7): 561-571.

El-Zein, A. 2008. A general approach to the modeling of contaminant transport through composite landfill liners with intact or leaking geomembranes. *International Journal Numerical and Analytical Methods in Geomechanics*, 32(3): 265-287.

Hambly, W.K., J. Pan, A.D. Crocombe, and P. Megalis. 1996. Diffusion laws governing wateruptake of adhesives. *Proceedings of EURADH '96 — ADHESION '96. Institute of Materials*. Cambridge, UK, pp: 281-286.

Holsen, T.M., J.K. Park, D. Jenkins, and R.E. Selleck. 1991a. Contamination of potable water by permeation of plastic pipe. *Journal AWWA*, 83(8): 53-56.

Holsen T.M., J.K. Park, L. Bontoux, D. Jenkins, and R.E. Selleck. 1991b. The effect of soils on the permeation of plastic pipes by organic chemicals. *Journal AWWA*, 83(11):85-91.

Hopman, R. and T.J.J. van den Hoven. 1992. Permeation of organic chemicals through plastic water pipes. *Aqua: Journal Water Supply Research and Technology*, 41(3): 158-162.

Jencen, D.A. and J.K. Hardy. 1988. Method for the evaluation of the permeation characteristics of protective glove materials. *Journal American Industrial Hygiene Association*, 49(6): 293-300.

Jencen, D.A. and J.K. Hardy. 1989. Effect of glove material thickness on permeation characteristics. *Journal American Industrial Hygiene Association*, 50(12): 623-626.

Joo, J.C., J.Y. Kim, and K. Nam. 2004. Mass transfer of organic compounds in dilute aqueous solutions into high density polyethylene geomembranes. *Journal Environmental Engineering*, 130(2): 175-183.

Joo, J.C., K. Nam., and J.Y. Kim. 2005. Estimation of mass transport parameters of organic compounds through high density polyethylene geomembranes using a modified double-compartment apparatus. *Journal Environmental Engineering*, 131(5): 790-799.

Kendaganna Swamy, B.K. and Siddaramaiah. 2003. Sorption and diffusion of chlorinated aliphatic hydrocharbon penetrants into diol chain extended polyurethane membranes. *Journal Hazardous Materials*, 99(2): 177-190.

Khoe, C., V. Bhethanabotla, and R. Sen. 2009. A new diffusion cell for characterizting oxygen permeation of fiber reinforced polymers. *COMPOSITES & POLYCON 2009. American Composites Manufactures Association*. January 15-17, Tampa, FL USA.

Larson, D. 2006. *Communication to AWWA Opflow*. Re: June 2006 Opflow, "Heat fusion process joints PE pipe". September 26, ,Opflow, Denver, CO.

Lin Y.W. and S.S. Que Hee. 1999. Glove permeation tests using novel microchemical techniques for 2,4-dichlorophenoxyacetic acid derivatives. *Archives of Environmental Contamination and Toxicology*, 36(4): 485-489.

Loh, W.K., A.D. Crocombe, M.M. Abdel Waugh, and I.A. Ashcroft. 2005. Modeling anomalous misture uptake and thermal characterisitics of a rubber toughened epoxy adhesive. *Int. Journal. Adhesion and Adhesives*, 25(1): 1-12.

Machado, D.R., D. Hasson, and R. Semiat. 1999. Effect of solvent properties on permeate flow through nanofiltration membranes. Part I: investigation of parameters affecting solvent flux. *Journal Membrane Science*, 163(1): 93-102.

Mao, F. 2008. Permeation of hydrocarbons through polyvinyl chloride (PVC) and polyethylene (PE) pipes. Ph.D. Dissertation, Iowa State University, Ames, IA, 269p.

Massey, L.K. 2003. *Permeability Properties of Plastics and Elastomers- A guide to packaging and barrier materials*. 2nd Ed. Plastics Design Library. William Andrew Publishing. Norwich, NY.

Morrissey, P. and D. Vesely. 2000. Accurate measurement of diffusion rates of small molecules through polymers. *Polymer*, 41(5): 1865-1872.

Naylor, T.deV. 1989. Permeation properties. In: Comprehensive Polymer Science. Edited by Colin B. and Colin P. Pergamon Press, Oxford, UK.

Nelson, G. O., B. Y. Lum, G. J. Carlson, C. M. Wong, and J. S. Johnson. 1981. Glove permeation by organic solvents. *Journal American Industrial Hygiene Association*, 42(3): 217-225.

Neofso, E.K. and S.E. Burns. 2007. Comparison of the equilibrium sorption of five organic compounds to HDPE, PP, PVC. Geomembranes. *Geotextiles and Geomembranes*, 25(6): 360-365.

Neogi, P., 1996. Diffusion in Polymers. Marcel Dekker, Inc, New York, NY.

Norenberg, H. T. Miyamoto, N. Fukugami, Y. Tsukahara, G. D. W. Smith, and G. A. D. Briggs. 1999a. Permeation of gases through polymer membranes investigated by mass spectroscopy. *Vacuum*, 53(1): 313-315.

Norenberg, H. T. Miyamoto, N. Fukugami, Y. Tsukahara, G. D. W. Smith, and G. A. D. Briggs. 1999b. Mass spectrometric estimation of gas permeation coefficients for thin polymer membranes. *Review of Scientific Instruments*, 70(5): 2414-2420.

Ong, S.K., J.A. Gaunt, F. Mao, C.L. Cheng, L. Esteve-Agelet, and C.R. Hurburgh. 2008. Impact of petroleum-based hydrocarbons on PE/PVC pipes and pipe gaskets. *Awwa Research Foundation Report No. 91204*. Awwa Research Foundation, Denver, CO.

Opflow. 2006. Heat fusion process joins PE pipe. Opflow, AWWA, Denver, CO.

Papiernik, S.K., S.R. Yates, and J. Gan. 2001. An approach for estimating the permeability of agricultural films. *Journal Environmental Science and Technology*, 35(6): 1240-1246.

Patterson, B.M., M.E. Grassi, B.S. Robertson, G.B. Davis, A. J. Smith, and A.J. Mckinley. 2004. Use of polymer mats in series for sequential reactive barrier remediation of ammonium-contaminanted groundwater: Field evaluation. *Journal Environmental Science and Technology*, 38(24): 6846-6854.

Park, J.K., L. Bontoux, T.M. Holsen, D. Jenkins, and R. E. Selleck. 1991. Permeation of polybutylene pipe and gasket material by organic chemicals. *Journal AWWA*, 83(10): 71-78.

Park, J.K. and L. Bontoux. 1991. Effect of temperature, repeated exposure, and aging on polybutylene permeation by organic chemicals. *Journal Applied Polymer Science*, 42(11): 2989-2995.

Park, J.K. and L. Bontoux. 1993. Thermodynamic modeling of the sorption of organic chemicals in thermoplastics and elastomers. *Journal Applied Polymer Science*, 47(5): 771-780.

Park, J.K. and M. Nibras. 1993. Mass flux of organic chemicals through polyethylene geomembranes. *Water Environment Research*, 65(3): 227-237.

Park, J.K., J.P. Sakti, and J.A. Hoopes. 1996a. Transport of organic compounds in thermoplastic geomembranes. I: Mathematical model. *Journal Environmental Engineering*, 122(9): 800-806.

Park, J.K., J.P. Sakti, and J.A. Hoopes. 1996b. Transport of aqueous organic compounds in thermoplastic geomembranes. II: Mass flux estimates and practical implications. *Journal Environmental Engineering*, 122(9): 807-813.

Perkins, J.L. and A.D. Tippit. 1985. Use of three-dimensional solubility parameter to predict glove permeation. *Journal American Industrial Hygiene Association*, 46(8): 455-459.

Perkins, J.L. and M.J. You. 1992. Predicting temperature effects on chemical protective clothing permeation. *Journal American industrial Hygiene Association*, 53(2): 77-83.

Pfau, J.P. 1985. Discussion: prediction of organic chemical permeation through PVC pipe-a scientist's perspective. *Journal AWWA*, 77(11): 65.

Phalen, R.N. and S.S. Que Hee. 2003. Permeation of captan through disposable nitrile glove. *Journal Hazardous Materials*, 100(3): 95-107.

Rahman, S. 2007. Sealing our buried lifelines. Opflow April, 2007, AWWA. Denver, CO, accessed on 5-9-08.

Rajani, B and Y. Kleiner. 2003. Protection of ductile iron water mains against external corrosion: review of methods and case histories. *Journal AWWA*, 95(11): 110-125.

Rajani, B. 2008. Long-term performance of ductile iron pipe. National Research Council Canada. http://irc.nrc-cnrc.gc.ca/ui/bu/ductile_e.html. (Expected to finish in 2009).

Rehan, S. 2008. Effect of aging water mains on water quality in distribution systems. National Research Council Canada. http://irc.nrc-cnrc.gc.ca/ui/bu/agingwater_e.html. accessed on 3-15-08.

Rogers, C.E. 1985. Permeation of gases and vapors in polymers. In: Comyn, J. (Ed.), Polymer Permeability. Elsevier Applied Science Publishers, London, UK.

Rowe, R.K., L., Hrapovic, and M.D. Armstrong. 1996. Diffusion of organic pollutants through HDPE geomembranes and composite liners and its influence on groundwater

quality. Geosynthetics: In: De Groot, DenHoedt, Termaat (Ed.), Applications, Design and Construction, A.A. Balkema, Rotterdam, The Netherlands: 737–742.

Rowe, R.K., 2005. Long-term performance of contaminant barrier systems, 45th rankine lecture. *Geotechnique*, 55 (9): 631-678.

Rowe, B.L., P.L. Toccalino, M.J. Moran, J.S. Zogorski, and C.V. Price. 2007. Occurrence and potential human-health relevance of volatile organic compounds in drinking water from domestic wells in the United States. *Environmental Health Perspectives*, 115(11): 1539-1546.

Saleem, M,. A.A Asfour, D. De Kee and B. Harison. 1989. Diffusion of organic penetrant through low density polyethylene (LDPE) films: effect of size and shape of the penetrant molecules. *Journal Applied Polymer Science*, 37(3): 617-625.

Sangam, H. and R.K. Rowe. 2001. Migration of dilute aqueous organic pollutants through HDPE geomembranes. *Geotextiles and Geomembranes*, 19(6): 329-357.

Schwope, A.D., R. Goydan, R.C. Reid, and S. Krishnamurthy. 1988. State-of-the-art review of permeation testing and the interpretation of its results. *Journal American Industrial Hygiene Association*, 49(11): 557-565.

Selleck, R.E. and B.J. Marinas. 1991. Analyzing the permeation of organic chemicals through plastic pipe. *Journal AWWA*, 83(7): 92-97.

Shishatskii, A.M., Y.P. Yampol'skii, and K.V. Peinemann. 1996. Effects of film thickness on density and gas permeation parameters of glassy polymers. *Journal Membrane Science*, 112(2): 275-285.

Silkowski, J.B., S.W. Horstman, and M.S. Morgan. 1984. Permeation through five commercially available glove materials by two pentachlorophenol formulations. *Journal American Industrial Hygiene Association*, 45(8): 501-504.

Soles, C.L., R.L. Jones, J.L. Lenhart, V.M. Prabhu, W.L. Wu, E.K. Lim, D.L. Goldfarb, and M. Angelopoulos. 2003. Polymer dynamics and diffusive properties in ultra-thin photoresist films. *Proceedings of SPIE*, Santa Clara, CA, 5039: 366-375.

Tseng, K.C., N.J. Turro, C.J. Durning. 2000. Molecular mobility in polymer thin films. *Physical Review E*, 61(2): 1800-1811.

Vahdat, N. 1987. Permeation of polymeric materials by toluene. *Journal American Industrial Hygiene Association*, 48(2): 155-159.

Vahdat, N. 1991. Estimation of diffusion coefficient for solute-polymer systems. *Journal Applied Polymer Science*, 42(12): 3165-3171.

Vahdat, N and V.D. Sullivan. 2001. Estimation of permeation rate of chemicals through elastometric materials. *Journal Applied Polymer Science*, 79(7): 1265-1272.

Vesely, D. 2001. Molecular sorption mechanism of solvent diffusion in polymers. *Polymer*, 42(9): 4417-4422.

Vogt, B.D., C.K. Soles, H.J. Lee, E.K. Lin, and W.L Wu. 2004. Moisture absorption and absorption kinetics in polyelectrolyte films: Influence of film thickness. *Langmuir*, 20(4): 1453-1458.

Vonk, M.W. 1985. Permeation of organic compounds through pipe materials. Publication No 85. KIWA, Neuwegein, Netherlands.

Wijmans, J.G. and R.W. Baker. 1995. The solution-diffusion model: a review. *Journal Membrane Science*, 107(1-2): 1-21.

Xu, W. and S.S. Que Hee. 2006. Permeation of a straight oil metalworking fluid through a disposable and a chemically protective nitrile glove. *Journal Hazardous Materials*, 137(2): 709-715.

Zainal, H. and S.S. Que Hee. 2006. Nitrile glove permeation of benomyl. *Archives of Environmental Contamination and Toxicology*, 50(3): 429-436.

CHAPTER 3. PERMEATION OF GASOLINE HYDROCARBON COMPOUNDS THROUGH GASKETED DUCTILE IRON WATER MAINS

CHU-LIN CHENG, SAY KEE ONG, JAMES A. GAUNT

A paper to be submitted to the Journal of American Water Works Association

3.1 Abstract

Contamination of drinking water from the permeation of hydrocarbon compounds into the drinking water pipes has been of public health concern for decades. In this study, permeation experiments and gravimetric sorption tests were conducted to understand the sorption and permeation behaviors of the benzene, toluene, ethylbenzene, and xylenes (BTEX) in gasoline through five polymeric gasket materials for ductile iron pipes. For the gravimetric sorption tests using premium gasoline as the contaminant, ethylene-propylene-diene monomer (EPDM) had the highest equilibrium sorption of gasoline of the five gasket materials, while fluoroelastomer rubber (FKM) had the lowest equilibrium sorption of gasoline. Each gasket was made up of a heel and a bulb portion consisting of the same polymer but different formulation. The heel portion sorbed less than the bulb portion implying that permeation through the heel portion may be slower than the bulb portion.

DI pipes with EPDM, CR and SBR gasket exposed to premium gasoline were found to be permeated within 50 days, while DI pies with SBR gasket exposed to 100% gasoline-saturated aqueous solutions was found to be permeated within 210 days of exposure. Pipe-drum experiments showed that acrylonitrile-butadiene rubber (NBR) was more resistant to BTEX permeation than styrene-butadiene rubber (SBR), the most commonly-used gasket materials in drinking water distribution systems. Sorption rates of contaminants into the heel portion of the gasket from the sorption experiments were found to correlate with the

permeation rates of BTEX compounds from the pipe-drum experiments. However, for DI pipes with SBR gaskets exposed to premium gasoline, the benzene concentration in the pipe-water with 8 hour of stagnation was estimated to exceed the EPA maximum contaminant level (MCL) for benzene but with flow in the pipe, the MCL will not be exceeded.

Keywords: Permeation, polymeric gaskets, BTEX, ductile iron pipe, sorption

3.2. Introduction

In a recent nation-wide examination of groundwater and drinking water supply wells, up to 55 different volatile and semi-volatile organic compounds were detected at low concentrations ranging from 0.01 µg/L to 100 µg/L (Zogorski et al., 2006). Many organic compounds including mono-aromatic compounds such as benzene, toluene, ethylbenzene, and xylenes have been found to be harmful to human health. Contamination of aquifers and soils as a result of gasoline spills, leaking underground storage tanks, and solvent spills from industrial sites, which may threaten drinking water mains and service lines due to organic compounds permeation through plastic pipes and gaskets of ductile iron pipes (Park et al., 1991; Holsen et al., 1991a; Glaza and Park, 1992). Many permeation incidents involving plastic pipes, such as polyvinyl chloride (PVC), polyethylene (PE), and polybutylene (PB), have been reported including several permeation incidents for water mains for ductile iron (DI) pipes with gaskets (Thompson and Jenkins, 1987; Park et al., 1991; Holsen et al., 1991a; Glaza and Park, 1992; Ong et al., 2008). Although DI pipe itself is resistant to permeation, the gaskets used to join and seal the pipes are susceptible to permeation by organic contaminants (Holsen et al., 1991a; Park et al., 1991; Selleck et al., 1991; Glaza and Park

1992; Ong et al., 2008). DI pipes are widely used with DI pipes accounting for almost half of the new water mains installed in North America (Rajani and Kleiner, 2003). Drinking water may be contaminated with the organic chemicals exceeding to MCL even though the odor and smell of the organic chemicals in drinking water may not be noticeable.

The most widely used and easiest to assemble joint for DI pipes is the push-on joint—two examples are given in Figure 1. To join the pipes, a single rubber gasket is placed in a groove inside a socket of the bell end of the pipe and the beveled end of the pipe (spigot) is pushed past the gasket into the bell end of the pipe. The gasket is compressed and a pressure-tight seal is formed. The gasket is made of polymeric material such as ethylene-propylene-diene monomer (EPDM), chloroprene rubber (CR; neoprene), styrene-butadiene rubber (SBR), acrylonitrile butadiene rubber (NBR), and fluoroelastomer rubber (FKM). SBR and CR are typically used for water distribution pipes while NBR and FKM gaskets are used for pipes conveying hydrocarbons and petroleum products or when hydrocarbon-resistant gaskets are required for water distribution pipes (Griffin Pipe Products Co., 2007; Ductile Iron Pipe Research Association, 2007). About 90% of the gaskets used in water distribution pipes are SBR gaskets due to its low cost and good durability (Park et al., 1991; Rahman 2007; Ong et al., 2008). SBR gaskets have been reported to be less resistant to gasoline permeation than NBR (Glaza and Park, 1991). However, there are very few studies on the susceptibility of contaminant permeation through SBR and NBR gaskets and other elastomeric gasket materials (Park et al., 1991; Glaza and Park, 1992). While numerous studies have focused on the permeation of contaminants through plastic pipes in the water industry (Berens, 1985; Holsen et al., 1991; Selleck and Marinas, 1991; Hopman and Hoven, 1992), not much is

known about the performance of commonly-used elastomeric gaskets in contact with organic contaminants, or the permeation mechanism of contaminants under commonly encountered field conditions.

The objectives of this study are: (1) to investigate the permeation of benzene, toluene, ethylbenzene, and xylenes (BTEX) in gasoline, through a commonly-used gasket for DI pipe joints under simulated environmental conditions; and (2) to evaluate the performance of different gasket materials at different contaminant concentrations; and (3) to assess the impacts of BTEX permeations on drinking water quality for various pipe sizes and stagnation and flow conditions in the pipe. Sorption of BTEX by various gasket materials using the gravimetric sorption tests, and the permeation rates and diffusion coefficients obtained from pipe-drum permeation experiments will be compared. Part of the study is to assess the threshold contamination under environmental conditions in the field that may result in exceeding of the MCLs for BTEX compounds in the drinking water.

3.3. Materials and Methods

3.3.1 Reagents and apparatus

The type of gasket used for the study is Tyton® gaskets. Tyton® gasket is the most common type of gasket used with a market share of 31% (Muller Water Products, 2006). Use of Tyton® gasket for this study is for experimental purposes and does not imply endorsement of the product.

Tyton® gaskets of five different polymer compounds (SBR, EPDM, NBR, CR and FKM) in 4-inch push-on DI pipe joints were used. The gaskets (manufactured by U.S. Pipe,

Birmingham, AL) and DI pipes were provided by Griffin Pipe Products Co. (Council Bluffs, IA). Examination of Tyton® gaskets indicated that a typical gasket consisted of a hard "heel" and a soft "bulb" portion (see Figure 1). The heel portion anchors the gasket in place during the assembly of the joint and the bulb forms the hydrostatic seal (Bird, 2006; Rahman, 2007). The heel and bulb are made of the same polymer but compounded differently with more carbon black for the heel portion to make it harder (Bird, 2006). No previous research has described the sorption or permeation characteristics of the bulb or the heel portion of a Tyton® gasket. Either portion may be the rate limiting step for the permeation of organic compounds.

3.3.2 Equilibrium sorption

To investigate the impact of different gasoline on gasket materials, equilibrium sorption tests were performed on the five gasket materials in premium gasoline, regular gasoline, 10% ethanol gasoline (E10) and premium gasoline with 10% methyl tertiary-butyl ether (MTBE). The samples were placed in 120 mL Teflon®-lined, screw-capped jars filled with gasoline and kept at room temperature (23 ± 1.5°C). Samples were removed at regular intervals, wiped dry using a paper towel and weighed using an electronic balance (Mettler Toledo AG204, Columbus, OH) with an accuracy of 0.001 gram. The samples were weighed until constant weight was reached and equilibrium sorption was reported as percent weight gain. Since premium gasoline showed the highest percent weight gain of the four gasolines for all gasket materials tested, premium gasoline was chosen as the solvent for all subsequent sorption tests and pipe-drum permeation experiments.

To study the impact of heel and bulb material on permeation, sample specimens of size 1 cm×1 cm×0.6 cm (0.4 inch×0.4 inch×0.25 inch) of the heel portion only, bulb portion only, and a cross-sectional portion of approximately equal heel and bulb portions for all five gasket materials were prepared. The specimens were immersed in premium gasoline and periodically removed and the weight measured as described earlier.

3.3.3 Pipe-drum permeation experiments

To study the permeation of gasoline through the gasket material of pipe joints, pipe-drum apparatuses were used to simulate a pipe joint buried in gasoline contaminated soils. The bell and spigot ends of the DI pipe were cut to lengths of 17.8 cm (7 inches) and 13 cm (5 inches), respectively. The end of each pipe was welded with a steel plate with a 0.6 cm (0.25 inch) fitting attached. A 0.6 cm (0.25 inch) copper tubing with a 0.6 cm ball valve for sampling of the water in the pipe was connected to the 0.6 cm fitting (see Figure 2). Welding was done by Home Welding and Metal Fabrication (Ames, IA). The bell and spigot were assembled according to the manufacturer's specification and efforts were made to ensure that the bell and spigot were properly aligned. The pipe joints were restrained from separating by using steel straps as shown in Figure 2. In a typical experiment, a pipe joint with a specific type of gasket material was placed in a 18 L (5 gallons) steel drum at an angle as shown in Figure 2. the drum was then filled with silica sand. The pipe-joint apparatus was filled with deionized water by introducing the deionized water into the bottom fitting until deionized water flowed out from upper fitting and valve. The valves were then closed. Contaminated water or gasoline were then slowly added to fill the drum. Each drum had a copper tube

extended from outside of the drum to the bottom of the drum and another copper tube at the rim of the drum to replenish the external contamination solution without opening the drum (see Figure 2). The space between the copper tubes and the holes in the lid and the side of the drum were sealed with gasoline-resistant, silicone caulking. The lid was secured to the pail with a lever-lock.

Samples for analysis were collected in 40-mL vials capped with Teflon®-coated silicone rubber seals by gently applying compressed air into the apparatus through the valve connected to the upper fitting. The samples collected from the pipe joint were analyzed with a gas chromatography (Tractor 540, Austin, TX) equipped with a packed column (1% SP1000 on 60/80 mesh Carbopack B), a photoionization detector, and an automated purge & trap concentrator (Tekmar LSC 2/ALS). After each sampling, the pipe joint was rinsed and flushed three times with deionized water before fresh deionized water was added from the bottom fitting to remove all air head space in the pipe joint. Samples were collected weekly or monthly depending on the external contaminant concentration used. The method detection limits for benzene, toluene, ethylbenzene, m-xylene and o+p xylene were 0.24 μg/L, 0.24 μg/L, 0.26 μg/L, 0.29 μg/L, and 0.53 μg/L, respectively.

Five pipe-drum apparatuses each with a different gasket material were set up with free product premium gasoline as the external contamination. In addition, eight pipe-drum apparatuses were set up to simulate environmental exposure of SBR and NBR gaskets to groundwater contaminated with gasoline with concentrations approximately equal to 100%, 50%, 20% and 5% of aqueous saturation. One apparatus was set up to simulate environmental exposure of FKM gasket to groundwater saturated with gasoline (100%). The

aqueous solutions of gasoline were replaced monthly by pumping fresh solutions into the bottom of the drum and collecting the overflow from the valve at the rim of the drum. Approximately 68%, 66%, 67% and 79% of the original concentrations of the aqueous solution remained at the end of each month. Water saturated with gasoline (100%) was prepared by mixing 1 L premium gasoline and 10 L deionized water in a 12-L glass bottle for 48 hours with constant stirring.

3.3.4 Data analysis

The "half-time method" was used to estimate the diffusion coefficient from the percent weight gain plots of the sorption tests (Crank, 1975; Neogi, 1996). The half-time method assumed a constant diffusion coefficient and no swelling effects during the uptake of the solvent by a polymer sheet. The equation for the total mass of contaminant adsorbed is given by:

$$\frac{M_t}{M_\infty} = 1 - \frac{8}{\pi^2}\sum_{m=0}^{\infty}\frac{1}{(2m+1)}\exp\left\{\frac{-D(2m+1)^2\pi^2 t}{\ell^2}\right\} \qquad [1]$$

where M_t = total mass of contaminant absorbed by the sheet at time t (mg)

M_∞ = equilibrium sorption attained, theoretically after infinite time (mg)

D = diffusion coefficient (cm^2/s)

ℓ = thickness of material (cm)

t = time (s)

Assuming that the concentration at the surface attains a value corresponding to the equilibrium uptake immediately after the sheet is placed in the contaminant and remains

constant, the value of $\frac{T_{1/2}}{\ell^2}$ when the mass gained is equal to half of the mass sorbed at equilibrium ($\frac{M_t}{M_\infty} = 1/2$), the equation is given as:

$$(\frac{T_{1/2}}{\ell^2}) = -\frac{1}{\pi^2 D}\ln\left\{\frac{\pi^2}{16} - \frac{1}{9}(\frac{\pi^2}{16})^9\right\} \quad [2]$$

Equation [2] (with an error of about 0.001%) can be simplified and rearranged to :

$$D_{T_{1/2}} = 0.049\frac{\ell^2}{T_{1/2}} \quad [3]$$

where $D_{T_{1/2}}$ = diffusion coefficient for $\frac{M_t}{M_\infty} = 1/2$ (cm^2/s)

$T_{1/2}$ = time required for mass sorbed to reach half of equilibrium mass sorbed (s).

The "time-lag method" was employed to estimate the diffusion coefficients from the plots of cumulative permeation mass curves for BTEX compounds with time (Crank, 1975; Park et al., 1991; Glaza and Park, 1992; Neogi, 1996; Chao et al., 2006). The time-lag method is derived from Fick's diffusion equation by assuming: the outer concentration of contaminant remains constant; the initial concentration of the contaminant in the polymer is zero; and the inner concentration of the contaminant is kept at zero.

The total mass of chemical diffusing through a plane sheet, Q_t (mg/cm^2), as a function of time t, is:

$$\frac{Q_t}{\ell C_0} = \frac{Dt}{\ell^2} - \frac{1}{6} - \frac{2}{\pi^2}\sum_1^\infty \frac{(-1)^n}{n^2}\exp(\frac{-Dn^2\pi^2 t}{\ell^2}) \quad [4]$$

where C_o = the concentration of contaminant on the outer side of the membrane (mg/L)

As t approaches infinity, the equation becomes:

$$Q_t = \frac{DC}{\ell}(t - \frac{\ell^2}{6D}) \quad [5]$$

Extending the asymptote of the curve of Equation [5] to the t axis, the intercept, T_L, is given by:

$$D_{T_L} = \frac{\ell^2}{6T_L} \quad [6]$$

where D_{T_L} = diffusion coefficient (cm^2/s) estimated from T_L

T_L = the lag time (s) at steady-state permeation (intercept of t axis).

3.4. Results and Discussion

3.4.1 Gravimetric sorption test

The results of sorption tests for five different Tyton® gasket materials were tested in three different types of gasoline and gasoline + 10% MTBE (Figure 3). Except for E10, the order of percent weight gain for gasoline, from highest to lowest, was EPDM, SBR, CR, NBR, FKM. For E10, the order of weight gain from highest to lowest was EPDM, SBR, NBR, CR, FKM. Equilibrium sorption for the SBR, NBR and EPDM gaskets was reached within one day. CR and FKM gaskets showed a slow increase with time. Since the sorption of premium gasoline for all gaskets showed higher percent weight gain than other gasoline, premium gasoline was used to conduct the pipe-drum permeation experiments to correlate with the sorption results.

For premium gasoline, the order of percent weight gain from highest to lowest for a gasket specimen was EPDM, SBR, CR, NBR, and FKM, with a percent weight gain of 127% for EPDM and less than 1% weight gain for FKM. The high sorption by EPDM implies that EPDM material may have more free volume to sorb premium gasoline or has more polymer interaction with the organic chemicals of gasoline resulting in larger extends of relaxation of the polymer molecule in respond to the solvent. A comparison of the percent weight gain of the heel and bulb portion showed that the bulb portion of all gasket materials except for CR were found to sorb more gasoline than the heel portion (Table 1). The percent weight gains for all gasket materials except for CR were roughly equal to the average of the percent weight gains of the bulb and heel portion.

Equilibrium sorption of a contaminant by polymeric materials has been correlated to the permeation property of polymer materials (Berens, 1985; Park and Bontoux, 1993; Altinkaya et al., 2006). Measurement of mass uptake in the sorption test is comparatively simple, but it yields no information on the breakthrough time and permeation rates of the contaminant through the gasket. Moreover, the sorption behavior can be complicated by factors, such as geometry of polymer materials, heat effects due to solvent absorption, area exposed to solvents, and swelling of the polymer material.

3.4.2 Permeation experiments

The results of pipe-drum apparatus experiments using premium gasoline showed that the order of total BTEX breakthrough for the various gasket materials matched the order of maximum sorption in sorption tests except for FKM gaskets (Figure 3). Without considering

FKM, the order of breakthrough was EPDM > CR = SBR > NBR at approximately 35, 50, 50, and 124 days, respectively. FKM is the most resistant of all the gaskets to hydrocarbon permeation based on the sorption data expressed as percent weight gain. It is possible that the BTEX permeated may be due to leakage since the relative hard FKM rubber created some difficulties in mounting the pipes (Bird, 2006).

The estimated permeation rates for total BTEX and individual compounds through the five different gaskets estimated from the slopes of the permeation curves of cumulative mass with time are presented in Table 2. SBR material has the highest permeation rates for total BTEX, followed by CR, EPDM, and NBR. In general, the permeation rates of toluene were higher than of benzene, ethylbenzene, and xylenes for all gasket materials.

A 4-inch DI pipe with SBR gasket exposed to a 100% saturated aqueous solution of gasoline in a pipe-drum apparatus showed a breakthrough time of 210 days while the breakthrough time for the SBR gasket exposed to a 50% saturated aqueous solution of gasoline was approximately 240 days (Figure 4). For pipes exposed to 20% or 5% saturated aqueous solutions of gasoline, no permeation was observed through SBR gaskets after more than 550 days of exposure. In the case of NBR or FKM gaskets exposed to gasoline-saturated water (100%), there were no measurable gasket permeation after 550 days. Gasket thickness, i.e. the length of permeation paths, is needed to estimate the diffusion coefficient using the time-lag approach. Since a gasket is compressed in the space of pipe joint and the gasket may swell due to sorption of the hydrocarbon compounds, the original gasket thickness before it was inserted into the joint was used in the estimation of the diffusion coefficients.

3.4.3 Correlation of sorption and permeation experiments

Since the sorption of the heel is much less than that of the bulb and the heel is most likely in contact with the external contaminants, the heel portion would impact the overall permeability of the Tyton® gaskets. Table 3 presents the estimated total BTEX permeation rates for 4-inch Tyton® gaskets and the percent weight gain, and sorption rate (percent weight gain/$min^{1/2}$) for the heel portion only. The heel portion of EPDM gasket had a 97% weight gain from the equilibrium sorption test. Both CR and SBR gaskets had 57% and 61% weight gains respectively but the permeation rates for these two gasket materials were higher than that of EPDM. The percent weight gain for NBR was about 27% but the BTEX permeation rate of 0.36 mg/joint/day was the lowest of the four gasket materials (excluding FKM). In general higher permeation rates were observed for gaskets that had high sorption rates.

Based on the above observations, simple linear correlations between the permeation rates and percent weight gain (W%) or sorption rates (W%/$min^{1/2}$) were attempted as shown in Figure 6. The R-squared value for a linear regression of permeation rates and sorption rates was 0.73, while the R-squared value was 0.63, for a linear regression of permeation rates and percent weight gain. Based on the data presented in Figure 6, there seemed to be a correlation between sorption rates or percent weight gain and the permeation rates.

3.4.4 Estimation of total BTEX diffusion coefficients for Tyton® gaskets

Total BTEX Diffusion coefficients for Tyton® gaskets were estimated from the results of the sorption tests and the pipe-drum experiments according to the half-time and time-lag

methods, respectively (Table 4). The length of gasket used in the estimation of the diffusion coefficients for the time-lag method was 2.54 cm. EPDM had the highest percent weight gain and the highest estimated diffusion coefficient for both methods, followed by CR, SBR and NBR. The estimated diffusion coefficient using the half-time method for a slice of SBR gasket (including bulb and heel) was 9.55×10^{-7} cm^2/s, while the estimated diffusion coefficient for a slice of NBR gasket was 3.20×10^{-7} cm^2/s. The estimated diffusion coefficients from sorption experiments were generally one order of magnitude larger than the estimated values from pipe-drum permeation experiments using the time-lag method. Unlike the other polymer materials tested, estimated diffusion coefficient using the half-time method for the FKM gasket was two order magnitudes smaller than estimated diffusion coefficient using the time-lag method. These results generally reflect the earlier explanation where the FKM gasket for the pipe-drum experiment was not installed or aligned properly due to the stiffness of the gasket and therefore may have experienced a minor leak.

3.4.5 Risk assessment of drinking water exposed to contaminated soils

To evaluate BTEX permeation and its impact on drinking water quality, the mass permeated per joint per day, M, and the permeation rate, F_m, in a pipe joint were employed. The permeation mass per joint used was based on the experimental data and is given by,

$$F_m = \frac{M}{A} \qquad [7]$$

where F_m = permeation rate in one pipe joint ($mg/cm^2/day$)

M = mass permeated per joint per day (mg/joint/day)

A = area of the gasket contacted by solvents (cm^2)

Using Fick's First Law

$$F_m = -D\frac{\partial C}{\partial x} = -D\frac{C_o - C_i}{\Delta x} \quad [8]$$

where D = diffusion coefficient of gasket material (cm^2/s)

C_o = solution concentration at outer boundary of the gasket (mg/L)

C_i = solution concentration at inner boundary of the gasket (mg/L)

Δx = permeation distance (cm) (gasket thickness)

By assuming the inside concentration, C_i, to be zero (drinking water within the pipe) and the thickness (i.e., length of permeation path) of the gasket to be ℓ, the equation becomes,

$$F_m = -D\frac{C_0}{\ell} \quad [9]$$

For the same type of gasket material (i.e., the same diffusion coefficient) and the same external concentration, the partitioning coefficients would be the same (same polymer-solvent pair) and is given by:

$$F_{m,1}\ell_1 = F_{m,2}\ell_2 = -D(C_0 - 0) \quad [10]$$

Substituting for the permeation rate, F_m, with equation [7], the equation [10] becomes,

$$\frac{M_1}{A_1}\ell_1 = \frac{M_2}{A_2}\ell_2 \quad [11]$$

Rearranging:

$$M_2 = M_1\frac{\ell_1}{\ell_2}\frac{A_2}{A_1}, \text{ or } M_2 = M_1\frac{\beta_A}{\beta_L} \quad [12]$$

where β_L = length factor $(=\frac{\ell_2}{\ell_1})$

β_A = area factor $(=\frac{A_2}{A_1})$

Knowing the dimensions of two gaskets, Equation [12] can be used to estimate the permeation rate for a gasket of different size by using the experimentally determined permeation rate of a single pipe. The estimated permeation rates for various sizes of gaskets as shown in Table 5 were based on the experimental permeation rates for benzene for a 4-inch DI pipe from pipe-drum experiments, which were 6.56 mg/joint/day for SBR gaskets exposed to free product gasoline; 0.159 mg/joint/day for SBR gaskets exposed to gasoline saturated water; and 0.073 mg/joint/day for NBR gaskets exposed to free product gasoline. The permeation rate of 6.56 mg/joint/day for SBR exposed to free product gasoline was based on eight pipe-drum experiments and equal to the mean plus three-standard-deviation margin (99.7% confidence level). The other two permeation rates were from single experiments. Based on Equation [12], the permeation rate of a single gasketed joint increased with larger sizes of DI pipe since the β_A for a larger DI pipe is larger than the β_L (based on manufacturer's data, Griffin Pipe Product Co., Council Bluffs, IA). For example, the permeation rates for 10, 16, and 24-inch pipe with SBR gasket exposed to free product gasoline were estimated to be 11.5, 21.0, and 30.7 mg/joint/day, respectively. The estimated total contact surface area for a 4-inch gasket used in the calculation was 44.41 cm^2, which was the area perpendicular to the push-in direction.

Typical flow velocities in water distribution pipes ranged from 2 to 10 feet per second (ft/s) (0.6 to 3 m/s). Using 2 ft/s, the flow rate for a 24-inch pipe is estimated to be 11,520

gpm. As presented in Figure 7, the estimated flow rate needed to obtain a contaminant level equal to the benzene MCL for 100 feet (5 joints) of a 24-inch DI pipe with SBR gaskets exposed to free product gasoline was approximately 6 gpm. This means that a minimal flow would easily provide sufficient volume per unit time so that the benzene MCL will not be exceeded. In the case of NBR gaskets exposed to gasoline, the flow rate needed so that the benzene was less than the MCL in a 24-inch pipe was 0.1 gpm (Figure 8).

The concentrations of benzene that might result from periods of stagnation were estimated using the benzene permeation rates in Table 5 and presented in Figure 9. Assuming a scenario of 100 ft of 4-inch DI pipe (with 5 gaskets) and containing 247 L of water exposed to free product gasoline, the benzene concentrations after 8 hours of stagnation were estimated to be 19 µg/L for SBR gaskets and 1.1 µg/L for NBR gaskets. In this scenario, the 5 µg/L MCL for benzene was exceeded for SBR gaskets but not for the NBR gaskets.

3.4.6 Impact in flowing water mains

Engineering decisions regarding permeation of gaskets by gasoline should be based on the rate of permeation by benzene since the MCL for benzene (5 µg/L) is 200 times lower than that of toluene (1,000 µg/L) and of the BTEX compounds, benzene is the most soluble in water. In the experiments involving 4-inch SBR Tyton® gaskets exposed to free product gasoline (a worst case scenario), the average rate of permeation by benzene was 2.72 ± 1.28 (standard deviation) mg/joint/day (based on the eight experiments conducted with SBR gaskets). Allowing for a safety margin of three standard deviations (99.7% confidence), a

benzene permeation rate of 6.56 mg/joint/day may be used to predict benzene concentrations in flowing mains. Assuming this permeation rate, a volume of 347 gallons (1,312 L)/joint/day of water would be required to obtain a concentration of benzene equal to the MCL of 5 µg/L. This corresponds to an average flow rate of 0.24 gpm for every joint exposed to contamination in 4-inch DI main. Since the analytical method detection limit (MDL) for benzene (0.24 µg/L) was about 21 times lower than the MCL, a flow of 5 gpm for every joint exposed to contamination would result in benzene concentration for DI pipe with SBR gaskets that are not analytically detectable.

For the experiment involving a 4-inch NBR gasket exposed to free product gasoline, the benzene permeation rate was experimentally found to be 0.159 mg/joint/day, which means that a flow of 0.0058 gpm for every joint exposed to contamination would be required to obtain benzene MCL concentration and a flow of 0.12 gpm would render the benzene concentration undetectable for one DI pipe joint.

For a 4-inch SBR gasket exposed to 100% saturated aqueous gasoline solution (containing about 168 mg/L total BTEX), the benzene permeation rate was found experimentally to be 0.073 mg/joint/day, which would require a flow rate of 2.7×10^{-3} gpm to obtain to the benzene MCL and a flow rate of 0.056 gpm would render the benzene concentration undetectable.

Clearly, only a minimal flow in a water main, even in the worst case scenario, will reduce benzene concentrations below the MCL and most likely render benzene undetectable. Since the benzene threshold odor limit is 190 µg/L, the benzene MCL can be exceeded before taste and odor are detected in the drinking water (Ong et al., 2008). According to the Ductile

Iron Pipe Research Association (DIPRA), the common flow velocity in DI pipe with cement/cement-mortar linings used for potable water is 2 to 10 feet per second (ft/s) or approximately 80 to 400 gpm for a 4-inch pipe. In realistic conditions, contaminants would be diluted to undetectable levels with a minimum flow of 2 ft/s in a 4-inch pipe.

3.5 Conclusion

Gravimetric sorption tests for five different Tyton® gasket materials (EPDM, SBR, CR, NBR and FKM) for DI pipes in premium gasoline indicate that EPDM had the highest sorption (127% weight gain) in comparison to the other gaskets, while FKM, known its resistance to gasoline permeation, exhibited very low sorption (about 0.65%). Tyton® gaskets consist of a hard "heel" and a soft "bulb" portion. Gravimetric sorption tests for the heel and bulb portion of the five gasket materials indicate that the bulb portion sorbed more than the heel for all gasket materials except for CR. For SBR Tyton® gaskets, the bulb portion sorbed about 66% more than the heel portion. While the bulb portion is known to provide the hydrostatic seal for the water in the pipe, observations indicated that an external contaminant must first pass through the less permeable heel portion. The permeability of the heel portion would, therefore, determine the overall permeability of an SBR gasket. This would not be the case for NBR gaskets since equilibrium sorption experiments showed the heel and bulb portions to be nearly identical.

Pipe-drum experiments with 4-inch DI joints using five different Tyton® gasket materials exposed to free product premium gasoline showed that EPDM and CR performed similarly to SBR with equilibrium permeation rate of 5.20 total BTEX/joint/day for SBR.

Breakthrough of gasoline was observed for the three gaskets after 35 days of experimentation. NBR was the most resistant (breakthrough time of 124 days) to permeation with equilibrium permeation rates of 0.36 mg total BTEX/joint/day. These pipe-drum experiments indicated that NBR was more resistant to permeation than SBR.

After 7 months of exposure to saturated solutions of gasoline in water (about 168 mg/L total BTEX), breakthrough time was observed through the SBR gasket after 210 days at a rate of 0.073 mg/joint/day of benzene (0.203 mg/joint/day of total BTEX). No permeation was observed through the NBR or FKM gaskets exposed to saturated solutions of gasoline for 550 days (18 months). Permeation was observed for the SBR gasket exposed to 50% aqueous solutions of gasoline after 240 days. No permeation was observed through NBR gaskets exposed to 50%, 20%, and 5% saturated aqueous solutions of gasoline and for SBR gaskets exposed to 20%, and 5% aqueous solutions of gasoline.

Under conditions of stagnation, such as in a service line, the 5 μg/L MCL for benzene will likely be exceeded during an 8-hour stagnation period for SBR gaskets in contact with free product gasoline. Under these circumstances, NBR gaskets would be sufficiently resistant to prevent permeation by benzene or other BTEX compounds in gasoline to a level that would exceed EPA MCLs. As long as there is at least a minimal flow of water in the main, benzene and other BTEX compounds in gasoline would not exceed EPA MCLs, even under the worst conditions of gasoline contamination, due to dilution.

The overall diffusion coefficients of intact 4-inch Tyton® gaskets were estimated from the results of the sorption test and pipe-drum experiments according to the half-time and time-lag methods. The estimated diffusion coefficient for a slice of SBR gasket using half-

time method of 9.55×10^{-7} cm^2/s, while the diffusion coefficient for a slice of NBR gasket gave a diffusion coefficient was 3.20×10^{-7} cm^2/s. The estimated diffusion coefficient from sorption experiments were generally one order of magnitude larger than estimated values from pipe-drum experiments using the time-lag method.

3.6 Reference

Altinkaya, S.A., N. Ramesh, and J.L. Duda. 2006. Solvent sorption in a polymer-solvent system-Importance of swelling and heat effects. *Polymer*, 47 (24): 8228-8235.

Berens, A.R. 1985. Prediction of organic chemical permeation through PVC pipe, *Journal AWWA*, 77(11): 57-64.

Bird, W. 2006. Personal communication. S&B Technical Products, 1300 East Berry St. Fort Worth 76119.

Chao, K.P., J.S. Lai, H.C. Lin, and Y.P. Hsu. 2006. Comparison of permeability determined by permeation cell and immersion methods for organic solvents through protective gloves. *Polymer Testing*, 25(7): 975-984.

Crank, J. 1975. The Mathematics of Diffusion. Clarendon Press. Oxdord, UK

Ductile Iron Pipe Research Association. 2007. DIPRA Gaskets Data Sheet (updated 3-02-08). http://www.dipra.org/pdf/gasketsForDIP.pdf, accessed on 10-20-08.

Glaza, E.C. and J.K. Park. 1992. Permeation of organic contaminants through gasketed pipe joints. *Journal AWWA*, 84(7): 92-100.

Griffin Pipe Products Co. 2007. Gasket materials used for ductile iron pipe in water and sewage service. Council Bluff, IA.

Holsen, T.M., J.K. Park, D. Jenkins, and R.E. Selleck. 1991 (a). Contamination of potable water by permeation of plastic pipe. *Journal AWWA*, 83(8): 53-56.

Hopman, R. and T.J.J. Van Den Hoven. 1992. Permeation of organic chemicals through plastic water pipes. *Aqua: Journal Water Supply Research and Technology*. 41(3): 158-162.

Neogi, P., 1996. Diffusion in Polymers. Marcel Dekker, Inc. New York, NY.

Ong, S.K., J.A. Gaunt, F. Mao, C.L. Cheng, L. Esteve-Agelet, and C.R. Hurburgh. 2008. Impact of petroleum-based hydrocarbons on PE/PVC pipes and pipe gaskets. *Awwa Research Foundation Report No. 91204.* Awwa Research Foundation, Denver, CO.

Park, J.K., L. Bontoux, T.M. Holsen, D. Jenkins, and R.E. Selleck. 1991. Permeation of polybutylene pipe and gasket material by organic chemicals. *Journal AWWA*, 83(10):71-78.

Park, J.K. and L. Bontoux. 1993. Thermodynamic modeling of the sorption of organic chemicals in thermoplastics and elastomers. *Journal Applied Polymer Science*, 47(5): 771-780.

Rahman, S. 2007. Sealing our buried lifelines. Opflow April, 2007, American Water Works Association. www.awwa.org/communication/opflow, accessed on 04-05-08.

Rajani, B and Y. Kleiner. 2003. Protection of ductile iron water mains against external corrosion: review of methods and case histories. *Journal AWWA*, 95(11): 110-125.

Selleck, R.E. and B.J Marinas. 1991. Analyzing the permeation of organic chemicals through plastic pipe. *Journal AWWA*, 83(7): 92-97.

Thompson C. and D. Jenkins. 1987. Review of water industry plastic pipe practices, report to AWWA Research Foundation NO. 90516. Denver, CO.

Zogorski, J.S., J.M. Carter, T. Ivahnenko, W.W. Lapham, M.J. Moran, B.L. Rowe, P.J. Squillace, and P.L. Toccalino. 2006. The quality of our nation's waters volatile organic compounds in the Nation's ground water and drinking-water supply wells. The U.S. Geological Survey Circular 1292: National Water-Quality Assessment program. Reston, VA.

Table 1 Percent weight gain (W%) per gram of gasket material in premium gasoline

	Total (Heel + Bulb)	Heel	Bulb
SBR	80.03 ± 1.35 %	61.11 ± 1.47 %	97.31 ± 2.78 %
NBR	27.72 ± 0.82 %	26.91 % ± 0.89	29.04 ± 1.48 %
EPDM	127.02 ± 1.86 %	97.34 ± 1.21 %	141.58 % ± 1.66 %
FKM	0.65 ± 0.09 %	0.81 ± 0.11 %	0.82 ± 0.11 %
CR	46.87 ± 1.06 %	57.13 ± 0.41 %	43.84 ± 1.34 %

Table 2 Measured permeation rates (mg/joint/day) through 4-inch Tyton® gaskets

Gasket	Benzene	Toluene	Ethylbenzene	m-Xylene	o+p Xylene	Total BTEX
EPDM	1.06	2.25	0.12	0.29	0.31	3.93
SBR#	2.72	2.22	0.068	0.164	0.185	5.20
CR	1.47	2.34	0.08	0.19	0.22	4.23
NBR	0.16	0.12	0.004	0.008	0.008	0.36
FKM*	0.15	0.23	0.013	0.030	0.033	0.49

[#: average values from 8 experiment; *: possible leakage]

Table 3 Heel rubber sorption and gasket permeation rates for premium gasoline

Experiments	4-inch Tyton® Gaskets				
	EPDM	CR	SBR	NBR	FKM
Equilibrium sorption for Heel (W%)	97.3%	57.1%	61.1%	26.9%	0.81%
Sorption rate for Heel (W% /min$^{1/2}$)	3.27	2.06	2.09	0.38	0.0073
Permeation rate (mg BTEX/day)	3.93	4.23	5.20#	0.36	0.49*

[# average of 8 values; * possible leakage]

Table 4 Estimated total BTEX diffusion coefficients for various gaskets

Estimation method	Diffusion coefficient (cm^2/s)				
	EPDM	CR	SBR	NBR	FKM
Half-time	1.20×10^{-6}	1.05×10^{-6}	9.55×10^{-7}	3.20×10^{-7}	6.73×10^{-9}
Time-lag#	2.29×10^{-7}	1.77×10^{-7}	1.46×10^{-7}	8.90×10^{-8}	1.62×10^{-7}*

* possible leaking of pipe joint in pipe-drum experiment
# estimation based on assumption of original gasket thickness of 2.54 cm

Table 5 Estimated permeation rates of benzene through 4-inch to 24-inch DI pipes with Tyton® gaskets

Pipe Diameter (ins)	Gasket width* (cm)	Contact area** (cm^2)	β_L	β_A	Permeation rate (mg/joint/day)		
					SBR-Gasoline^{+}	SBR-100%$^{++}$	NBR-Gasoline^{+}
4	3.63	44.41	1.00	1.00	6.56^{ζ}	0.073^{ζ}	0.159^{ζ}
6	3.63	62.28	1.00	1.40	9.20	0.102	0.223
8	4.72	89.63	1.30	2.02	10.18	0.113	0.247
10	5.08	108.94	1.40	2.45	11.51	0.128	0.279
12	5.08	128.72	1.40	2.90	13.59	0.151	0.329
14	5.84	201.63	1.61	4.54	18.52	0.206	0.449
16	5.84	228.22	1.61	5.14	20.96	0.233	0.508
18	5.84	254.81	1.61	5.74	23.40	0.260	0.567
20	5.84	281.40	1.61	6.34	25.84	0.288	0.626
24	5.84	334.57	1.61	7.53	30.73	0.342	0.745

* width (thickness) of gasket as provided by manufacturer
** largest cross section area of gasket (estimated from manufacturer's data)
$^{+}$ gasket in contact with pure premium gasoline
$^{++}$ gasket in contact with gasoline-saturated water
$^{\zeta}$ from experimental data

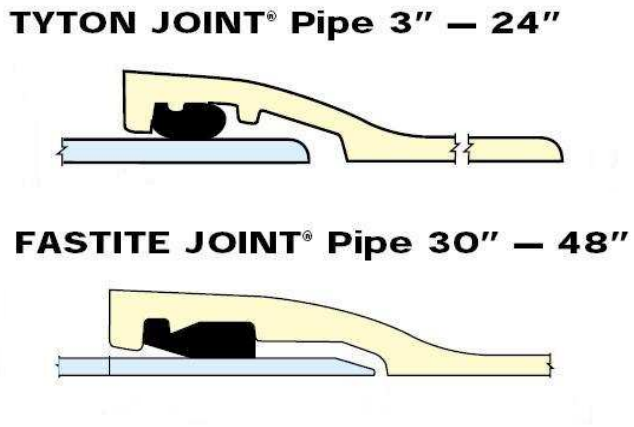

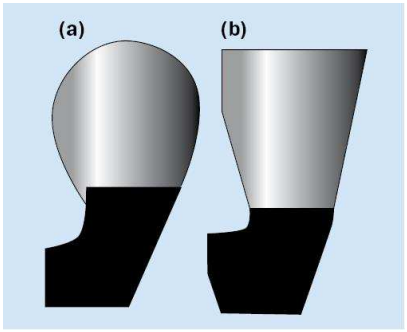

Figure 1 (left) Cross-sections of push-on joints of DI pipe (Griffin Pipe Products Co., Council Bluffs, IA); (right) cross-sections of push-on gaskets including heel (black) and bulb (gray): (a) Tyton® (b) Fastite® (Rahman, 2007)

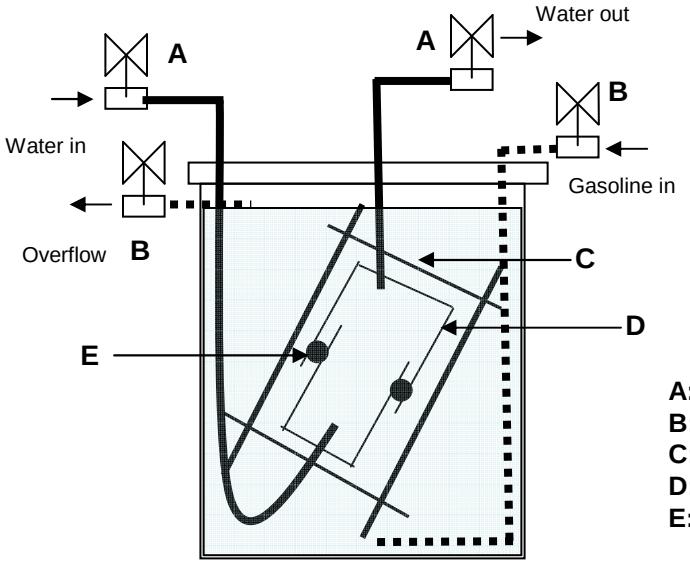

A: Pipe water sampling and replenishing tubing
B: Drum solution replenishing tubing
C: Steel restraining strap
D: Ductile iron pipe joint
E: Gasket

Figure 2 Pipe-drum apparatus used for permeation experiments

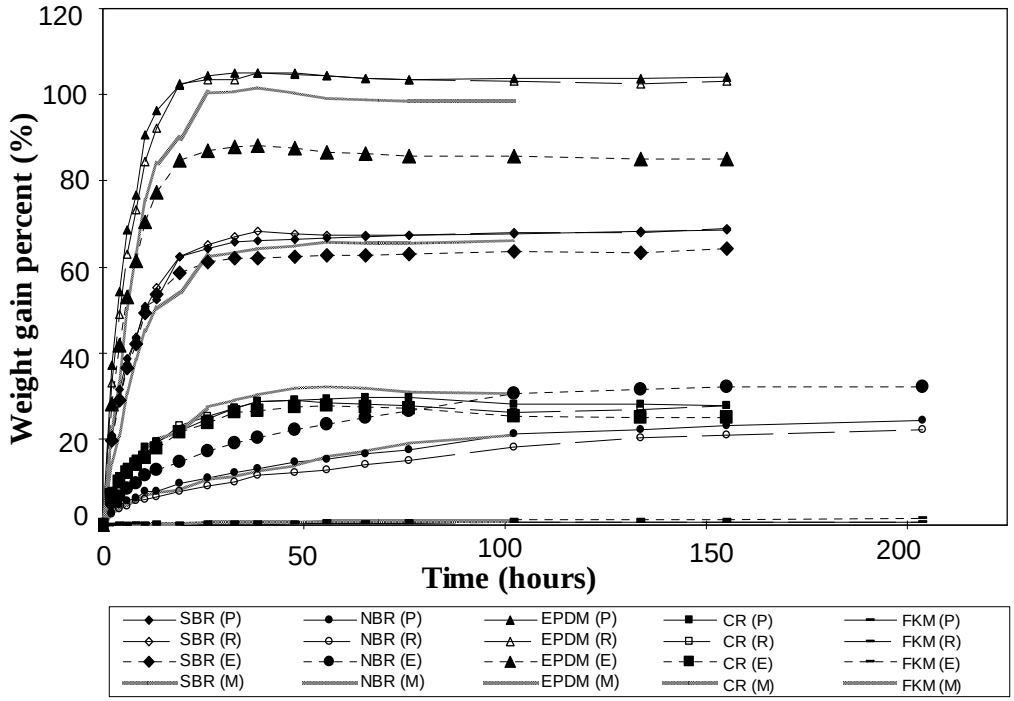

Figure 3 Equilibrium sorption tests for 5 different gasket materials in 4 contaminants (P: premium gasoline, R: regular gasoline, E: 10% ethanol gasoline (E10) and M: premium+10% MTBE)

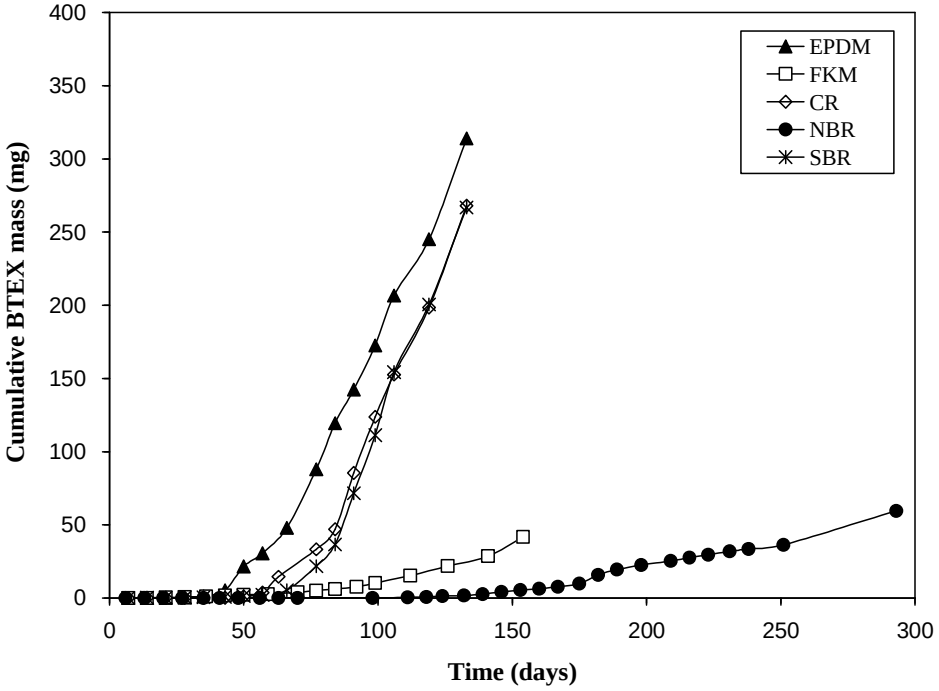

Figure 4 BTEX permeation through five types of gaskets exposed to premium gasoline

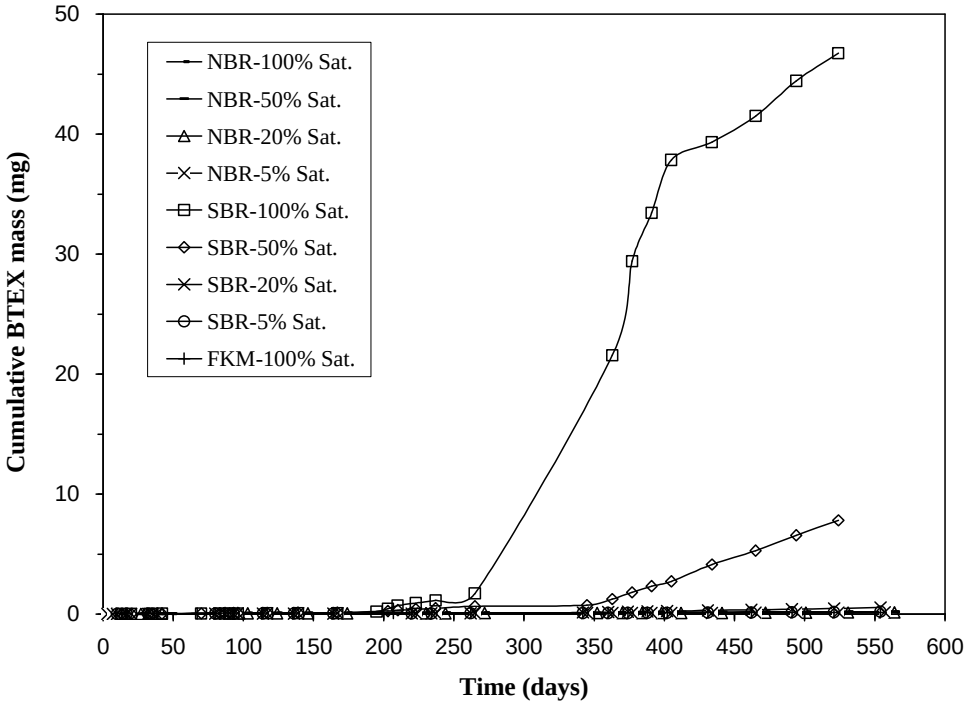

Figure 5 BTEX permeation through SBR, NBR and FKM gaskets exposed to aqueous gasoline solutions of 100%, 50%, 20% and 5% saturation.

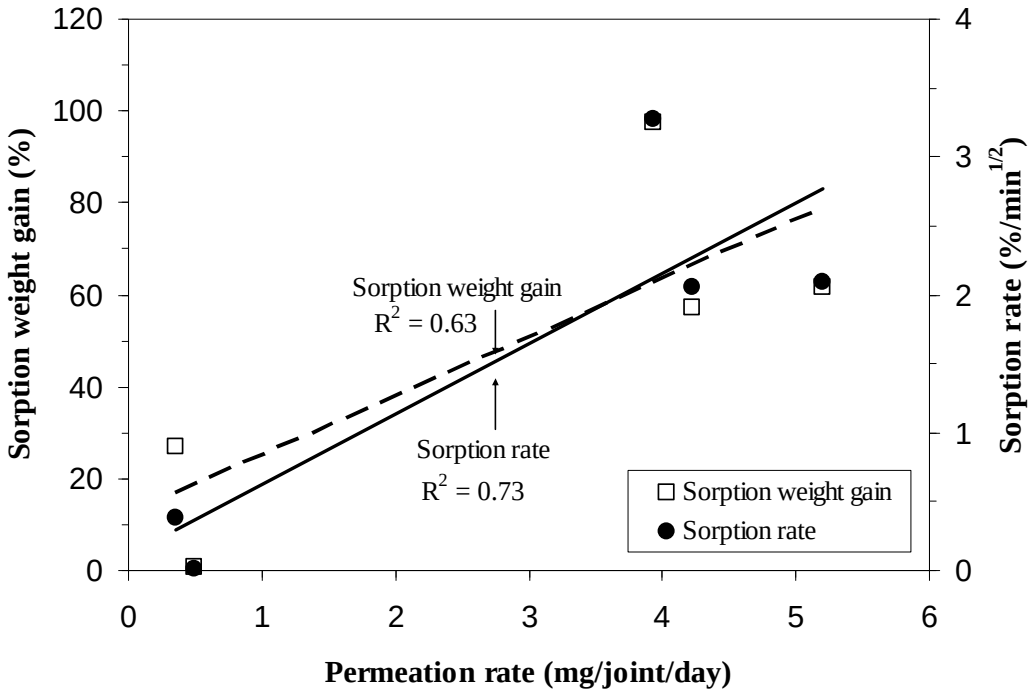

Figure 6 Correlation of permeation rate with percent weight gain (W%) and sorption rate

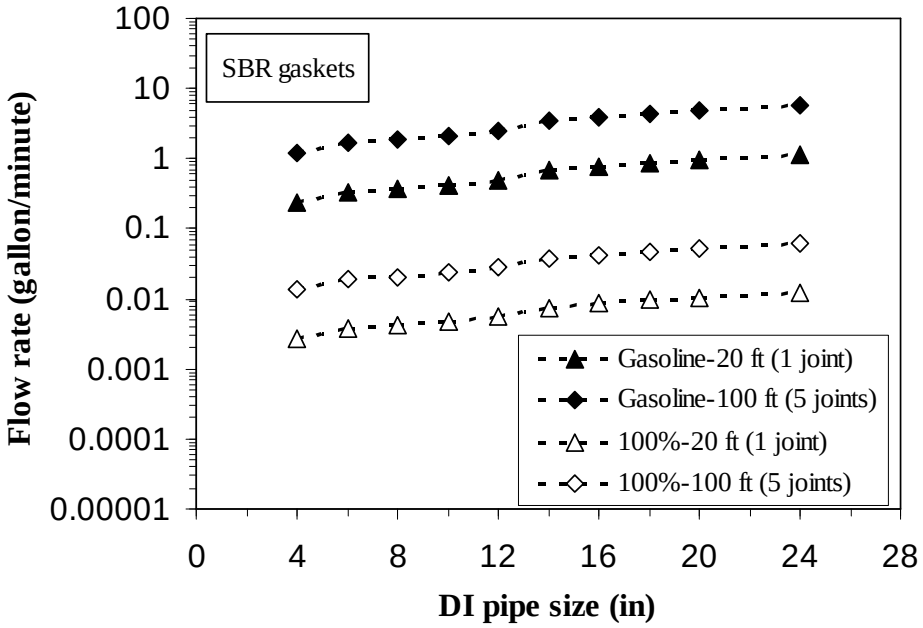

Figure 7 Flow rates needed to obtain MCL concentration of benzene of 5 µg/L for 20 ft and 100 ft of 4-inch to 24-inch DI pipes with SBR Tyton® gaskets.

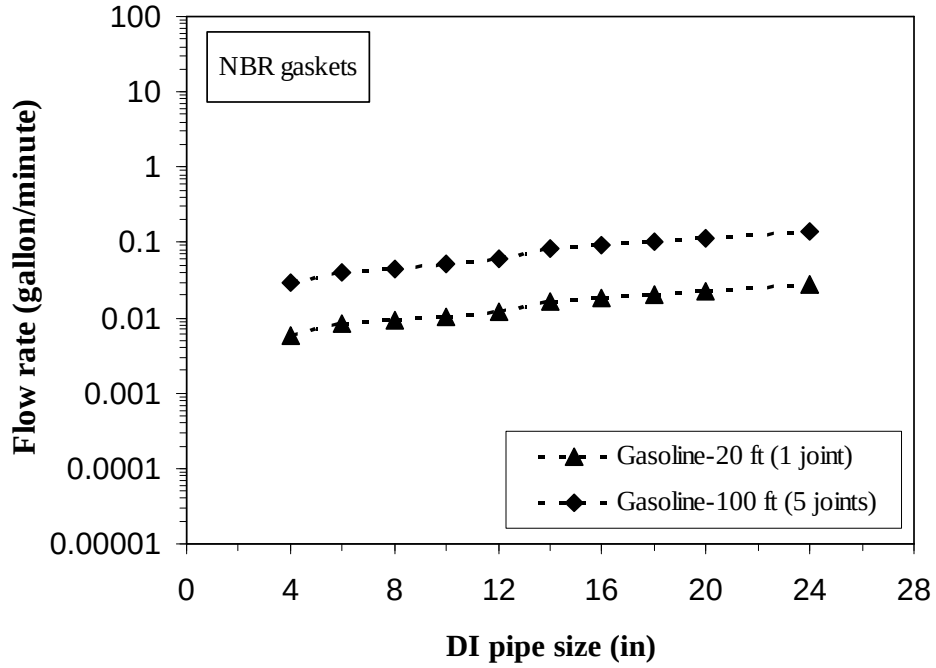

Figure 8 Flow rates needed to obtain MCL concentration of benzene of 5 µg/L for 20 ft and 100 ft of 4-inch to 24-inch DI pipes with NBR Tyton® gaskets.

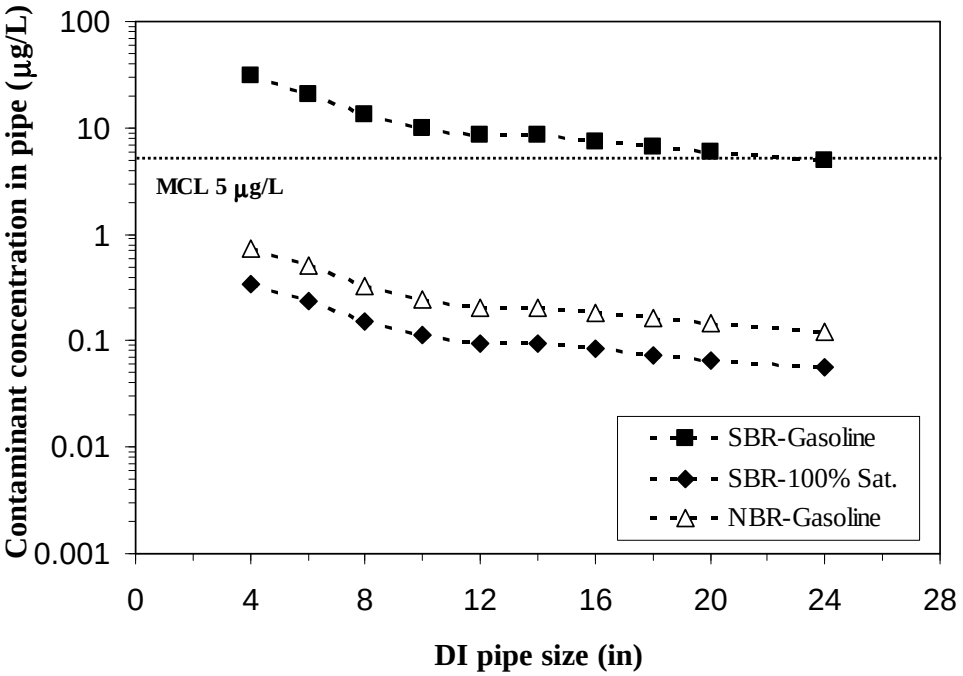

Figure 9 Benzene concentrations after 8 hours of stagnation in various sizes of DI pipes with SBR and NBR Tyton® gaskets (100 ft of pipe with 5 joints) [Note: Concentrations for SBR-gasoline were calculated using a permeation rate equal to the mean obtained from 8 experiments plus 3 standard deviations (99.7% confidence).]

CHAPTER 4. THICKNESS EFFECTS ON GASOLINE HYDROCARBON PERMEATIONS THROUGH GASKET MATERIALS: EXPERIMENTS AND NUMERICAL MODELING

CHU-LIN CHENG, SAY KEE ONG, JAMES A. GAUNT

A paper to be submitted to the Journal of American Water Works Association

4.1 Abstract

A cost-effective experimental device was developed to investigate the impact of material type and material thickness on the permeation of benzene, toluene, ethyl benzene, and xylenes (BTEX) in gasoline through ductile iron (DI) pipe gaskets. Experiments were conducted for styrene-butadiene rubber (SBR), acrylonitrile butadiene rubber (NBR), fluoroelastomer rubber (FKM) prepared from 4-inch DI pipe gaskets. Diffusion coefficients were inversely estimated from the experimental data by using the MULTIPHYSICS software for a diffusion model.

The estimated diffusion coefficients of BTEX compounds for SBR and NBR gasket materials were in the range of 10^{-7} cm^2/s and 10^{-8} cm^2/s, respectively. Experimental results for FKM material indicated that FKM material was considered impermeable to BTEX. Estimated diffusion coefficients using experimental data from diffusion cell experiments were in good agreement with those obtained from gravimetric sorption experiments using intact gaskets.

Diffusion coefficients for benzene and toluene through various thicknesses and different portions of SBR gaskets were estimated and compared with the estimations using the traditional time-lag method. The results of model simulations showed that steady-state

permeation rates had a linear correlation with polymer thickness, while no correlation was found between material thickness and diffusion coefficients for material thicknesses ranging from 2 mm to 5 mm.

Key words: Diffusion cell, permeation, gaskets, BTEX, ductile iron pipe, modeling

4.2. Introduction

Ductile iron pipes are widely used as drinking water mains for drinking water distribution system. The most popular and easy-to-assemble joint and fitting for DI pipe is the push-on joint where polymeric gasket is placed in a groove inside the socket of the bell end of a pipe (Figure 1) and the spigot end of another pipe is pushed into the bell end of the first pipe, compressing the gasket and forming a pressure-tight seal. The most popular gasket type used for DI pipe with diameters ranging from 3 to 24 inches without use of other accessories or tools for assembly is the Tyton® gasket (Figure 1). Styrene-butadiene rubber (SBR) is the most commonly used synthetic material (more than 90%) due to its low cost (Ong et al., 2008). Nitrile (NBR), ethylene propylene diene monomer (EPDM), neoprene (CR), and fluoroelastomer rubber (FKM) are other materials available and are used for specific environmental applications. For example, NBR and FKM gaskets are recommended by the water industry for use in contaminated soils since the materials have good resistance to organic chemicals permeation (DIPRA, 2006).

Chemical permeation through polymeric gaskets involves sorption onto the outer surface of the gasket in contact with the contamination, followed by diffusion within the gasket, and desorption from inner surface of the gasket into the water in the pipe (Holsen et

al., 1991a; Duncan et al., 2005; Rowe, 2005). Of interest in many chemical permeation studies are the impact of material type, thickness and geometrics on chemical breakthrough time, permeation rate and diffusion coefficient of the chemical. Berardinelli and Hall (1985) studied the permeation of latex neoprene gloves by acetone and reported that the breakthrough times were directly proportional to the square of the material thickness, and that the steady-state permeation rates, or steady-state concentrations of diffusants were inversely proportional to material thickness. Jencen and Hardy (1988), examining the permeation of toluene and 1,1,1-trichloroethane through different thicknesses of neoprene gloves and acetone through natural rubber gloves, found that the square root of the breakthrough times were linearly related to the thickness of the gloves while the steady-state permeation rates were inversely proportional to material thickness. Schwope et al. (1988) used the open-loop and closed-loop mode of American Society for Testing and Materials (ASTM) Method F739 to test the permeation of protective cloth and found that the breakthrough times were not proportional to the square of the material thickness. Work done by Vahdat (1987) on the permeation of toluene through butyl nomex, neoprene, polyvinyl alcohol (PVA) and butyl gloves showed that the permeation rates were dependent on the challenge concentration, thickness of material and the area exposed, but the estimated diffusion coefficients were independent of these factors. A study by Park et al. (1991) on the permeation of mixtures of organic chemicals through polybutylene, low-density polyethylene (LDPE) pipes and SBR gaskets showed that the estimated diffusion coefficients for the polymeric materials decreased exponentially as the thickness of the polymer material increased. In other studies, Park et al. (1996a; 1996b) reported that the diffusion coefficients of methylene chloride,

toluene, trichloroethylene (TCE), and m-xylene decreased exponentially with material thickness for the permeation of mixtures of these chemicals at concentrations of 10-100 mg/L through high-density polyethylene (HDPE), very low-density polyethylene (VLDPE), and polyvinyl chloride (PVC) geomembranes. A study by Tseng et al. (2000), using positron annihilation lifetime spectroscopy to measure dye-probe diffusion coefficients in thin films of monodisperse polystyrene, found that the diffusion coefficients decreased exponentially with film thicknesses at temperature below 150 $^{\circ}$C but diffusion coefficients increased when the film thickness at about 350 nm. Soles et al. (2003) examined permeation of water vapor through polytert-butoxycarboxystyrene (PBOCSt) by using incoherent neutron scattering measurements and found that the diffusion coefficients increased exponentially as film thicknesses increased. Vogt et al. (2004) investigated moisture diffusion through poly(4-ammonium styrenesulfonic acid) films using Fickian and two-stage absorption models and found that water diffusion coefficients into the films increased exponentially as a function of initial film thickness. Studies on the influences of thickness on the diffusion coefficients of a polymeric material exposed to organic chemicals are limited with data showing both linear and exponential correlations, while a study showed no correlation.

The objectives of the study are to investigate the permeation of benzene, toluene, ethylbenzene, and xylenes (BTEX) in gasoline through gasket materials of DI pipe under controlled conditions using a simple and cost-effective diffusion cell and to study the influence of polymeric materials and material thickness on the permeation of organic compounds.

4.3 Materials and Methods

4.3.1 Sorption experiments

Tyton® gaskets made of SBR, NBR, EPDM, CR, and FKM (Griffin Pipe Products Co., Council Bluffs, IA) were tested in this study. A typical gasket consists of a hard "heel" and a soft "bulb" portion as shown in Figure 2. The heel and bulb are made of the same polymer but the heel is typically compounded with extra carbon black to make it harder (Bird, 2006). To the author's knowledge, no research has reported chemical permeations through the bulb or heel portion of a gasket.

Gasket specimens from both heel and bulb portion were carefully cut from a 4-inch gasket using a razor blade. Each specimen had a thickness of 1 cm (0.4 inch) and a surface area of approximately 3.2 cm^2 (0.5 $inch^2$). The specimens were immersed in free product gasoline in 120 mL Teflon®-lined, screw-capped jars and periodically taken out and their weight gains measured using an electronic balance (Mettler Toledo AG204, Columbus, OH) with an accuracy of 0.001 gram. Before weighing, the samples were wiped dry with paper towels to remove free product gasoline that may be present on the sample surface.

The times needed for the mass sorbed to be equal to the maximum sorbed were estimated from the plots of percent weight gain versus time of the sorption test and the times were used to estimate the diffusion coefficients using the "half-time method" (Crank, 1975; Neogi, 1996). The half-time approach describes the mass uptake of organic chemicals by a polymer sheet with the assumptions of constant diffusion coefficient and no swelling of the polymer sheet. The equation is given by:

$$\frac{M_t}{M_\infty} = 1 - \frac{8}{\pi^2}\sum_{m=0}^{\infty}\frac{1}{(2m+1)}\exp\left\{\frac{-D(2m+1)^2\pi^2 t}{\ell^2}\right\} \quad [1]$$

where M_t is the total amount of contaminant absorbed by the sheet at time t (sec), M_∞ the equilibrium mass absorbed theoretically after infinite time (sec), D is diffusion coefficient (cm^2/s), m is an exponent, and ℓ is the material thickness (cm). The equation assumes that the concentration at each surface immediately attains a value corresponding to the equilibrium uptake when the sheet is placed in the contaminant and remains constant afterwards. The value of $\frac{t}{\ell^2}$ when $\frac{M_t}{M_\infty}$=1/2 with $t = T_{1/2}$, is given by:

$$\left(\frac{T_{1/2}}{\ell^2}\right) = -\frac{1}{\pi^2 D}\ln\left\{\frac{\pi^2}{16} - \frac{1}{9}\left(\frac{\pi^2}{16}\right)^9\right\} \quad [2]$$

The above equation can be further reduced with the error of about 0.001% as:

$$D_{T_{1/2}} = 0.049\frac{\ell^2}{T_{1/2}} \quad [3]$$

where $D_{T_{1/2}}$ is the diffusion coefficient (cm^2/s) for the time $T_{1/2}$ when the mass absorbed is equal to half of the infinite equilibrium mass absorbed.

4.3.2 Diffusion experiment

To analyze chemical permeation through gasket materials, a diffusion cell based on the ASTM F739 method of a closed-loop system was developed as shown in Figure 3. The diffusion cell consisted of two 40 mL glass vials (I-CHEM, Rockwood, TN) representing the collection chamber and the challenge chamber. A 2-inch outer diameter (OD) steel flat washers was attached to each vial (Figure 3a), followed by attching a 1-inch OD steel flat

washer to the 2-inch OD washers with epoxy resin as shown in Figure 3. The gasket specimen was placed between the two vials and the vials were held together with three 0.48 cm (3/16 inch) hex head cap screws through three 0.51 cm (0.2 inch) holes on the washers (Figure 3b). Each gasket specimen was cut into shape of square pieces with dimensions of 15 mm × 15 mm × 3.8 mm (0.6 inch × 0.6 inch × 0.15 inch). The space between the two 2-inch washers was then filled with epoxy resin (Figure 4c and 4d). This was to minimize possible chemical permeation through the sides of the gasket specimen. Preliminary sorption experiments using epoxy resin samples were conducted by immersing the resin samples in free product premium gasoline and the weight gains were less 0.1 % after 44 days (1053 hrs) indicating that interaction between the resin and gasoline was very limited. The collecting chamber was filled with distilled water while the challenge chamber was filled with gasoline or gasoline-saturated aqueous solution. Glass beads were added in the collection chamber to assist mixing of the solution. Before sampling, the diffusion cell was gently agitated back and forth to assure that the solution within the collection chamber was well mixed.

For diffusion cell experiments, only SBR, NBR and FKM gasket specimens were used. EPDM and CR were found to be quite susceptible to the permeation of BTEX when exposed to premium gasoline (Ong et al. 2008) and were not used in diffusion cell tests.

The permeation behavior of the bulb and heel portions was studied using specimens of 2 mm thickness from the SBR gaskets. The impact of thickness on permeation was studied using specimens with thicknesses of approximately 2 mm, 3 mm, 4 mm, and 5 mm from the bulb portion of SBR gaskets.

A total of seven diffusion cells with different thicknesses of the bulb and heel portions of SBR gasket and one with bulb portion of NBR gasket were set up and were exposed to free product premium gasoline. Two diffusion cells each with 2.53 mm thick SBR and 2.33 mm thick NBR bulbs were prepared with 100% gasoline saturated solutions.

Since the FKM material is nearly impermeable to petroleum-based organic chemicals, an experiment using a 2.69 mm thick bulb portion of the FKM gasket in contact with free product gasoline was prepared to provide information to assess that diffusion cell through FKM material and verify that diffusion cell was indeed setup properly and there were no leakages.

The data from the diffusion cell were summarized as cumulative mass permeated with time and the diffusion coefficients were estimated based on the "time-lag method" (Crank, 1975). The time-lag method is an estimation technique derived from Fick's diffusion equation. The total mass of chemical diffusing through a plane sheet, Q_t (μg), assuming the: concentration of chemicals on the challenge chamber side remained constant (C); the initial concentration of the chemicals in the polymer was zero; the concentration of the chemicals on the collection chamber side was zero, is given by:

$$\frac{Q_t}{\ell C} = \frac{Dt}{\ell^2} - \frac{1}{6} - \frac{2}{\pi^2}\sum_{1}^{\infty}\frac{(-1)^n}{n^2}\exp\left(\frac{-Dn^2\pi^2 t}{\ell^2}\right) \qquad [4]$$

where C is concentration (μg/L), D is the diffusion coefficient (cm^2/s) calculated by time-lag method; and ℓ is the thickness of material (cm). As t (sec) approaches infinity, then

$$Q_t = \frac{DC}{\ell}\left(t - \frac{\ell^2}{6D}\right) \qquad [5]$$

Equation [5] has an intercept T_L on the t axis defined as the lag time and is given by:

$$T_L = \frac{\ell^2}{6D} \text{ or } D = \frac{\ell^2}{6T_L} \quad [6]$$

4.3.3 Chemical analysis

Water samples from the collection chamber were analyzed for BTEX using a gas chromatograph (Tractor 540, Austin, TX) equipped with a packed column (6 ft × 2 mm; 1% SP1000 on 60/80 mesh Carbopack B), a photoionization detector, and an automated purge & trap concentrator (Tekmar LSC2/ALS). The detection limits for the gas chromatography method for benzene, toluene, ethylbenzene, m-xylene and o+p-xylene were 0.24 μg/L, 0.24 μg/L, 0.26 μg/L, 0.29 μg/L, and 0.53 μg/L, respectively.

4.3.4 Numerical simulations

MULTIPHYSICS 3.2 (previous FEMLAB, COMSOL, Stockholm, Sweden) was employed to simulate the permeation process of organic compounds through polymeric gasket materials. The module employed in MULTIPHYSICS 3.2 was the "Transient Analysis of Diffusion" program under the Mass Balance of Chemical Engineering module. The diffusion process can be described by the classic Fickian diffusion equation:

$$\frac{\partial C}{\partial t} + \nabla(-D_e \nabla C) = 0 \quad [7]$$

where D_e is the diffusion coefficient of contaminants in the polymeric material. The gasket specimens were modeled as shown in Figure 5 with the various dimensions and boundaries.

Each polymeric specimen (bulb and heel portion of a gasket) was assumed to be homogeneous, its diffusion coefficient assumed isotropic within the particular material and

the polymeric materials assumed to have no reaction with the experimental solvents. Any possible impact of uneven surface of the gasket samples and small gaps between specimens and the stainless washers of diffusion cell apparatus were neglected.

The extra polymer material, about 0.5 mm, that was not in contact with attacking solvents and distilled water (opening window on each side of the chambers) was also examined for its impact on the overall result. It was found that the influence of the extra polymer volume on BTEX permeation was very low (less than 0.0001%) based on model simulations.

The initial and boundary conditions for the diffusion cell specimen are as follow (Figure 5):

Initial condition $t < 0$, $C = 0$; throughout specimen

Boundary conditions $t \geq 0$, $C = C_0$; at the attacking side

$t \geq 0$, $C = 0$; at the collecting side

$t \geq 0$, $\nabla C = 0$; at the edge of the specimen

The concentrations, C_0, on the challenge side was calculated based on the equilibrium soption experiments where it was assumed that the specimen was saturated instantaneously with attacking chemicals.

Numerical simulations for permeation of BTEX were conducted for: (i) exposure of SBR bulb and heel portion to premium gasoline for four thicknesses of approximately 2 mm, 3 mm, 4 mm, and 5 mm, (ii) exposure of NBR bulb portion for thickness of 2 mm to premium gasoline, and (iii) exposure of SBR and NBR bulb portions to saturated gasoline aqueous solution for a thickness of approximately 2 mm. Simulations were conducted by

using Equation [7] with an initial diffusion coefficient based on the time-lag method followed by adjusting the diffusion coefficient to provide the "best fit" by minimizing the root mean squared errors (RMSE). In addition, simulations were conducted with $C = C_{avg}$ for the collecting side of the diffusion cell. C_{avg} is the average of the zero concentration in the freshly added water and the concentration when the water was sampled.

4.4 Results and Discussion

4.4.1 Sorption experiment

The order of percent weight gain for the five gasket materials when exposed to free product gasoline from high to low was EPDM, SBR, CR, NBR, and FKM (see Table 1 and Figure 6). The mass of free product gasoline absorbed by EPDM was approximately 127% of its own weight, while FKM showed the lowest increase, with less than 1% increase in its weight indicating that EPDM and SBR gaskets were susceptible to BTEX permeation when in contact with gasoline spills or contaminated soils.

Table 1 shows that for all five gasket materials except for CR, the bulb portion of a gasket sorbed more than heel portion. The mass absorbed by the bulb portion of SBR was about 30% higher than the mass sorbed by the heel portion while the mass absorbed by the bulb portion of NBR gasket was about 10% higher than the mass absorbed by the heel portion. The sorption results suggested that the bulb portion of the SBR gasket may be more susceptible to gasoline permeation than the heel portion, while the bulb and heel portion of a NBR gasket may have similar permeation behavior to gasoline. Estimated diffusion coefficients of gasoline using the half-time method for the sorption experiments were

3.20×10^{-7} cm^2/s and 3.81×10^{-7} cm^2/s for bulb and heel portions of SBR, and 1.62×10^{-7} cm^2/s and 1.35×10^{-7} cm^2/s for the bulb and heel portions of NBR, respectively. The slight difference in diffusion coefficients between bulb and heel for the SBR gasket were not as expected since the percent weight gain was 30% more for the bulb portion. The sorption test is relatively simple providing the total mass of chemicals absorbed but it does not yield information on the breakthrough time of the contaminant. Moreover, the sorption of chemical by the gaskets is complicated by factors such as the geometry of polymer materials, swelling of the polymer materials, and heat effects due to solvent absorption. Nevertheless, the results from sorption tests can be used to provide preliminary information on chemical permeation before more intensive tests such as diffusion cell methods are used.

4.4.2 Diffusion cell experiments

A typical plot for the cumulative mass permeated versus time for total BTEX and individual compounds is shown in Figure 7. In addition, Figure 8 compares benzene permeation for different materials and thicknesses for 100% aqueous solutions. Using the "time-lag" method for a given thickness of the specimen, the estimated permeation rates are presented in Table 2. The diffusion coefficients for BTEX for various thicknesses for premium gasoline were found to range from 4.57×10^{-7} cm^2/s to 5.27×10^{-8} cm^2/s. Benzene and toluene were the more permeated compounds in terms of both concentration and time. Benzene was the first compound to be detected in the collecting chamber while the cumulative mass of toluene permeated with time was the highest due to its abundance in

gasoline. In general, the permeated masses of benzene and toluene were approximately twenty-five times more than ethylbenzene and four times more than xylenes.

The estimated total BTEX diffusion coefficient for SBR-Bulb was 4.57×10^{-7} cm^2/s based on the time-lag method, while the diffusion coefficients for benzene, toluene, ethylbenzene, and xylenes were 5.24×10^{-7} cm^2/s, 3.75×10^{-7} cm^2/s, 4.14×10^{-7} cm^2/s, and 3.69×10^{-7} cm^2/s, respectively. The bulb portion of a SBR gasket in contact with 100% gasoline aqueous solution gave a time lag of about 255 hours (Figure 8 or Table 2). With a thickness of 2.53 mm, the BTEX diffusion coefficient was 1.16×10^{-8} cm^2/s. The permeation rate was estimated to be 0.0031 mg/hr, which is about 10 times less than the permeation rate of 0.028 mg/hr in contact with free product premium gasoline. Furthermore, the diffusion coefficients of BTEX through SBR-Bulb and SBR-Heel materials exposed to free product premium gasoline were within the same order of magnitude with a value of 10^{-7} cm^2/s, but were one order of magnitude smaller for SBR-Bulb exposed to 100% gasoline aqueous solution.

The time lag for the NBR-Bulb in contact with premium gasoline was about 63.6 hours (2.65 days). With a thickness of 2.69 mm, the estimated diffusion coefficient for total BTEX was 5.27×10^{-8} cm^2/s and the permeation rate was 0.0151 mg/hr. The NBR-Bulb exposed to 100% gasoline aqueous solution gave a time lag of 436 hours (18 days) with an estimated BTEX diffusion coefficient of 5.8×10^{-9} cm^2/s for a specimen thickness of 2.33 mm.

No permeation was found for the FKM-Bulb specimen of 2.92 mm thickness after more than 1085 hours (45.2 days) exposure to free product premium gasoline (Figure 8).

Within the testing period and for a thickness of 3 mm, results showed that FKM was resistant to BTEX permeation.

4.4.3 Estimation of diffusion coefficients using numerical models

Figure 9 to Figure 11 show representative curve fitting of the experimental data using the numerical model by minimizing the RMSE (assuming $C = 0$, at the collecting side). Figure 9 and Figure 10 show the curve fit for SBR bulb and heel materials for various thicknesses for free product gasoline while Figure 11 provide results contrasting NBR and SBR bulb materials with 100% gasoline-saturated solution.

As shown in Figure 9, the model was able to curve fit the experimental data by adjusting the diffusion coefficients except for a thickness of 2 mm. The predicted curves captured the main trend of the experimental data, showing the breakthrough of the chemicals followed by a transient state to steady-state permeation of chemicals. A possible reason for the over prediction of the model for 2 mm thick of heel portion and 3 mm thick of the bulb portion of SBR gasket is that the collecting side of the chamber may not be at "zero" concentration, which was the assumed boundary condition for the model. And therefore, this would mean that mass permeated in the experiment would be lower than if the concentration in the collection chamber was truly at zero concentration (as shown in Figure 9a and 10a). To minimize this condition, the water in the collecting side should be changed more frequently. This simulation was investigated by curve fitting the experimental data by using $C = C_{avg}$ at the collecting side.

The estimated diffusion coefficients for BTEX and individual compounds through the bulb and heel portions of SBR and NBR materials using numerical modeling for both $C = 0$ and $C = C_{avg}$ for the collecting side are at the same magnitude. As observed before for the time-lag method, diffusion coefficients of same material exposed to premium gasoline were about 10 times larger than that of 100% gasoline aqueous solution (see Table 3). The estimated diffusion coefficients using model simulations were generally smaller than the values estimated using time-lag methods (see Table 3, Figure 12, Figure 13). Using $C = C_{avg}$ in models simulating SBR Heel 2 mm and Bulb 3 mm, the curve fittings improved slightly from that of using $C = 0$. For other thicknesses, permeation curve fittings using both concentrations at the collecting side were identical.

4.4.4 Effect of thickness and permeation parameters

Presented in Figure 14 is the plot of benzene permeation rates and the thickness of the specimens. As shown in Figure 14, benzene diffusion coefficients were poorly correlated with the thickness of the specimens implying that thickness has limited impact on diffusion coefficients. Although the work was conducted for a limited range of thicknesses (from approximately 2 mm to 5 mm), the results were similar to that of Vahdat (1987) but were different from other researchers (Berardinelli and Hall, 1985; Park, 1991; Park et al. 1996a; 1996b; Shishatskii et al., 1996; Papiernik et al., 2001), where diffusion coefficients were found to vary with thicknesses. Steady-state permeation rates were found to linearly correlate with the thickness of the specimens. These results were similar to that found by others (Vahdat, 1987; Jencen and Hardy, 1988).

4.5 Conclusion

A simple diffusion cell device was successfully used in obtaining experimental data for the estimation of permeation parameters such as diffusion coefficients and permeated masses. The diffusion cell provided sufficient data within a short period of time as compared to use of actual pipe joints. An advantage of the diffusion cell is that the environment is well-controlled by reducing the various uncertainties. Another advantage is that it is time efficient while investigations in permeation of BTEX compounds through an intact gasket carried in pipe-drum apparatus take months.

Diffusion coefficients estimated by numerical cure fitting with $C = 0$ and $C = C_{avg}$ at the collecting side were found to be at the same order of magnitude as the coefficients estimated by time-lag method. Steady-state permeation rates were found to inversely correlate exponentially with polymer thickness. Diffusion coefficients were found to be unaffected by the polymer thickness from 2 mm to 5 mm.

4.6 Reference

Ash, R. 2001. A note on permeation with boundary-layer resistance. *Journal Membrane Science*, 186(1): 63-69.

Berardinelli, S.P. and R. Hall. 1985. Site-specific whole glove chemical permeation. *Journal American Industrial Hygiene Association*, 46(2): 60-64.

Berardinelli, S.P. and R. Hall. 1985. Site-specific whole glove chemical permeation. *Journal American Industrial Hygiene Association*, 46(2): 60-64.

Berens, A.R. 1985. Prediction of organic chemical permeation through PVC pipe, *Journal AWWA*, 77(11): 57-64.

Bird, W. 2006. Private Communication. S&B Technical Products. 1300 East Berry St, Fort Worth, TX 76119.

Chao, K.P., J.S. Lai, H.C. Lin, and Y.P. Hsu. 2006. Comparison of permeability determined by permeation cell and immersion methods for organic solvents through protective gloves. *Polymer Testing*, 25 (7): 975-984.

Chao, K.P., P. Wang, and Y.T. Wang. 2007. Diffusion and solubility coefficients determined by permeation and immersion experiments for organic solvents in HDPE geomembrane. *Journal Hazardous Materials*, 142(1-2): 227-235.

Crank, J. 1975. The Mathematics of Diffusion. Clarendon Press. Oxford, UK.

Ductile Iron Pipe Research Association (DIPRA). 2006. DIPRA gaskets data sheet. Birmingham, AL. http://www.dipra.org/pdf/gasketsForDIP.pdf, accessed on 10-20-08.

Duncan, B., J. Urquhart, and S. Roberts. 2005. Review of measurement and modeling of permeation and diffusion in polymers. *Report of National Physical Laboratory*, London, U.K.

Glaza, E.C. and J.K. Park. 1992. Permeation of organic contaminants through gasketed pipe joints. *Journal AWWA*, 84(7): 92-100.

Holsen, T.M., J.K. Park, D. Jenkins, and R.E. Selleck. 1991. Contamination of potable water by permeation of plastic pipe. *Journal AWWA*, 83(8): 53-56.

Jencen, D.A. and J.K. Hardy. 1988. Method for the evaluation of the permeation characteristics of protective glove materials. *Journal American Industrial Hygiene Association*, 49(6): 293-300.

Lee, C.H. 2003. Time lag and permeation rate in liquid/liquid dialysis. Journal Applied *Polymer Science*, 19 (11): 3087-3091.

Mao, F. 2008. Permeation of hydrocarbons through polyvinyl chloride (PVC) and polyethylene (PE) pipes and pipe gaskets. Doctoral dissertation. Department of Civil, Construction, and Environmental Engineering, Iowa State University. Ames, IA. 269p.

Ong, S.K., J.A. Gaunt, F. Mao, C.L. Cheng, L. Esteve-Agelet, and C.R. Hurburgh. 2008. Impact of petroleum-based hydrocarbons on PE/PVC pipes and pipe gaskets. *Awwa Research Foundation Report No. 91204*. Awwa Research Foundation, Denver, CO.

Park, J.K., L. Bontoux, T.M. Holsen, D. Jenkins, and R. E. Selleck. 1991. Permeation of polybutylene pipe and gasket material by organic chemicals. *Journal AWWA*, 83(10): 71-78.

Park, J.K. and L. Bontoux. 1993. Thermodynamic modeling of the sorption of organic chemicals in thermoplastics and elastomers. *Journal Applied Polymer Science*, 47(5): 771-780.

Park, J.K., J.P. Sakti, and J.A. Hoopes. 1996a. Transport of organic compounds in thermoplastic geomembranes. I: Mathematical model. *Journal Environmental Engineering*, 122(9): 800-806.

Park, J.K., J.P. Sakti, and J.A. Hoopes. 1996b. Transport of aqueous organic compounds in thermoplastic geomembranes. II: Mass flux estimates and practical implications. *Journal Environmental Engineering*, 122(9): 807-813.

Rowe, R.K., 2005. Long-term performance of contaminant barrier systems, 45th rankine lecture. *Geotechnique* 55 (9): 631-678.

Rutherford, S.W. and D.D. Do. 1999. Permeation time lag with multilayer adsorption and surface diffusion. *Chemical Engineering Journal*, (74): 155-160.

Schwope, A.D., R. Goydan, R.C. Reid, and S. Krishnamurthy. 1988. State-of-the-art review of permeation testing and the interpretation of its results. *Journal American Industrial Hygiene Association*, 49(11): 557-565.

Shishatskii, A.M., Y.P. Yampol'skii, and K.-V. Peinemann. 1996. Effects of film thickness on density and gas permeation parameters of glassy polymers. *Journal Membrane Science*, 112(2): 275-285.

Tseng, K.C., N.J. Turro, C.J. Durning. 2000. Molecular mobility in polymer thin films. *Physical Review E*, 61(2): 1800-1811.

Vahdat, N. 1987. Permeation of polymeric materials by toluene. *Journal American Industrial Hygiene Association*, 48(2): 155-159.

Table 1 Percent weight gain of various gasket materials in premium gasoline

Heel + Bulb	Percent weight gain	Half time $T_{1/2}$ (hr)	Estimated diffusion coefficient (cm^2/s)
SBR	80.03 ± 1.35 %	4.97	3.23×10^{-7}
NBR	27.72 ± 0.82 %	15.85	1.43×10^{-7}
EPDM	127.02 ± 1.86 %	5.89	1.20×10^{-6}
FKM	0.65 ± 0.09 %	51.27	6.91×10^{-8}
CR	46.87 ± 1.06 %	5.62	1.15×10^{-6}
Heel only			
SBR	61.11 ± 1.47 %	3.57	3.81×10^{-7}
NBR	26.91 % ± 0.89 %	17.99	1.35×10^{-7}
EPDM	97.34 ± 1.21 %	3.72	1.90×10^{-6}
FKM	0.81 ± 0.11 %	33.38	9.39×10^{-8}
CR	57.13 ± 0.41 %	3.10	1.01×10^{-6}
Bulb only			
SBR	97.31 ± 2.78 %	5.06	3.20×10^{-7}
NBR	29.04 ± 1.48 %	12.42	1.62×10^{-7}
EPDM	141.58 % ± 1.66 %	6.42	1.10×10^{-6}
FKM	0.82 ± 0.11 %	43.62	7.34×10^{-8}
CR	43.84 ± 1.34 %	7.63	4.19×10^{-6}

Table 2 Diffusion coefficients from experimental data and model for bulb and heel portions of a SBR and NBR gasket exposed to premium gasoline

SBR		Time lag approach (cm^2/s)				Numerical curve fitting (cm^2/s)			
Heel 2mm	Compounds	Time lag (hr)	Bulb (—)	Time lag (hr)	Heel (1.93 mm)	Time lag (hr)	Bulb (—)	Time lag (hr)	Heel (1.93 mm)
	BTEX			2.4	7.15×10^{-7}				
	B			1.7	1.03×10^{-7}			3.8	4.20×10^{-7}
	T			1.9	8.94×10^{-7}			3.9	4.00×10^{-7}
	E			3.3	5.16×10^{-7}			5.7	2.85×10^{-7}
	X			3.1	5.59×10^{-7}			3.8	4.20×10^{-7}
Bulb/ Heel 3mm			Bulb (3.11 mm)		Heel (2.55 mm)		Bulb (3.11 mm)		Heel (2.55 mm)
	BTEX	5.6	8.06×10^{-7}	9.3	3.23×10^{-7}				
	B	3.0	1.51×10^{-7}	8.1	3.73×10^{-7}	7.1	6.00×10^{-7}	8.7	3.35×10^{-7}
	T	5.5	8.21×10^{-7}	9.5	3.18×10^{-7}	6.6	6.22×10^{-7}	9.4	3.05×10^{-7}
	E	8.0	5.60×10^{-7}	14	2.15×10^{-7}	8.4	5.06×10^{-7}	17	1.65×10^{-7}
	X	10.4	4.29×10^{-7}	12.9	2.34×10^{-7}	6.1	6.70×10^{-7}	8.6	3.35×10^{-7}
Bulb/ Heel 4mm			Bulb (3.84 mm)		Heel (3.86 mm)		Bulb (3.84 mm)		Heel (3.86 mm)
	BTEX	15	4.57×10^{-7}	9.3	7.43×10^{-7}				
	B	13	5.24×10^{-7}	12.4	5.55×10^{-7}	13	4.98×10^{-7}	15.8	4.15×10^{-7}
	T	18.2	3.75×10^{-7}	12.9	5.35×10^{-7}	14	4.48×10^{-7}	15.8	4.15×10^{-7}
	E	16.5	4.14×10^{-7}	17.9	3.85×10^{-7}	22.1	2.48×10^{-7}	24.2	2.35×10^{-7}
	X	18.5	3.69×10^{-7}	19.6	3.52×10^{-7}	14.7	4.04×10^{-7}	15	4.15×10^{-7}
Bulb/ Heel 5mm			Bulb (5.09 mm)		Heel (4.84 mm)		Bulb (5.09 mm)		Heel (4.84 mm)
	BTEX	14.6	8.19×10^{-7}	21.9	4.95×10^{-7}				
	B	16	7.50×10^{-7}	20.9	5.18×10^{-7}	16.9	5.42×10^{-7}	21.2	4.00×10^{-7}
	T	21.1	5.69×10^{-7}	22.4	4.85×10^{-7}	21.8	5.22×10^{-7}	21.5	3.78×10^{-7}
	E	21.3	5.62×10^{-7}	23.4	4.64×10^{-7}	27.3	3.92×10^{-7}	25	2.55×10^{-7}
	X	26.6	4.51×10^{-7}	23.7	4.58×10^{-7}	19.4	5.92×10^{-7}	20.8	3.98×10^{-7}
NBR		Time lag approach (cm^2/s)				Numerical curve fitting (cm^2/s)			
Bulb 2mm	Compounds	Time lag (hr)	Bulb (2.69 mm)	Time lag (hr)	Heel (—)	Time lag (hr)	Bulb (2.69 mm)	Time lag (hr)	Heel (—)
	BTEX	63.6	5.27×10^{-8}						
	B	63	5.32×10^{-8}			68.9	3.68×10^{-8}		
	T	68.3	4.91×10^{-8}			81	2.95×10^{-8}		
	E	68.3	4.90×10^{-8}			96	1.90×10^{-8}		
	X	67.9	4.94×10^{-8}			84.4	2.48×10^{-8}		

B-benzene, T-toluene, E-ethylbenzene, X-xylenes

Table 3 Diffusion coefficients from experimental data and model for bulb portions of a SBR and NBR gasket exposed to 100% gasoline saturated aqueous solution

SBR		Time lag approach (cm^2/s)		Numerical curve fitting (cm^2/s)	
Bulb 2mm	Compounds	Time lag (hr)	Bulb (2.53 mm)	Time lag (hr)	Bulb (2.53 mm)
	BTEX	254.6	1.16×10^{-8}		
	B	175	1.69×10^{-8}	264.1	8.67×10^{-9}
	T	370	8.01×10^{-8}	245.7	8.98×10^{-9}
	E	241.3	1.23×10^{-8}	328.6	5.75×10^{-9}
	X	277.4	1.07×10^{-8}	286.8	7.67×10^{-9}
NBR		Time lag approach (cm^2/s)		Numerical curve fitting (cm^2/s)	
Bulb 2mm	Compounds	Time lag (hr)	Bulb (2.33 mm)	Time lag (hr)	Bulb (2.33 mm)
	BTEX	435.5	5.77×10^{-9}		
	B	423	5.94×10^{-9}	469.8	3.91×10^{-9}
	T	437.2	5.75×10^{-9}	462.2	3.66×10^{-9}
	E	429.5	5.85×10^{-9}	510.3	3.05×10^{-9}
	X	485	5.18×10^{-9}	530.4	2.75×10^{-9}

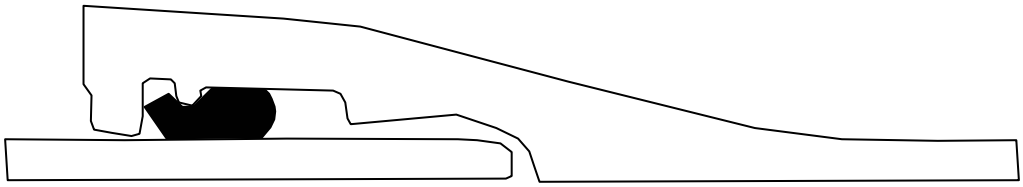

Figure 1 Cross-section view of a push-on joint of DI pipe with a Tyton® gasket (adapted from Griffin Pipe Products Co., Council Bluffs, IA)

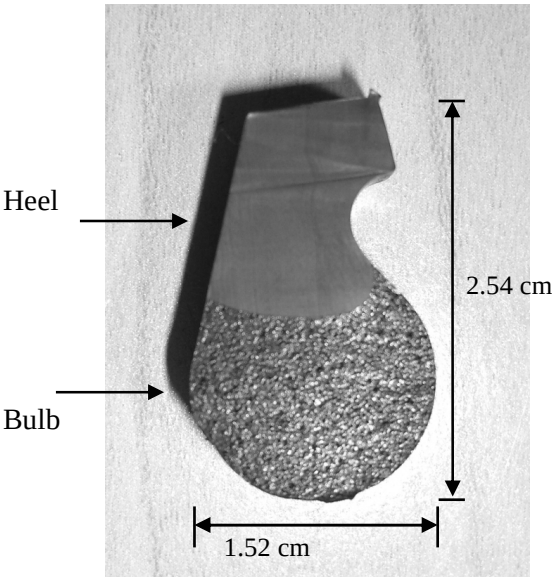

Figure 2 Cross-section view of a 10 cm (4-inch) SBR gasket showing heel and bulb portion and various dimensions

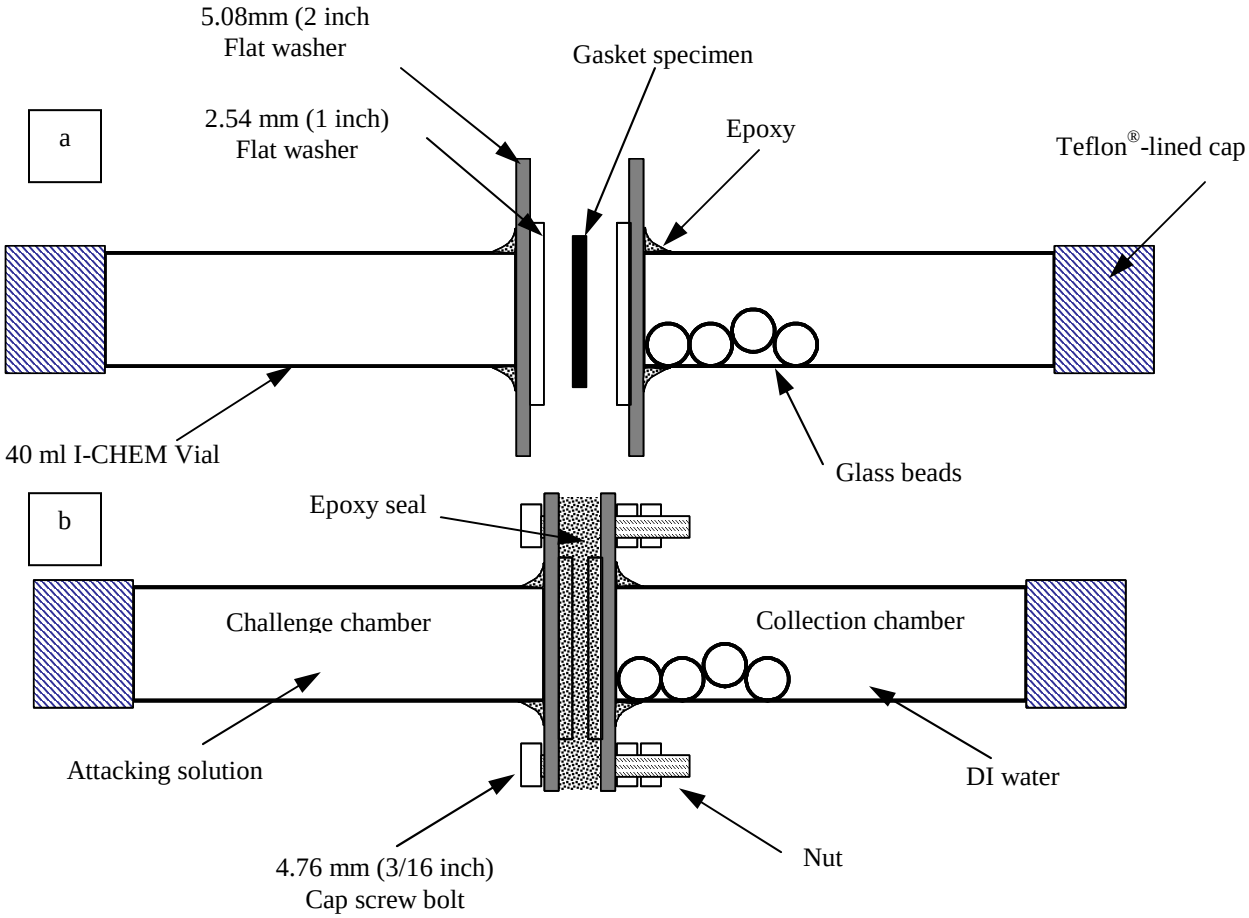

Figure 3 Schematic layout of a diffusion cell device.

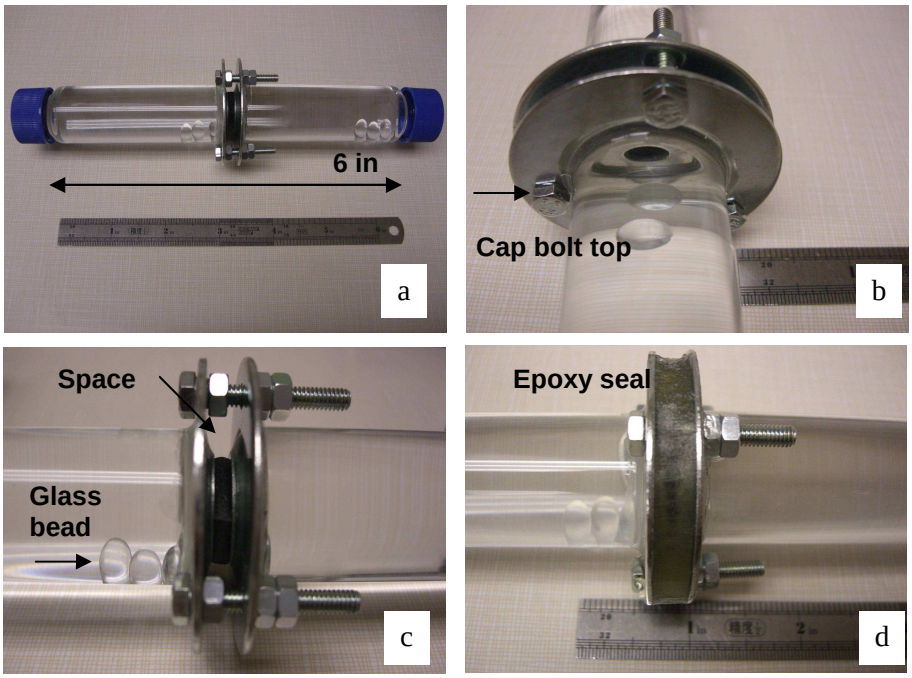

Figure 4 Diffusion cell before and after sealing the gasket specimen: (a) full view of a diffusion cell; (b) view showing blot; (c) view showing space between washers; (d) view of space washers filled with epoxy seal

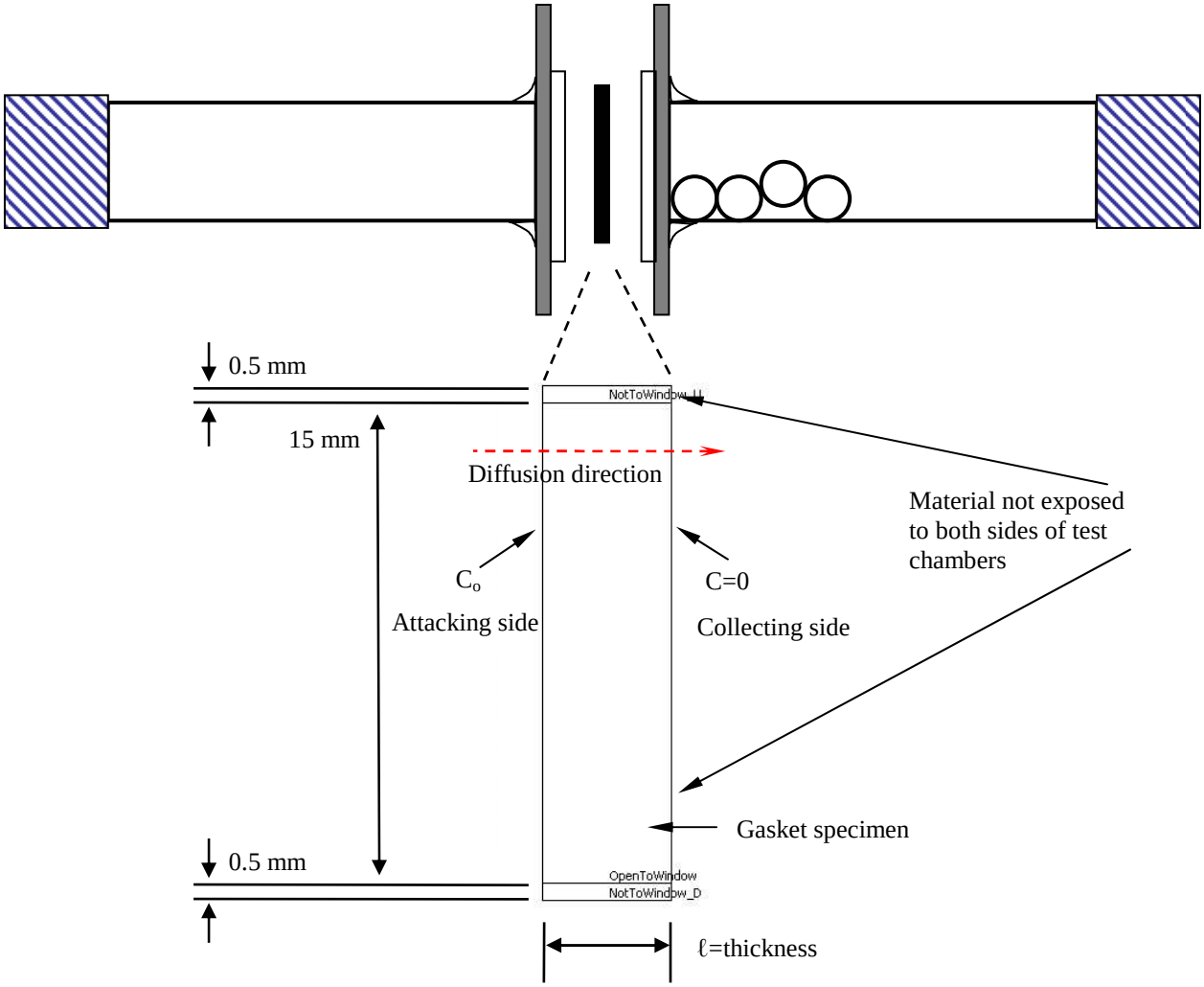

Figure 5 Boundary conditions for gasket specimen setup for MULTIPHYSICS simulation of experimental data

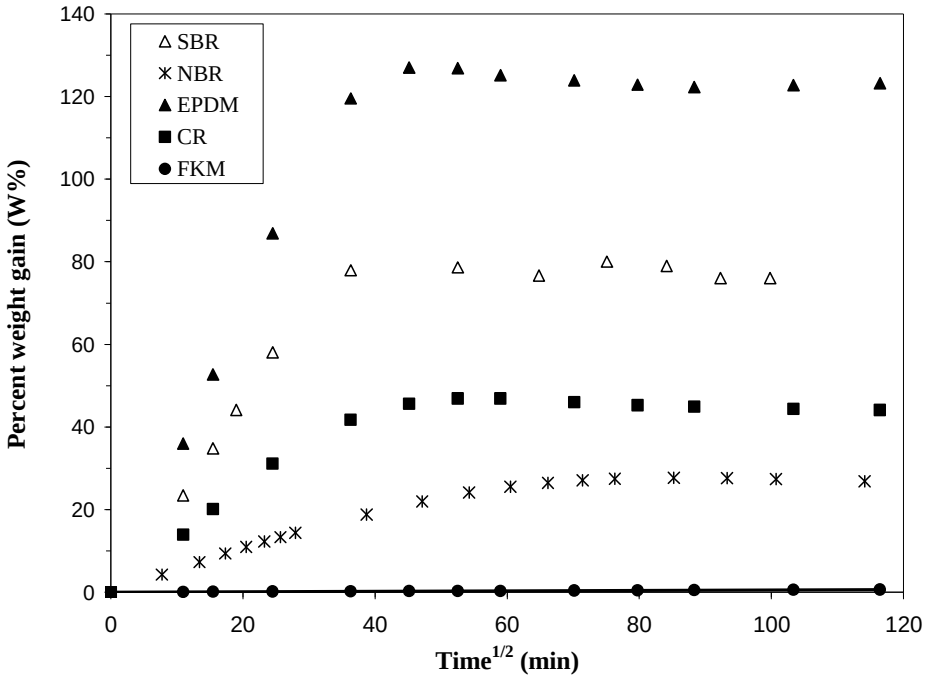

Figure 6 Sorption uptake of premium gasoline by five types of gaskets

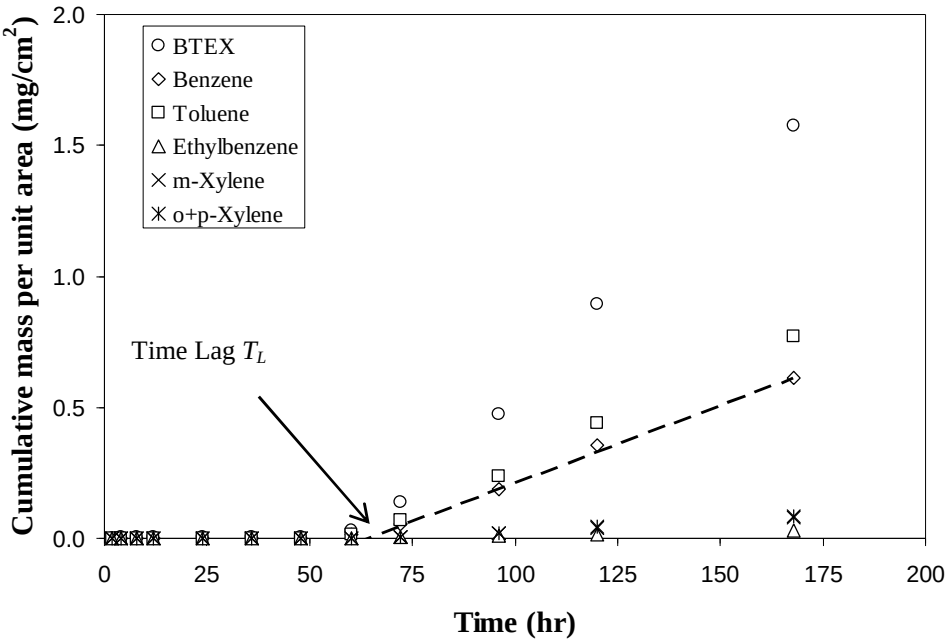

Figure 7 Cumulative mass permeated per unit area for BTEX compounds through bulb portion of NBR gasket exposed to free product premium gasoline (Concentrations of benzene – 19.8 g/L; toluene – 75.9 g/L; ethylbenzene – 14.7 g/L; m-xylene – 33.7 g/L; o+p-xylene – 32.5 g/L)

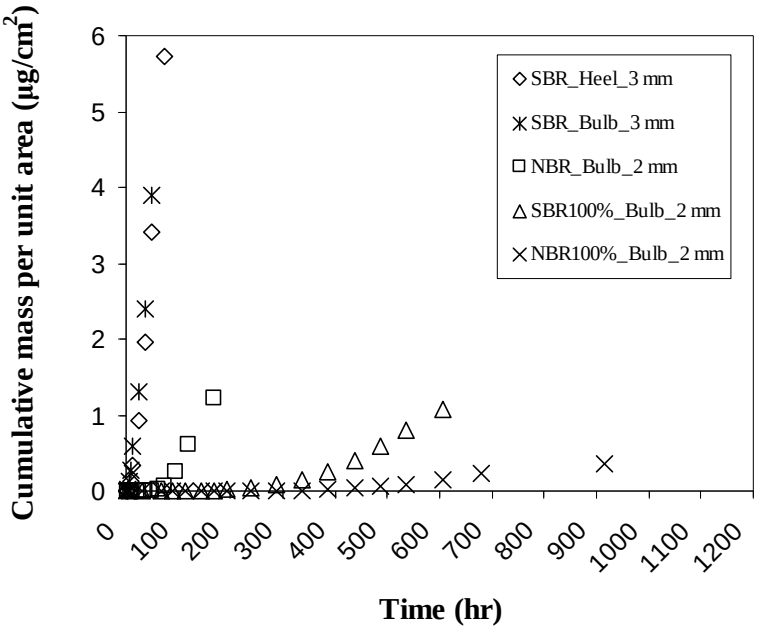

Figure 8 Permeation of benzene through bulb/heel portions of SBR and NBR gasket with different thicknesses and concentrations (100% represents specimens exposed to 100% gasoline saturated aqueous solution, while others exposed to premium gasoline)

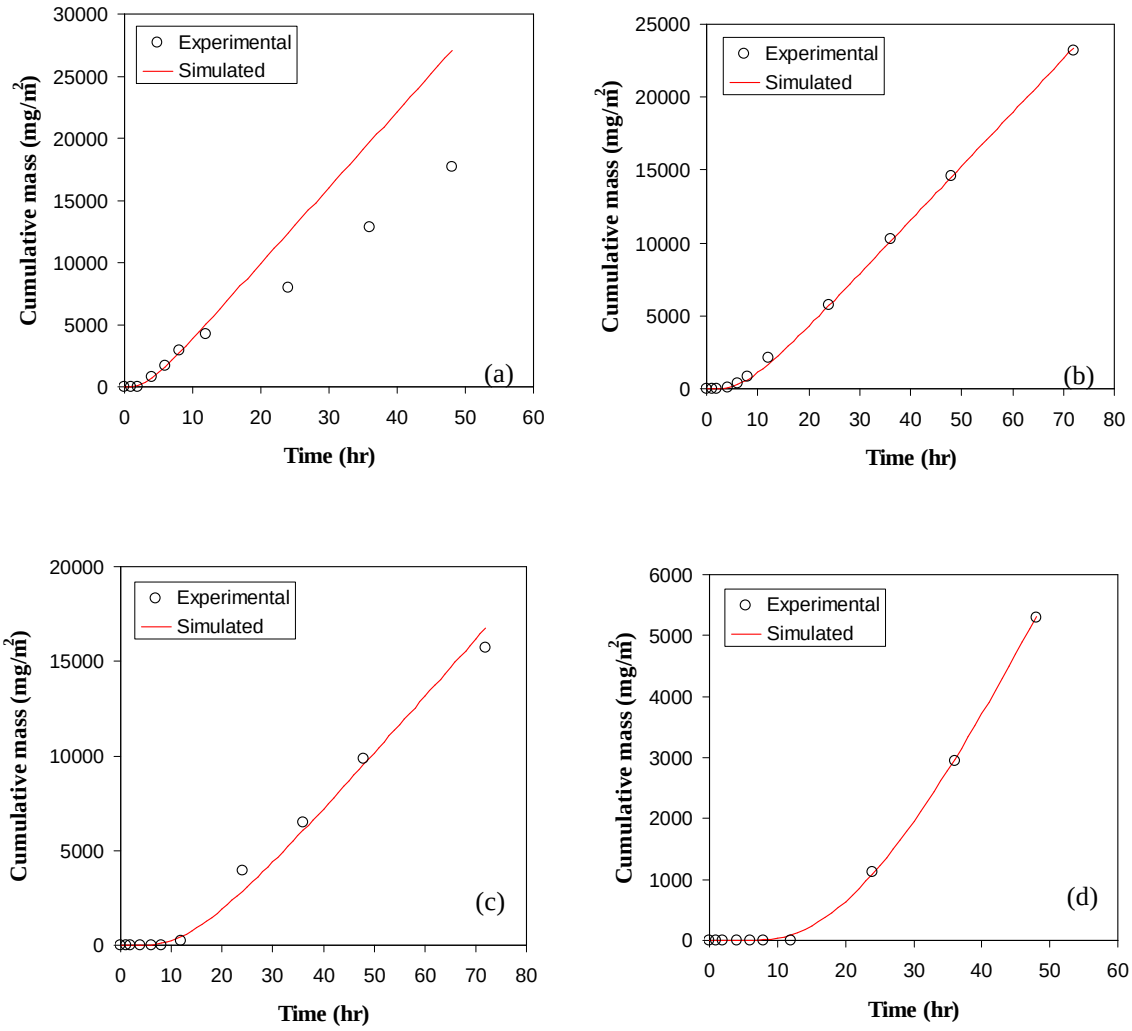

Figure 9 Simulated cumulative mass of benzene permeation through SBR heel portion when exposed to premium gasoline for thickness of (a) 2 mm, (b) 3 mm, (c) 4 mm, and (d) 5 mm

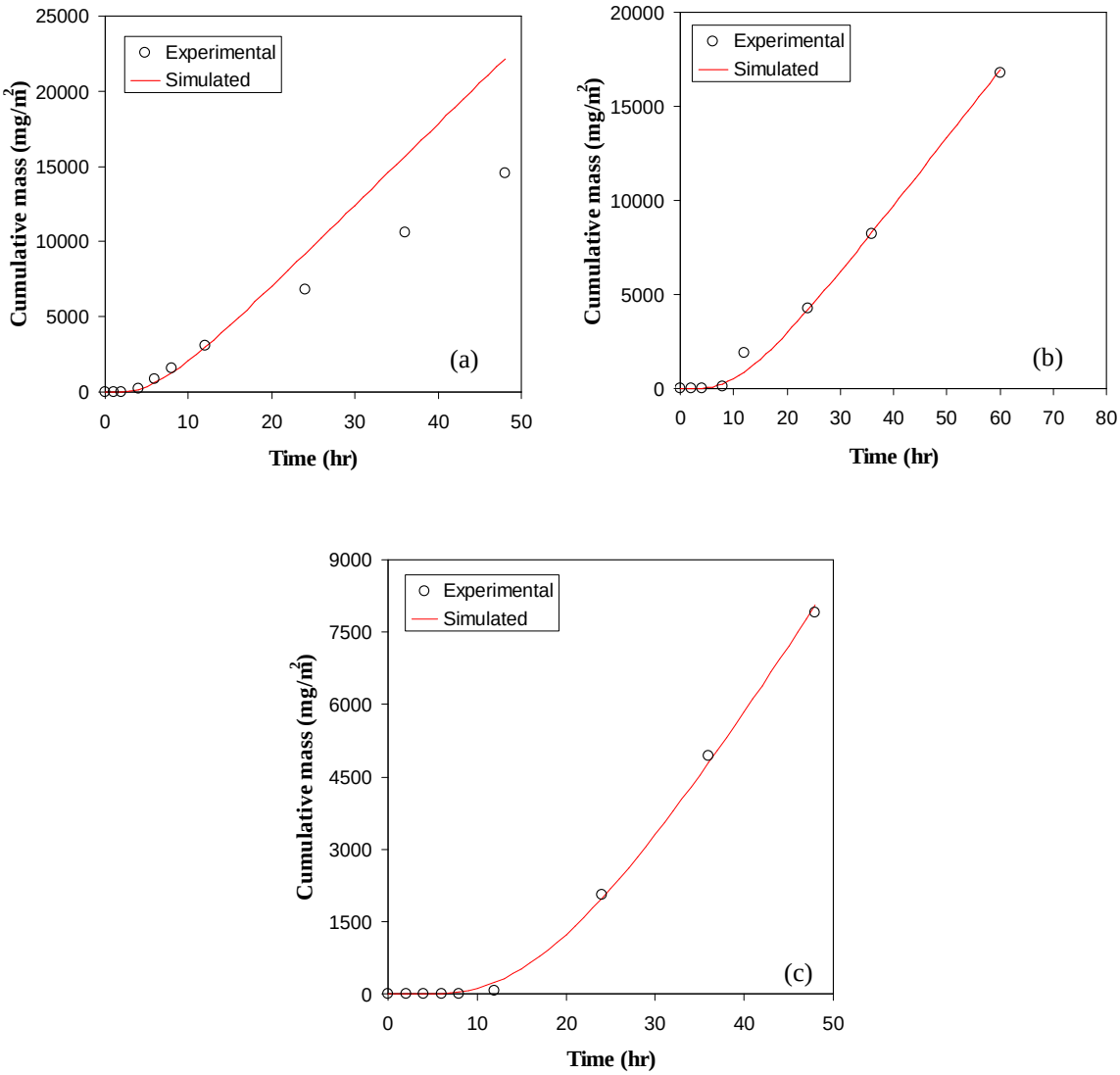

Figure 10 Simulated cumulative mass of benzene permeation through SBR bulb portion when exposed to premium gasoline for thicknesses of (a) 3 mm, (b) 4 mm, and (c) 5 mm

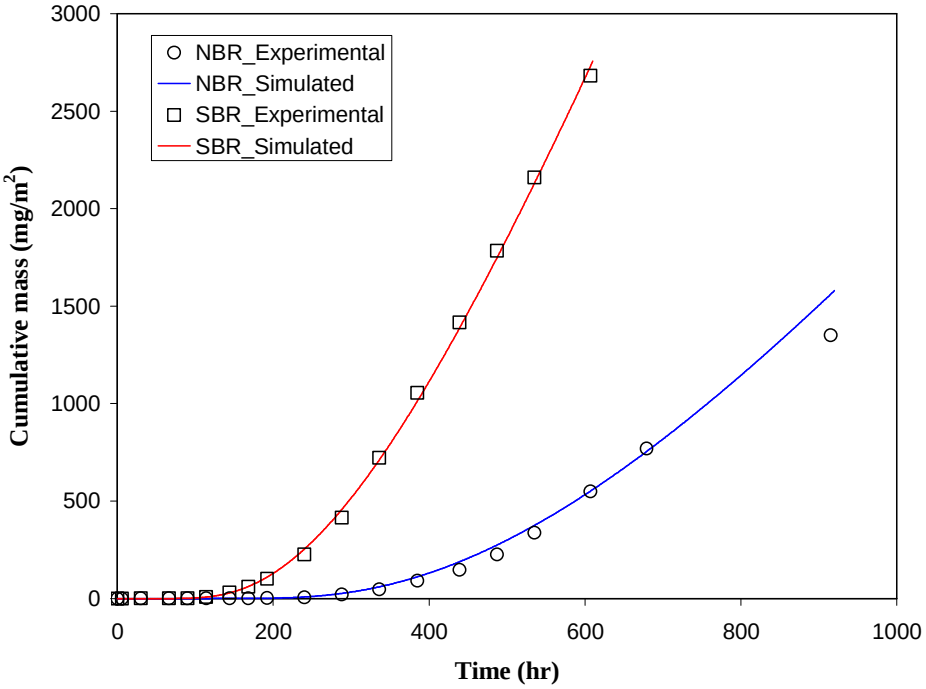

Figure 11 Simulated cumulative mass of benzene permeation through SBR and NBR bulb portion exposed to 100 % gasoline saturated aqueous solution for thickness of approximately 2 mm

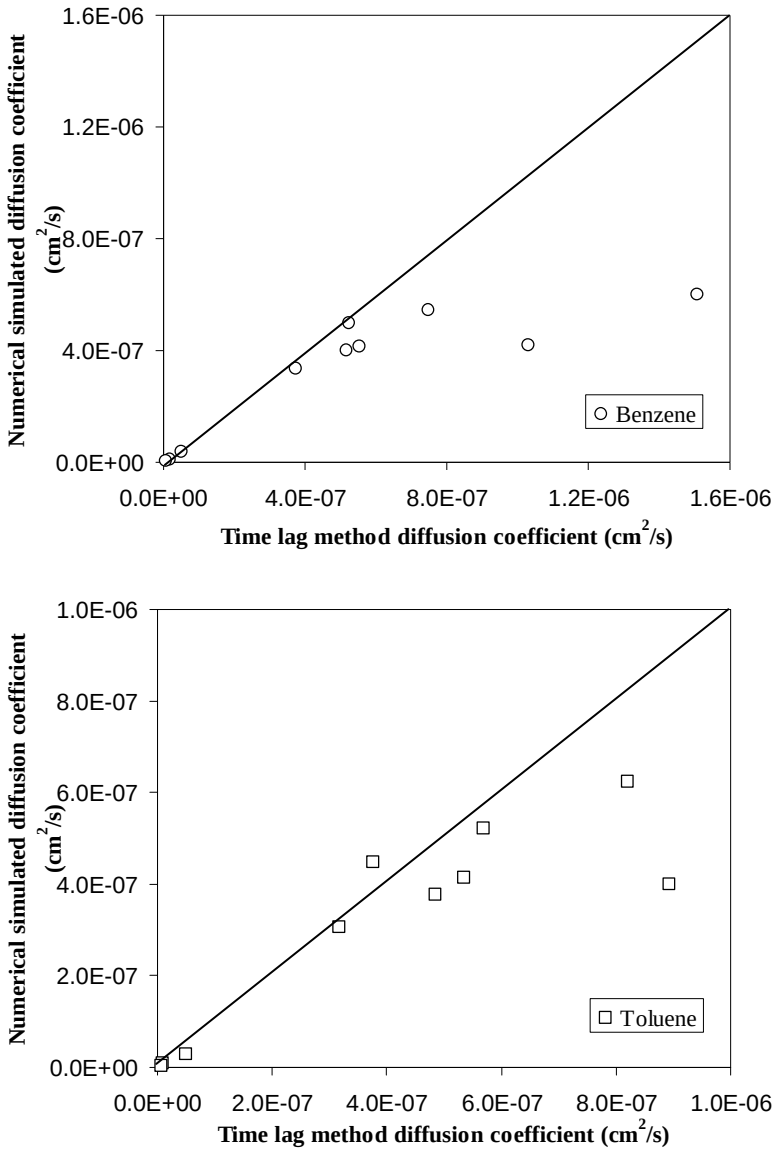

Figure 12 Comparison of estimated diffusion coefficients of benzene and toluene for different thickness from experiments and simulations for all thickness, and material types and concentrations.

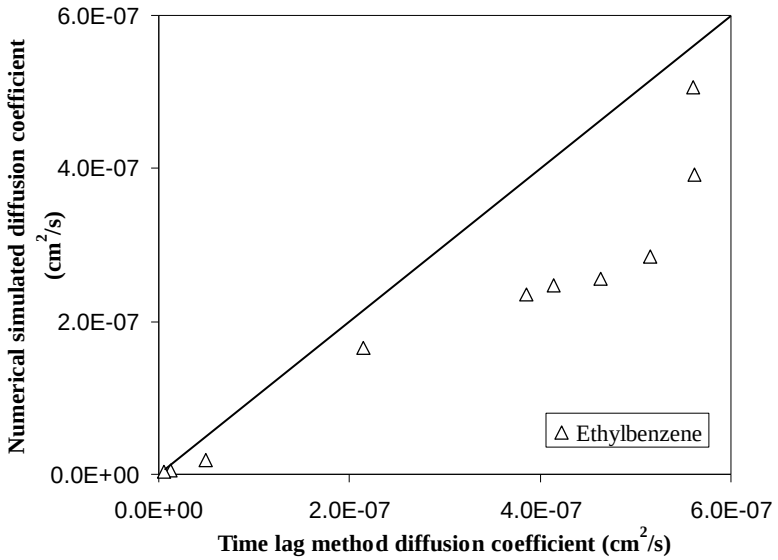

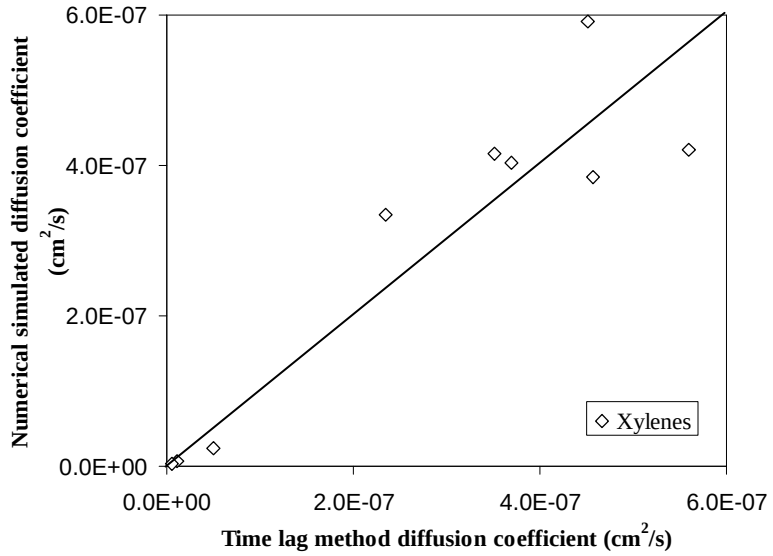

Figure 13 Comparison of estimated diffusion coefficients of ethylbenzene and xylenes for different thickness from experiments and simulations for all thickness, and material types and concentrations.

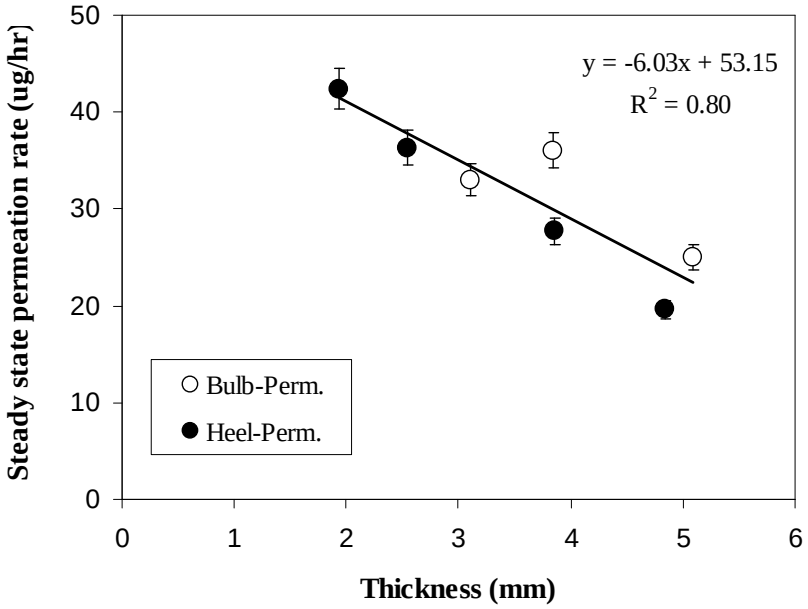

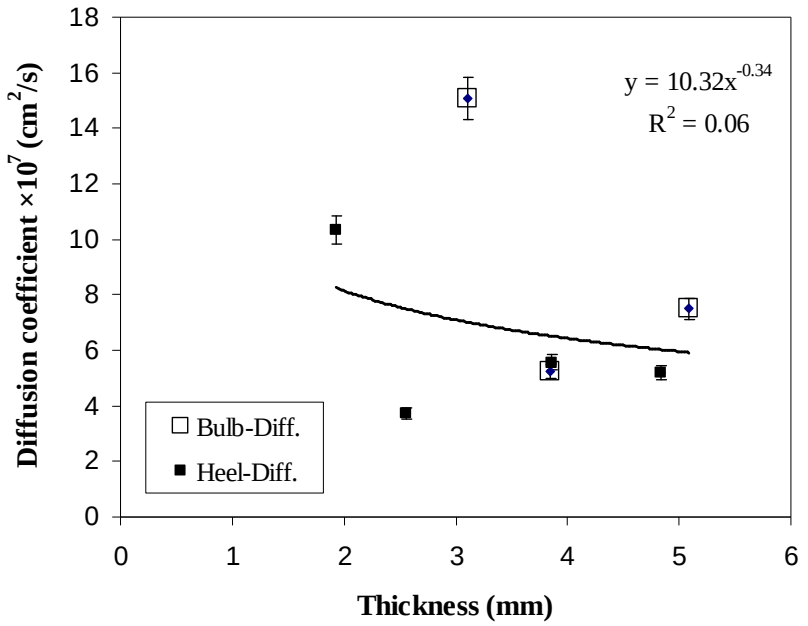

Figure 14 Correlations between steady-state permeation rates and estimated diffusion coefficients for benzene with different thicknesses for bulb/heel specimens of SBR (Diff.: diffusion coefficient; Perm.: steady state permeation rate)

CHAPTER 5. NUMERICAL SIMULATIONS AND PREDICTIONS OF BENZENE PERMEAITON THROUGH TYTON® GASKETS AND ITS IMPACT ON WATER QUALITY

CHU-LIN CHENG, SAY KEE ONG, JAMES A. GAUNT

A paper to be submitted to the Journal of American Water Works Association

5.1 Abstract

The objective of this study was to investigate possible permeation paths and potential patterns of organic compounds permeating through polymeric gasket materials of ductile iron (DI) pipe joints in drinking water distribution system. Numerical models for various boundary conditions were developed using Multiphysics 3.2. Numerical simulations were conducted to fit the permeation data from pipe-drum experiments by minimizing the root mean square error.

Numerical simulations of an intact SBR gasket using diffusion coefficients determined by a separate diffusion cell device showed that the heel portion and part of the bulb portion of a gasket were likely to be in contact with the contaminants after assembly. Compression of the gasket under hydrostatic pressure may pose greater risk to contaminant permeations mainly due to an increase in exposed surface area of the heel portion. If the length/size of the bulb portion of a 4-inch SBR gasket was increased from 10% to 30%, the permeated mass of benzene were found to be reduced about 29% to 71%.

Key words: Permeation, swelling, SBR, NBR, organic compounds, DI pipe, FEM simulation

5.2. Introduction

In recent years, almost half of all new water mains installed in North America are ductile iron (DI) pipes (Rajani and Kleiner, 2003). Some of the advantages of DI pipes over plastic pipes include: higher tensile strength, strength not affected under typical variations of temperature, ability to withstand four times higher hydrostatic pressure and eight times higher crushing load, and strength not compromised over time (DIPRA, 2003). Iron pipe have been used for more than 100 years in 600 or more utilities in the United States and Canada (Bonds et al., 2005). Although DI pipe itself is resistant to permeation, the gasketed joints between pipe segments are susceptible to permeation by organic contaminants (Holsen et al., 1991a; Park et al., 1991; Selleck et al., 1991; Glaza and Park, 1992; Ong et al., 2007). Water mains and service lines consisting of plastic and ductile iron pipes are known to be impacted by petroleum products from gasoline spills or leakages from underground storage tanks (Park et al., 1991; Holsen et al., 1991a; Glaza and Park, 1992; Ong et al., 2007; Mao, 2008). The vast majority of the permeation incidents of plastic piping and polymeric gaskets involve soils contaminated with petroleum products. Permeation incidents involving plastic pipes, such as polyvinyl chloride (PVC), polyethylene (PE), and polybutylene (PB), have been reported while few contamination incidents for water mains using ductile iron (DI) pipes joints with gaskets have also been reported (Thompson and Jenkins, 1987; Park et al., 1991; Holsen et al., 1991a; Glaza and Park, 1992; Ong et al., 2008). There are direct methods to observe contaminant permeations through a gasket. Studies on chemical permeations of pipes and gaskets are typically conducted using pipe-drum experiments or diffusion cells. Several nondestructive testing methods such as infra-red (IR) spectroscopy, refractive index,

reflection spectroscopy, X-ray diffraction (XRD), and nuclear magnetic resonance (NMR) can be used to measure optical and interior properties of the polymer material (Duncan et al., 2005), but have not been used for an intact DI pipe gasket. It is not possible to directly monitor the permeations of chemicals through the gaskets of DI pipe joints since the gasket is hidden within the bell and spigot assembly and the metal of the DI pipe would shield the gasket from spectroscopy methods. Even if spectroscopy methods can be used, the carbon black in gasket materials may prevent the direct observation of polymer-organic chemical interaction within the polymer material. As such, study of chemical permeations would rely on pipe-drum experiments and numerical modeling of the permeation data. To date, there are no numerical modeling studies that can predict organic chemicals permeating through an intact gasket of a pipe joint.

The goal of this chapter is to numerically simulate the permeation of gasoline through intact DI pipe joints for the pipe-drum experiments of Chapter 3. The objectives of the modeling work were to investigate: (1) contaminant exposure area of a gasket; (2) impacts of net swelling of the polymer on permeation; (3) possible permeation path of contaminant; and (4) potential diffusion limiting portion (heel or bulb) of a gasket.

5.3. Materials and Methods

Permeation of BTEX through SBR and NBR gasket materials in the pipe-drum experiments (Chapter 3) were the main focus of the numerical modeling. The 4-inch SBR and NBR gaskets obtained from the supplier were similar in shape and dimensions. The percent area of heel and bulb portion for the two gasket materials was found to be

approximately the same. A cross-section view of the polymeric 4-inch Tyton® gasket installed in DI pipes is shown in Figure 1. For the pipe-drum experiments, one side of the gasket was in contact with deionized water while the opposite side was exposed to attacking solvents which were gasoline or different concentrations of gasoline aqueous solutions. To estimate the surface of a Tyton® gasket in a pipe joint where contaminants come in contact with, paint was applied to the area between the bell and the spigot of an assembled pipe joint. After one week, the joint was disassembled and the white paint on the gasket (Figure 2) indicated that the heel portion of the gasket was primarily exposed to paint. The contact area of heel portion of the gasket can be viewed as consisting of three parts: a rectangular area (a1), a ring area (a2), and a trapezoid-like area (a3) as shown (Figure 2). While the actual contact area might vary somewhat due to variations in field assembly techniques, these three surfaces approximate the surface area of the gasket exposed to external contamination.

5.3.1 Model setup

The program used to model the permeation process of organic compounds through Tyton® gaskets for different conditions and secnarios was the Transient Analysis of Diffusion under the Mass Balance of Chemical Engineering module in Multiphysics 3.2 (previously FEMLAB, COMSOL, Stockholm, Sweden). To simplify the complexity of the permeation process, the model simulations assumed a tight seal and neglect possible impact of incomplete contact or seal between gasket and the DI pipe bell and spigot. The conceptual model used for modeling purposes was constructed in two-dimension (2-D) as shown in Figure 3. The boundary of the pipe spigot and bell and the gasket were digitized and

delineated using AutoCAD 2007 (Autodesk, Inc., 2007) then imported into Multiphysics. The coordinate system of the modeled gasket was defined accordingly and the dimensions of the intact gasket were added in scale with extra caution.

The heel and bulb portion were assigned as separate subdomains (D1 and D2), in which the diffusion coefficient for each subdomain can be adjusted accordingly during the simulations. Two additional subdomains were identified between the bell and the gasket (D3') and between the spigot and the gasket (D3) (see Figure 3) to represent the possible gap/space. These two subdomains might be exposed to contaminants or be filled with air. Diffusion coefficients of contaminants in the air of Subdomain D3 and D3' were set to 0.096 cm^2/s for benzene (Schwazenbach et al., 1993). As per the photo of cross-section of the DI pipe (Figure 1), the volume of subdomain D3' might vary due to the hydrostatic pressure or swelling of the gasket.

The diffusion process can be modeled using the classic Fickian diffusion equation:

$$\frac{\partial C}{\partial t} + \nabla(-D_e \nabla C) = 0 \qquad [1]$$

where D_e is the diffusion coefficient of contaminants in the polymeric material. The polymeric material of the bulb and heel portion was assumed to be homogeneous and their diffusion coefficient assumed isotropic within the particular material. Another assumption was that the solvents used did not interact and dissolve the polymer materials.

Boundary and initial conditions

The surface of the gasket exposed to the contamination indicated by Boundary B1 was assigned a boundary condition with a fixed concentration of contaminant (Figure 2). When

the heel portion does not form a hydrostatic seal with the bell, it is possible that the contaminants may advance into Subdomain D3'. In this case, surface B3 consisting of both heel and bulb portion will be exposed to the contaminants and the boundary conditions assigned for B3 was a fixed concentration. The bulb portion of a gasket had revealed greater vulnerability than the heel portion (see Chapter 3). It is possible that the bulb portion being directly in contact with organic pollutants may result in faster permeation and greater risk of drinking water contamination. The surface of the gasket open to the drinking water (B2) was assumed to have a concentration of zero. The surfaces of the gasket in contact with the pipe bell and spigot were assigned a boundary condition of no flow, or zero concentration gradient normal to the surface.

The boundary and initial conditions are summarized as follow:

$t < 0$, Subdomain area D1, D2, D3, D3', D5, $C = 0$; [2]

$t \geq 0$, Boundary B1 and/or B3, $C = C_0$;

$t \geq 0$, Boundary B2, $C = 0$;

$t \geq 0$, Boundary (all other surfaces of gasket in contact with the bell and spigot of the pipe), $\nabla C = 0$;

The concentrations (C_0) for boundary B1 and/or B3 was calculated on the basis of the concentration in the solvent/aqueous phase and the polymer partition coefficient by assuming that boundary was saturated instantaneously with contaminants.

Modeling scenarios

Even though Figure 1 provided an excellent picture of how the gasket would sit in the bell and spigot section of the pipe, there is still much uncertainty with regards to its actual position and exposed areas. As such various scenarios were developed to examine whether each situation has an impact on the permeation of chemicals through the gasket.

Gaskets restrained in a pipe joint are limited to expand longitudinally in the space between the spigot and bell. Changes in the length of the gasket may be due to compression during pipe joint installation, compression from hydrostatic pressure under operation, and swelling of the gasket due to the solvent soprtion of gasket polymers. The actual length changes for each of the above effects are unknown but it is possible that each of the above effect can act in opposite directions resulting in an unknown net change in the length of the gasket.

The various modeling scenarios are summarized in Table 1. Briefly, Scenario 1 was setup to examine the impact of the water within this additional space in the socket on the permeated benzene concentration. The additional space between the gasket and the bell exposing to drinking water is filled with drinking water as shown in Figure 1. The water in the space might be stagnant and chemicals coming out from the gasket will have to diffuse towards the opening between the beveled end of the spigot and bell into the pipe. Subdomain D5 was assigned to the space with a diffusion coefficient of contaminant in the water, which is 1.02×10^{-5} cm^2/s for benzene (Banat and Simandl, 1996).

The purpose of Scenario 2 is to examine the possible contaminant exposure area. Using the position of the gasket as per Figure 1 and Figure 2, the concentration tested were:

(i) only heel portion (boundary B1) exposed to the contaminant with D3' and D3' filled with air; (ii) boundary B1 and B3 exposed to contaminant with D3 filled with air, and (iii) B1 and B3 exposed to contaminants with D3 filled with lubricant. During the assembly of pipe joints, lubricant is applied to the spigot and the lubricated spigot is then pushed past the gasket into the bell. The film of lubricant was applied to the inside surface of gasket which will come in contact with plain end of the pipe (Griffin, 2006; US Pipe, 2008; ACIPCO, 2009). In addition to the previous paint experiment, the Subdomain D3 can be either filled by trapped air or lubricant.

Whether the hydrostatic pressures will promote or prevent contaminant permeations is still debatable. It is generally believed that an increase in the contaminant pressure may result in two opposing effects: (a) increase the concentration of the contaminant dissolved in the polymer material, and (b) decrease the "free volume" due to the increase of pressure on the polymeric material (Stern, 1972). The shorter permeation path (thickness) due to the compression of material may occur under hydrostatic pressure. Meanwhile, swelling as a result of sorbate-induced structural rearrangements/relaxation would open up the free volume and enhance permeation. Ong et al. (2008) conducted a serial of pipe-drum experiments on Tyton® SBR gasket under pressures of 0, 20, 40, and 60 psi and found that the correlations between hydrostatic pressure and BTEX permeation through SBR gaskets were insignificant. Scenario 3 was to test the effect of possible changes in the length of the gasket due to hydrostatic pressure and swelling. The starting configuration for the gasket is as shown in Figure 4 where the hydrostatic pressure has pushed the gasket outwards. The boundaries and subdomains were the same as Figure 2 except for the exposed area of Boundary B3 and B1,

which may be decreased and increased, respectively, due the redistribution of an intact gasket from hydrostatic pressure. Meanwhile, the Boundary B2 exposing to drinking water remained the same. Total of six conditions were run with a bulb portion length ranging between -30% to +30% of the original length, which were 1.05 cm, 1.2 cm, 1.35 cm, 1.65 cm, 1.8 cm, and 1.95 cm respectively (Figure 5).

5.3.2 Determination of diffusion coefficients

For each of the scenarios, diffusion coefficients of benzene in intact gasket simulations were initially given a value based on the time-lag estimation from previous diffusion cell results (Chapter 4). The diffusion coefficients were then adjusted through several trials until the experimental data points matched the theoretical permeation curve plotted. The adjustments were made and the least-squares method was applied to determine the diffusion coefficient of benzene that led to the "best fit". The least-squares method employed in this study was the root mean squared error (RMSE). The fitting of the benzene permeation curves were the experimental data of SBR gasket from pipe-drum experiment.

5.4. Results and Discussion

5.4.1 Conversion of permeation mass through one joint to unit area

In order to produce the proper cumulative mass per unit area over time ($mg/cm^2/s$) from pipe-drum experiment data (mg/joint/s) for modeling calibration, estimation of exposed surface area was needed. The paint experiment showed that the estimated exposed area was 57.78 cm^2. However, it is possible that the exposed area may be larger than the painted area

(Figure 6). The area represented the possible maximum surface area of a gasket contacting with outside organic compounds after the pipe was joined and the gasket compressed. Looking towards the heel portion of a gasket, the contaminant exposed area consisted of three portions, which were the rectangular area (A1), ring area (A2), and trapezoid-like area (A3) as shown (Figure 6). The estimated areas were 20.78 cm^2, 36.99 cm^2, and 29.55 cm^2, respectively. The total potential contacting surface was 87.32 cm^2. This was larger than the estimated area from the paint experiment. This larger estimated area assumed that contaminants not only can be in contact with the perpendicular side of heel portion (A2) but also some of the areas (A1 and A3) adjacent to it. The actual exposed area might vary due to the nature of the installation of a push-on pipe joint with the same size of gasket. Some bulb portion might be exposed to contaminants if the application of lubricant is improper.

5.4.2 Validation of initial boundary condition and diffusion coefficients

The numerical model was set up using the boundary conditions as shown in Figure 3. The diffusion coefficients for heel (D1) and bulb (D2) were initially assigned using the benzene diffusion coefficient estimations from Chapter 3 and Chapter 4. The initial results are presented in Figure 7. The benzene diffusion coefficients used for both heel and bulb portion from Chapter 3 were 1.47×10^{-7} cm^2/s, while the benzene diffusion coefficients from Chapter 4 were 4.0×10^{-7} cm^2/s and 5.42×10^{-7} cm^2/s, respectively. It was found in the simulation that the estimated permeation mass was higher than the experimental data, implying that assigned diffusion coefficients were too large. The RMSE of using diffusion coefficients from Chapter 3 was 12.0 (mg/cm^2), while the RMSE of using diffusion

coefficients from Chapter 4 was 74.9 (mg/cm^2). The same procedures were conducted with the boundary conditions in Scenario 1.1 and Scenario 1.2. The simulation results were identical implying that the boundary conditions here may not be the main factors. Efforts were made by adjusting diffusion coefficients of heel and bulb portion to curve fit the benzene permeation data from pipe-drum experiment using trial and error procedure. Adjustments were made based on the results found in the previous experiments, where the diffusion coefficients of bulb should be larger than the heel portion and the difference in value of the diffusion coefficient between the bulb and heel portion of a SBR gasket should be within one order of magnitude. With the trial and error procedure, it was found that diffusion coefficients were likely in the order of 10^{-8} cm^2/s.

5.4.3 Evaluation of possible exposure area

The influence of Subdomain D5 on benzene permeation were simulated as shown in Figure 8. The simulation of Scenario 1.1 and 1.2 both started with assigning diffusion coefficients for heel and bulb portions from Chapter 4. As presented in Figure 8 (b), the assigned diffusion coefficients for the gasket fitted the permeation data poorly with RMSE of 1.5 (mg/cm^2). When diffusion coefficients for both heel and bulb were assigned to the order of 10^{-8} cm^2/s, the simulated permeation curve fitted closer with RMSE 0.08 (mg/cm^2). However, the simulation did not capture most of the data from experiments as shown in Figure 8. Efforts were made to try to fit the curve but were unsuccessful. In addition, Scenario 1.2 the RMSE ranged from 0.1-1.5 (mg/cm^2), while Scenario 1.1 had RMSE

ranging from 0.01-0.02 (mg/cm^2). Based on simulations, the influence of Subdomain D5 to contaminant permeations seemed limited under the boundary conditions.

Following the estimation of the magnitude of diffusion coefficients for heel and bulb portion, the possible exposure areas were then adjusted to improve the curve fitting of the experimental data. A model was set up according to the boundary condition as Scenario 2.1 with only heel portion of the gasket (B1) was exposed to contaminant. By trial and error, the diffusion coefficients with least RMSE of 0.028 (mg/cm^2) for heel and bulb portion of a gasket were 2.13×10^{-8} cm^2/s and 5.43×10^{-8} cm^2/s, respectively. However, it was found that although it had least RMSE, the simulated permeation curve cannot capture the intermediate or the latter stage of the experimental permeation data. Scenario 2.2 was then conducted with Boundary B3 exposed to contaminants. The diffusion coefficients estimated from this scenario for heel and bulb portion of a gasket were 1.13×10^{-8} cm^2/s and 2.43×10^{-8} cm^2/s, respectively, and the RMSE was 0.020 (mg/cm^2). As shown in Figure 9, the simulated permeation curve under this scenario covered most of the permeation indicating that the heel portion only acts as an anchor to place the gasket at proper position in the socket during the pipe joint assembly and does not form the hydrostatic seal like bulb portion (Bird, 2006; Rahman, 2007). According to the results from Scenario 2.1 and 2.2, it is highly probable that the part of the bulb portion of a gasket was likely to be exposed to the external contaminants (Figure 10). Therefore, the part of the bulb portion of a gasket may serve as a means for contaminant permeation when pipe joint is not under hydrostatic pressure. This boundary setting (Scenario 2.2) was also tested for toluene permeation. The prediction had an RMSE of 0.089 (mg/cm^2) with fairly good curve fit and the estimated diffusion coefficients of

toluene for heel and bulb portion of a gasket were 1.13×10^{-8} cm^2/s and 3.03×10^{-8} cm^2/s, respectively.

Scenario 2.3 was setup to study the possible impacts of lubricant on benzene permeations within the SBR gasket. The oil-based lubricant was assumed to be inactive or close to impermeable to benzene and, therefore Subdomain D3 was assigned a diffusion coefficient of 2×10^{-16} cm^2/s. The simulated permeation curve was similar to the result from Scenario 1.2, implying that the space trapped with air or lubricant would have limited impact on benzene permeation through SBR gasket.

5.4.4 Influences of hydrostatic pressure on permeations

Under hydrostatic pressure, the gasket was assumed to be pushed by internal pressure and relocated closer to socket (Figure 5). In addition, compression or swelling will change the length of the gasket (Figure 5). The boundary conditions remained the same except for Boundary B1 and B3, where B1 became larger and B3 became smaller. Assigning the heel and bulb portion with diffusion coefficients estimated from Scenario 2.2, it was found that the permeated mass increased about 40% (Figure 11).

Figure 12 showed the range of cumulative mass of benzene permeated through an intact SBR gasket within a range of ±30% length increments of bulb portion. It was evident as shown that the permeated mass of benzene decreased with an increase in length in bulb portion of a SBR gasket. The simulation results of an intact DI gasket showed that the pipe joints under hydrostatic pressures were likely to increase permeation, which were similar to the results of Rieber SBR gasket used in PVC pipe systems done by Mao (2008). For the

same boundary conditions, the permeation length is likely to be the main controlling factor to permeation rates of benzene, which corresponds to the results in Chapter 4. Accordingly, by increasing the length/size of the bulb portion of a 4-inch SBR gasket from 10% to 30%, the estimated permeated mass of benzene may be reduced by about 29% to 71% within 150 days of exposure to gasoline.

5.4.5 Permeation path and limiting portion of a gasket

Figure 13 showed the predicted permeation pathways of contaminants under simulated conditions without influence of hydrostatic pressure. Scenarios were run with D3 filled with lubricants and D5 filled with water to present field conditions. Both simulations in Figure 13 indicated that depending on the exposure areas of a 4-inch SBR gasket to contaminants, either bulb or heel portions of a 4-inch SBR gasket might be the limiting portion to permeations.

5.5. Conclusion

The simulations of an intact SBR gasket in a pipe joint showed that part of the bulb portion of a gasket was likely to be in contact to contaminants after assembly. In addition, hydrostatic pressure may push the gasket outwards slightly resulting in high contaminant permeations due to a larger exposed surface area.

The domain of water in contact with the gasket on the drinking water side was found to have minimal impact on benzene permeation.

With the heel and part of the bulb portion of a SBR gasket exposed to gasoline, increasing the length/size of the bulb portion of a 4-inch SBR gasket from 10% to 30%, resulted in a reduction of about 29% to 71% of the permeated mass within 150 days of exposure to gasoline. The results from this study can be used as a basis reference for manufacturing an ideal gasket in improving the reliability of infrastructure of water distribution system.

Based on the simulation results, either bulb or heel portions of a 4-inch SBR gasket might be the limiting portion to permeations depending on the exposure areas of a 4-inch SBR gasket to contaminants.

5.6. References

ACIPCO. 2009. American Cast Iron Pipe Company . AMERICAN Ductile Iron Flex-Lok Boltless Ball Joint Pipe Assembly.Instructions. http://www.acipco.com/adip/pipe/ball/assembly.cfm, accessed on 2-5-09.

Banat, F.A. and J. Simandl. 1996. Removal of benzene traces from contaminated water by vacuum membrane distillation. *Chemical Engineering Science*, 51(8): 1257-1265.

Bonds, R.W., M. Barnard, A.M. Horton, and G.L. Oliver. 2005. Corrosion and corrosion control of iron pipe: 75 years of research. *Journal AWWA*, 97(6): 88-98.

DIPRA. 2000. What is the pressure and vacuum capacity of the push-on joint? Birmingham, AL. http://www.dipra.org/faq/design.cfm, accessed on 2-12-08.

DIPRA. 2003. Ductile iron pipe versus PVC. Ductile Iron Pipe Research Association. Birmingham, AL.

Griffin Pipe Products Co. 2006. Push-on Joint Pipe. Council Bluffs, IA.

Rockaway, T.D., G.A. Willing, and R.M. Nasisetty. 2007. Life predictions of elastomers in drinking water distribution systems. *Journal AWWA*, 99(12): 99-110.

Rajani, B. and Y. Kleiner. 2003. Protecting ductile-iron water mains: what protection method works best for what soils condition? *Journal AWWA*, 95(11):110-125.

Rowe, B.L., P.L., Toccalino, M.J. moran, J.S. Zogorski, and C.V. Price. 2007. Occurrence and potential human-health relevance of volatile organic compounds in drinking water from domestic wells in the United States. *Environmental Health Perspectives*, 115(11): 1539-1546.

Stern, S.A., S.M. Fang, and H.L. Frisch. 1972. Effects of pressure on gas permeability coefficients. A new application of "free volume" theory. Journal Polymer Science Part A-2: *Polymer Physics*, 10(2): 201-219. (Published online: 2003)

Mao, F. 2008. Permeation of hydrocarbons through polyvinyl chloride (PVC) and polyethylene (PE) pipes and pipe gaskets. Ph.D. thesis. Iowa State University. Ames, IA. 269p.

US Pipe. 2008. International TYTON JOINT® Pipe & Fittings, 2008 Edition http://www.uspipe.com/Files/20071218851390.TYTON.pdf, accessed on 1-19-08

Table 1 Scenarios for numerical simulation for benzene through a SBR gasket

	Purpose	Model settings
Scenario 1	Examine impacts of addition water in the space within the socket	
1.1	With water in the socket	B1=C_0 B2=0 B3= C_0 D3=Air D5=Water D1, D2 adjusted
1.2	With water but B2 at the end of the gasket	B1=C_0 B2=0 (at the end of bulb of the gasket) B3= C_0 D3=Air D5=Water D1, D2 adjusted
Scenario 2	Examine possible exposure areas	
2.1	Only heel portion exposed to contaminants	B1=C_0 B2=0 D3=Air D3'=Air D1, D2 adjusted
2.2	Both heel and bulb portion exposed to contaminants	B1=C_0 B2=0 B3= C_0 D3=Air D1, D2 adjusted
2.3	Impact of lubricant trapped between gasket and spigot	B1=C_0 B2=0 B3= C_0 D3=Air/Lubricant D1, D2 adjusted
Scenario 3	Evaluate impact of change the length on benzene permeation	B1=C_0 B2=0 B3= C_0 D3=Air D1, D2 from Scenario 1.2

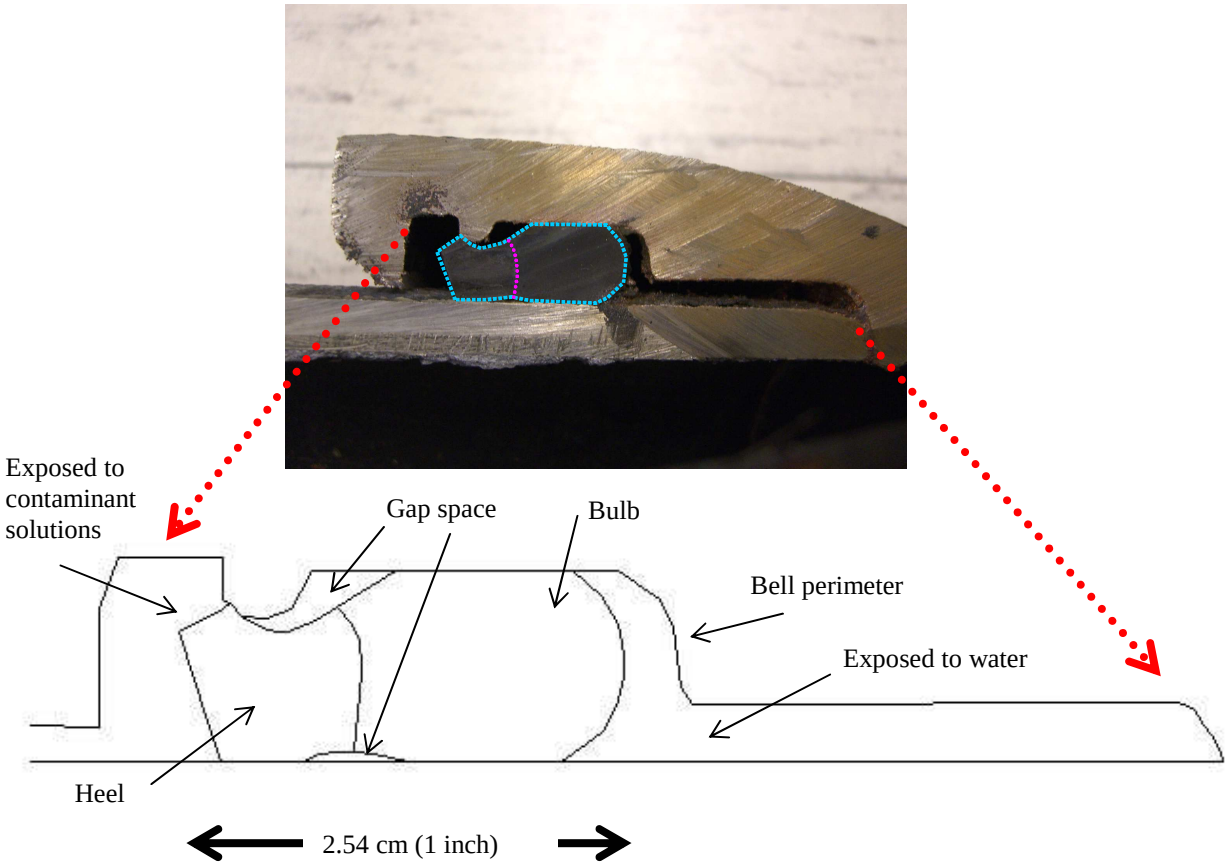

Figure 1 Cross-section of a 4-inch DI pipe joint showing a Tyton® gasket and possible surface exposed to exterior contaminants and interior drinking water

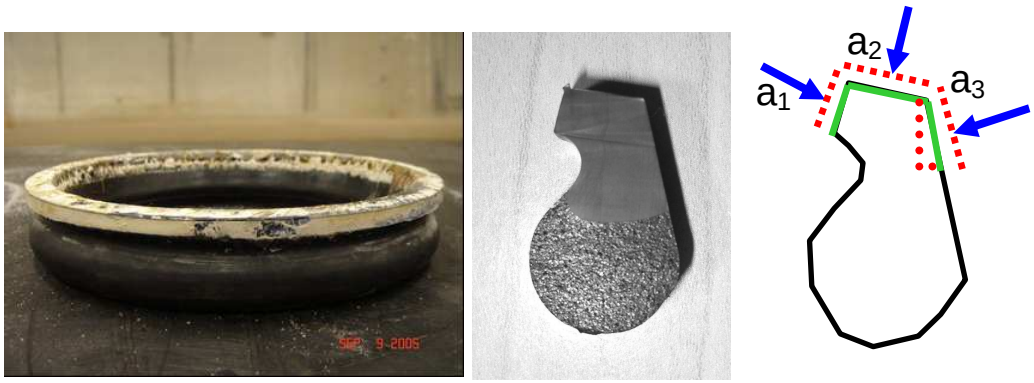

Figure 2 Cross section of a gasket showing contact area with paint

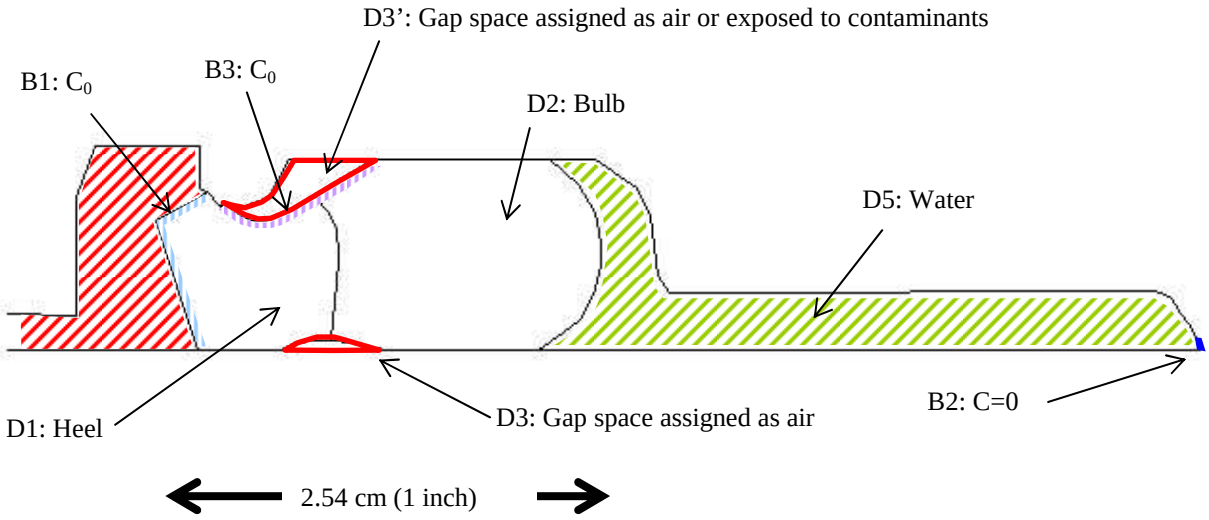

Figure 3 Schematic setup of a DI pipe jointed with a Tyton® gasket in a model (B1 and B3: boundary with concentration of benzene, B2: boundary with zero concentration, D1: heel portion, D2: bulb portion, D3': trapped air or exposed to contaminants, D3: trapped air, D5: fresh water)

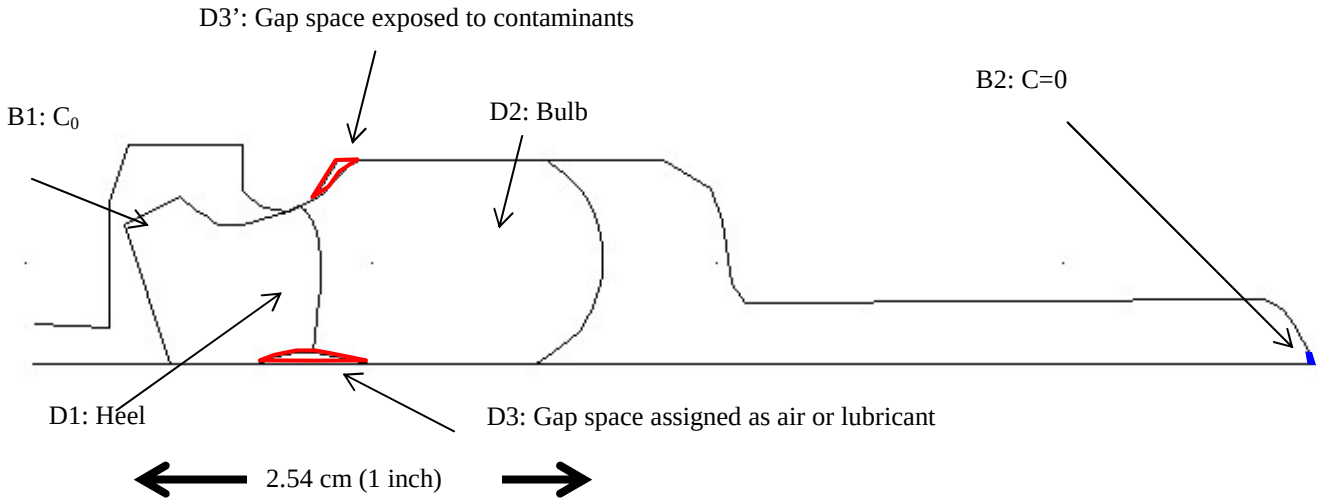

Figure 4 Scheme of a gasket relocated by hydrostatic pressure (B1 and B3: boundary with concentration of benzene, B2: boundary with zero concentration, D1: heel portion, D2: bulb portion, D3: trapped air or lubricant)

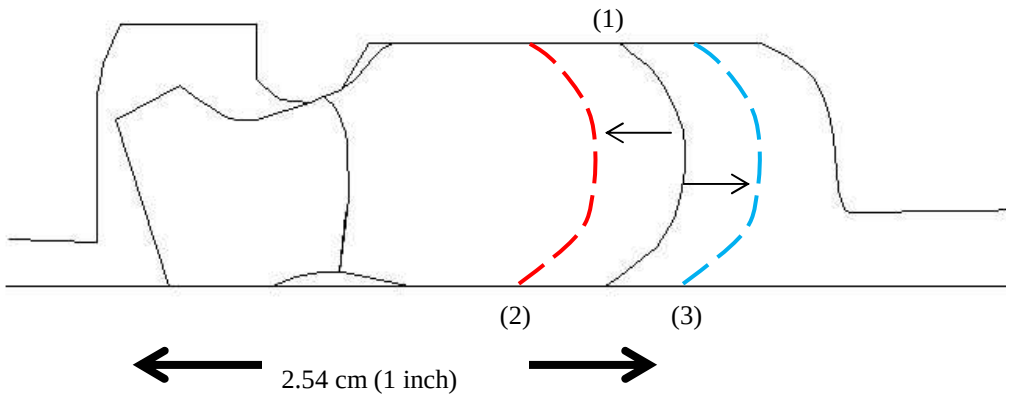

Figure 5 Net change of length of bulb portion due to hydrostatic pressure and swelling (1-original length; 2-compressed 30%; 3-swolen 30%)

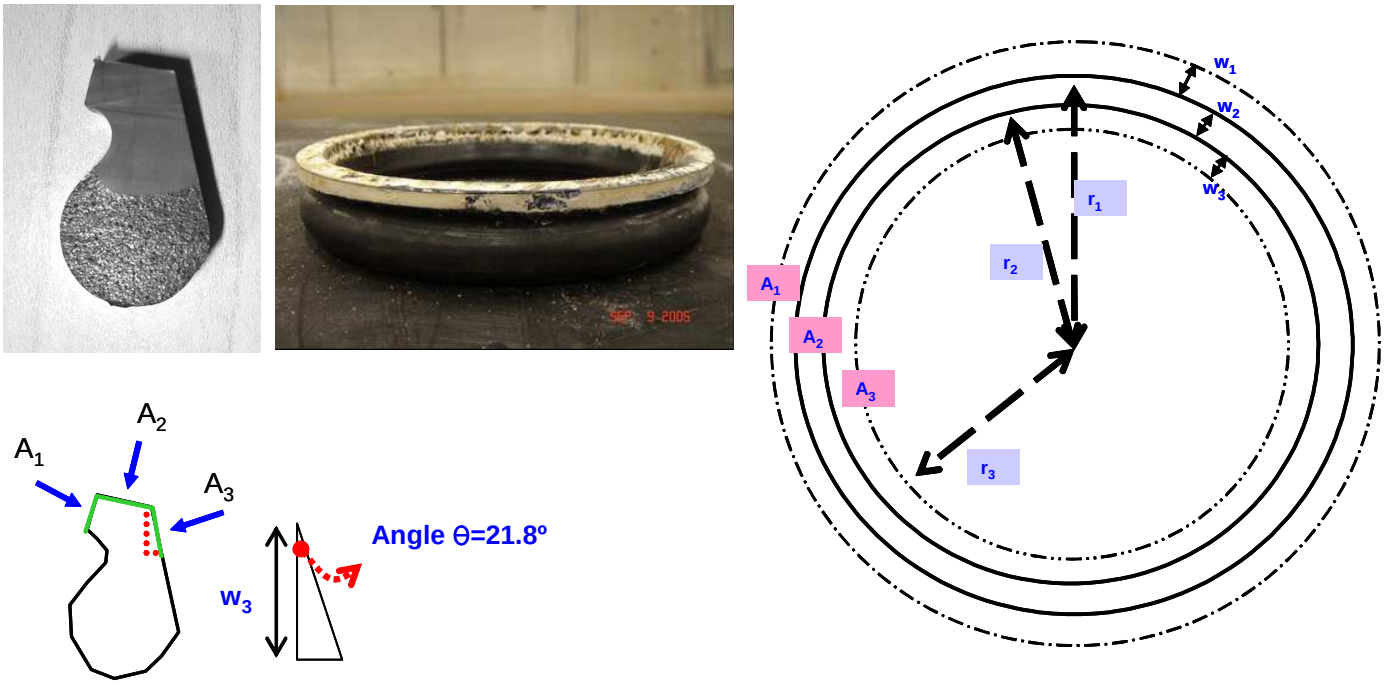

Figure 6 Estimation of possible contact surface as compared to paint experiment

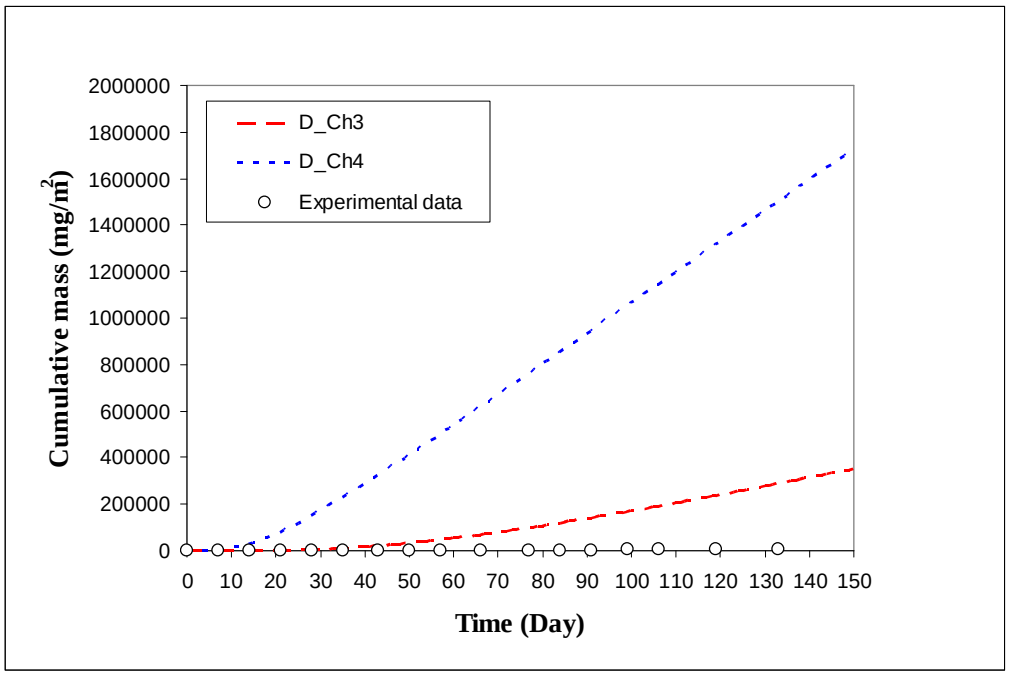

Figure 7 Simulated cumulative mass permeated through a SBR gasket using diffusion coefficients estimated from Chapter 3 and Chapter 4

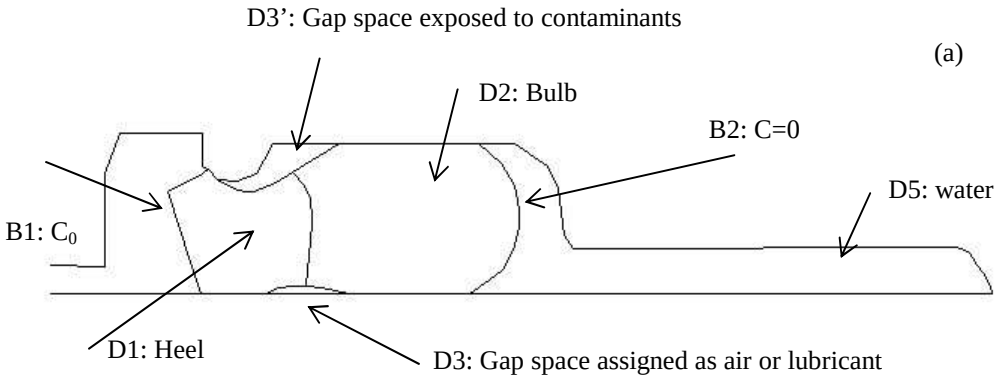

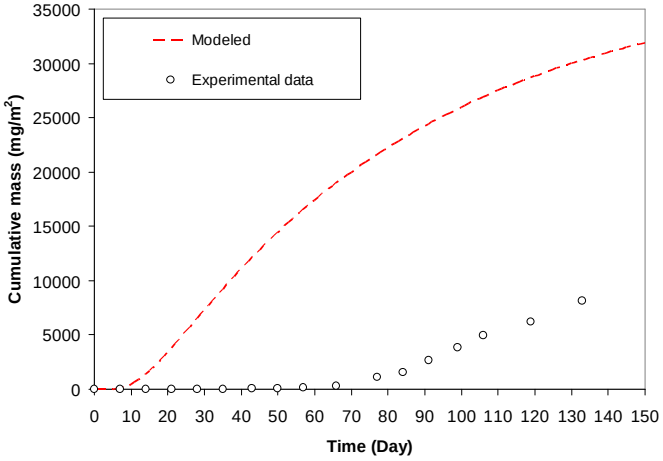

(b)

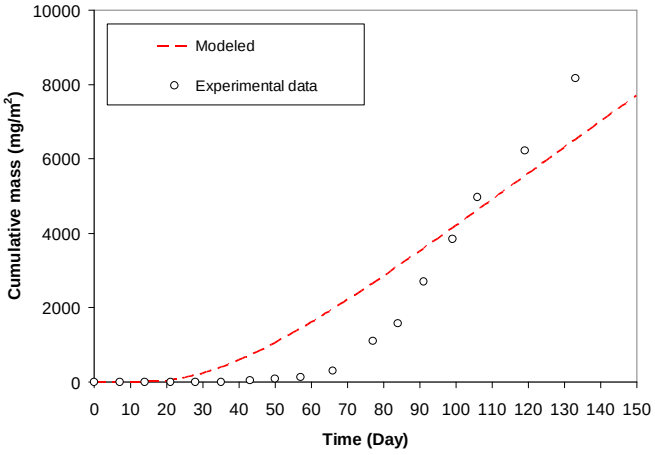

(c)

Figure 8 Simulation of the influence of space filled with water, (a): model setting, (b): result with RMSE of 1.5, (c): result with RMSE of 0.08 (Scenario 1)

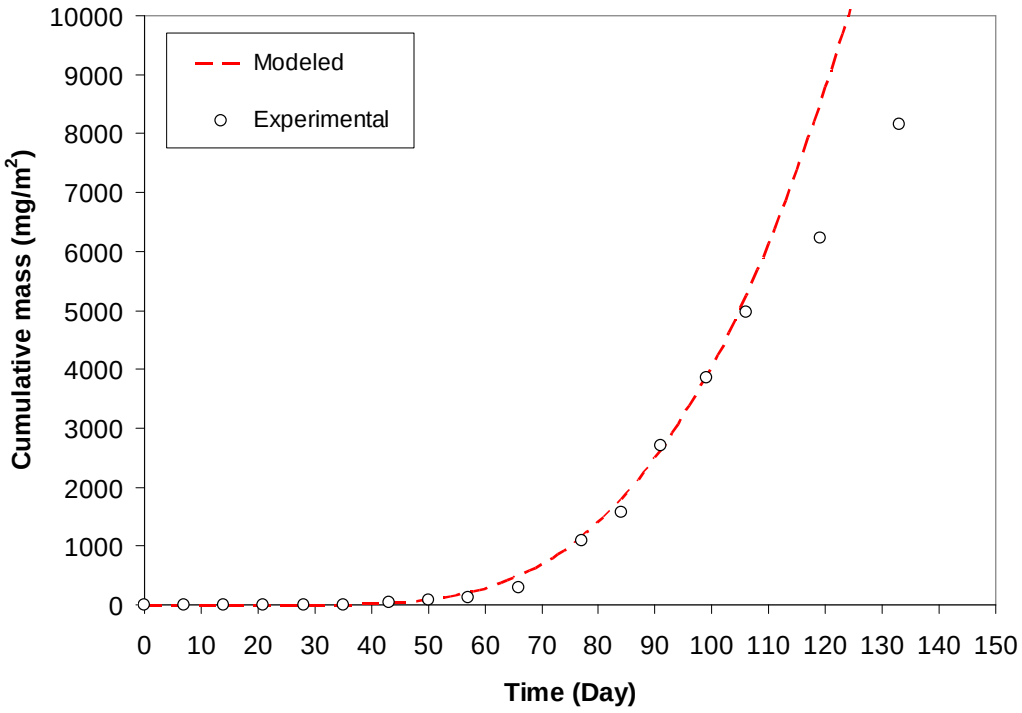

Figure 9 Simulated permeation curve for an intact SBR gasket exposed to free product premium gasoline by adjusting the diffusion coefficients of heel and bulb portion (Scenario 2.2)

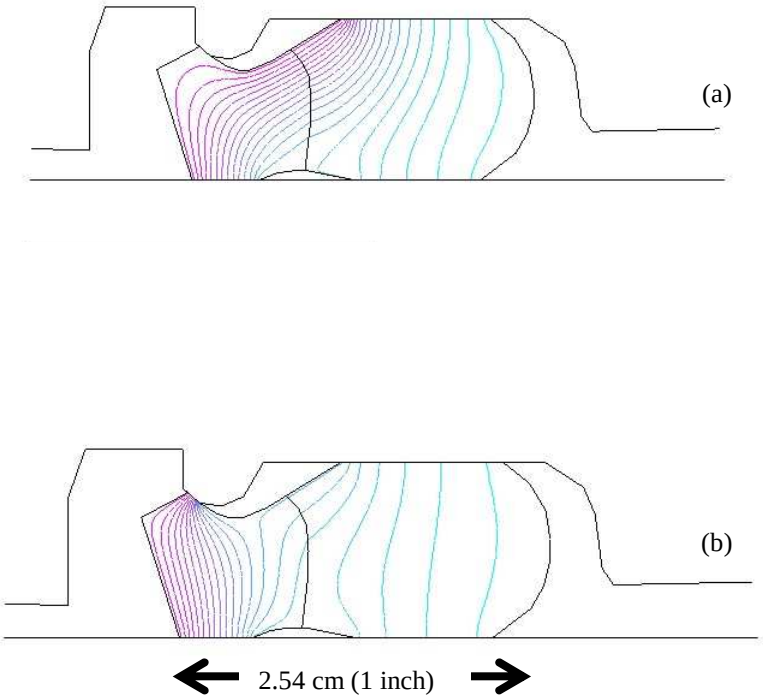

Figure 10 Simulations of possible exposure surface area and permeation path of benzene in a SBR gasket (a: in contact with heel and bulb portions, b: in contact with only heel portion of a gasket) (Scenario 2.2 and Scenario 2.1)

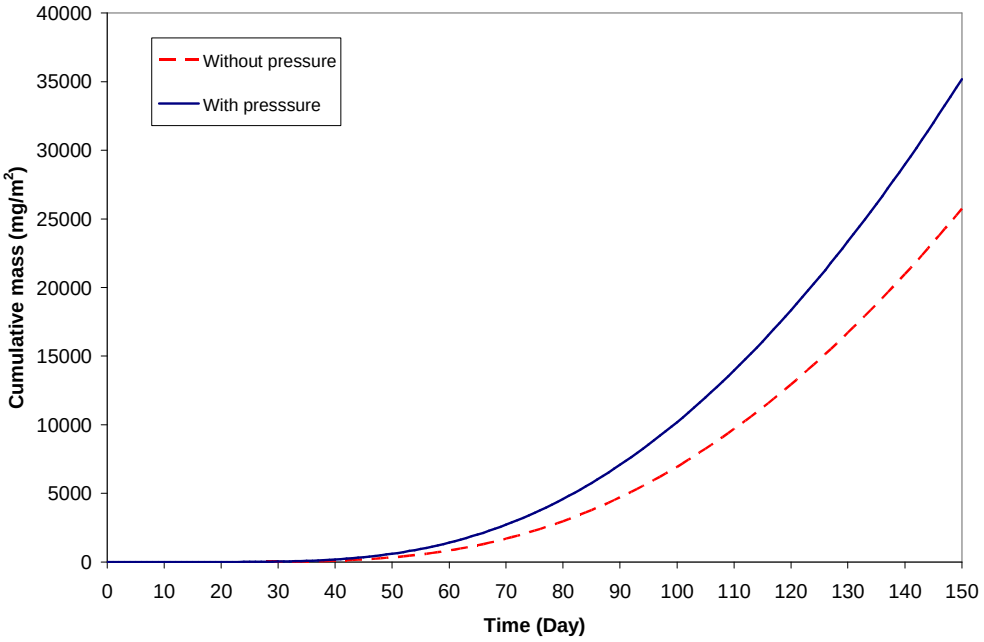

Figure 11 Permeation curves showing increased cumulative permeation mass through a SBR gasket under hydrostatic pressure without deformation

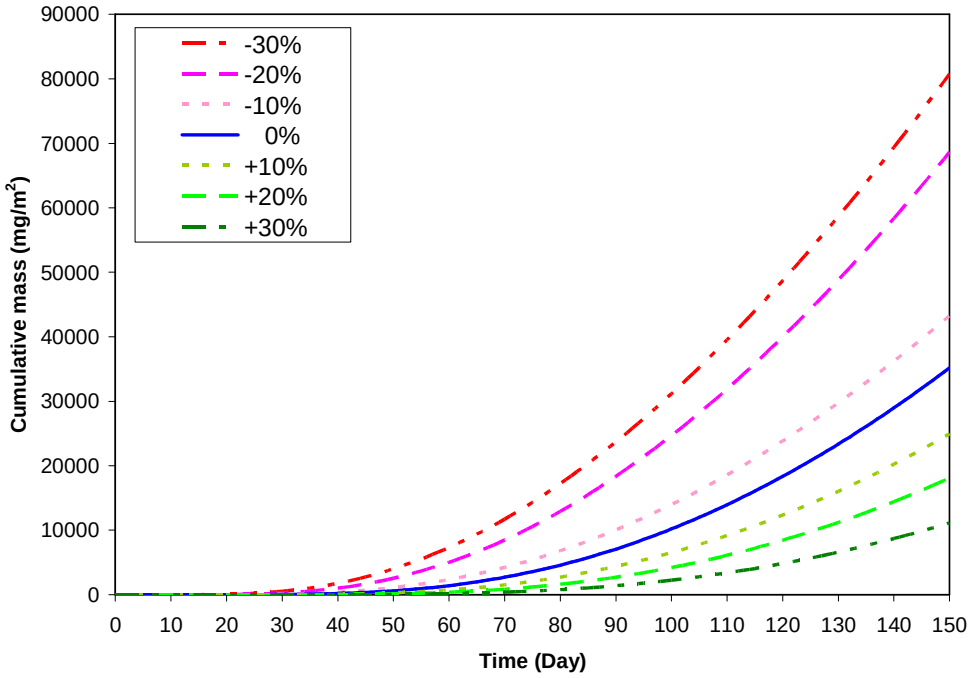

Figure 12 Cumulative mass permeated for a SBR gasket with changes in length of bulb portion from -30% and +30%. (Scenario 3)

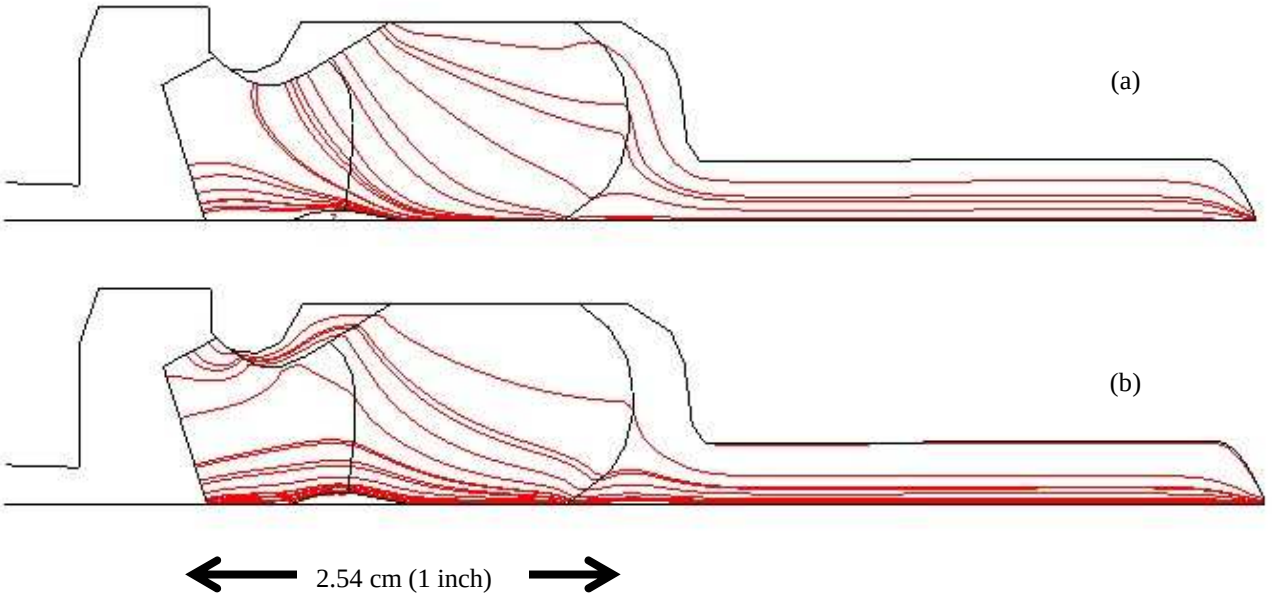

Figure 13 Predicted permeation path of contaminants through an intact gasket: (a) both heel and bulb portions exposed to contaminants, (b) only heel portion exposed to contaminants

CHAPTER 6. CONCLUSION

The purpose of this study was to advance the water industry's understanding of the impact of organic contaminants through commonly-used gaskets used in DI pipes in drinking water distribution systems. The major findings were:

Of the five gasket materials tested, gravimetric sorption tests showed that EPDM had the highest sorption, while FKM exhibited the lowest sorption. The order of percent weight gain for the five gaskets from highest to lowest was EPDM, SBR, CR, NBR, and FKM with a percent weight gain of 127.02±1.86% for EPDM and less than 1±0.11% percent weight gain for FKM. The heel and bulb portions of the Tyton® gasket showed different sorption affinity with the bulb portion sorbing more organic compounds in gasoline than the heel portion for all gasket materials except for CR.

Pipe-drum experiments with premium gasoline showed that the order of breakthrough time from earliest to longest for total BTEX for the various gasket materials were EPDM > CR = SBR > NBR. SBR material has the highest BTEX permeation rates of 5.20 mg/joint/day, followed by CR, EPDM, FKM, and NBR.

Pipe joints with NBR and FKM gaskets were not susceptible when exposed to gasoline saturated aqueous solutions, while SBR was found to be susceptible to chemical permeation. The BTEX breakthrough times for 4-inch SBR gaskets exposed to 100% and 50% saturated aqueous solutions of gasoline were 210 and 240 days, respectively. For pipes exposed to 20% or 5% saturated aqueous solutions of gasoline, no permeation was observed through SBR gaskets after more than 550 days of exposure.

With regards to threats to drinking water, under conditions of water stagnation in the pipe, the 5 μg/L MCL for benzene will likely be exceeded during an 8-hour stagnation period for SBR gaskets in contact with free-product premium gasoline. NBR gaskets were found to be sufficiently resistant to permeation by benzene or other BTEX compounds in gasoline with benzene concentration unlikely exceed EPA MCLs.

Using a low cost diffusion cell, the estimated diffusion coefficient for total BTEX through SBR material in contact with premium gasoline was 4.57×10^{-7} cm^2/s, while the estimated total BTEX diffusion coefficient in contact with 100% gasoline aqueous solution was 1.14×10^{-8} cm^2/s using time-lag method. Using diffusion cell and numerical curve fitting, the diffusion coefficients of BTEX through the bulb and heel portions of a SBR gasket exposed to premium gasoline were found to be of the same order of magnitude of 10^{-7} cm^2/s. When exposed to 100% gasoline aqueous solution, the estimated diffusion coefficients for SBR bulb portion were in the order of 10^{-8} cm^2/s. The estimated diffusion coefficient of total BTEX for the bulb portion of NBR gasket exposed to premium gasoline was 5.28×10^{-8} cm^2/s while the estimated BTEX diffusion coefficient of the bulb portion of NBR gasket exposed to 100% gasoline aqueous solution was 5.8×10^{-9} cm^2/s. Within the testing period and for a thickness of 3 mm, the diffusion cell experiments suggested that the bulb portion of a FKM gasket was resistant to BTEX permeation. The steady state permeation rates had an inverse exponential relationship with the thickness of SBR gasket materials while the diffusion coefficients were found to correlate poorly with the thickness of the gasket materials.

Actual surface area of a gasket exposed to contaminants may vary due to assembly and may influence the permeation. Modeling with an intact gaskets suggested that part of the

surface of the bulb portion of a gasket may be likely the pathway to contaminant permeation. The estimated diffusion coefficients for heel and bulb portion of a gasket using numerical modeling of data from the pipe-drum experiments were 10 times less than estimations from the diffusion cell experiments. The opening space occupied by lubricant or air were small compared to the gasket itself and the influence of the space being a sink or a source to benzene permeation was found to be limited. In addition, a 4-inch SBR gasket under hydrostatic pressure with only change in its length would result in higher contaminant permeations mainly due to an increase in exposed surface area of the heel portion. The water in the space on the drinking water side of the gasket was found to be not a factor in benzene permeation.

Future Research

This study used new gasket materials. The research can be extended using old, used, or compromised gaskets. However, the age, exposure, history, and conditions must be documented to fully correlate permeation rates with the properties of the gasket. Under field conditions, gasket materials may suffer degradation or deterioration due to soil-water conditions, physical stress variation, and biological degradation. Such degradation or deterioration may result in the loss of material strengths, especially the bulb portion making the gasket more susceptible to chemical permeation.

Direct observation of the advance of permeated compounds within the gasket is the preferred approach. Several high resolution microscopic methods may allow this observation. Positron annihilation lifetime spectroscopy (PALS) is one technique which can

be used to verify the permeation data. Since the heel and bulb portion have different permeation properties, PALS technique may be able to discriminate the permeation characteristics of bulb and heel portions of a gasket.

Measurement of the free volume fraction for future studies may provide in foundation and correlations with the chemical permeation rates and diffusion coefficients. Numerical simulations can be conducted in 3 dimensions of an intact gasket and may provide improved estimation of the chemical diffusion coefficients. Permeation studies using a series of similar organic compounds or compound with different functional groups may further elucidate the physical-chemical properties of the organic compounds that impact permeation rates and diffusion coefficients. The issue of the impact of thickness on the diffusion coefficient of a give gasket material needs to be further investigated by using a larger range of material thicknesses.

APPENDIX

A.1 Pipe-drum Experiment Data for Chapter 3

Data for Ch3_Figure 4

SBR

Water volume of pipe joint=1.88 L

Concentration of BTEX in pipe joint (μg/L)

Time (Day)	7	14	21	28	35	43	50	57	66	77	84	91	99	106	119	133
Benzene	11	10	6	7	13	137	186	250	740	3748	2242	5177	5370	5211	5805	9008
Toluene	29	31	22	27	24	58	81	184	746	4347	4255	10236	11695	12807	13460	19528
Ethyl benzene	2	2	2	2	2	2	4	4	19	100	196	480	614	768	798	1011
m-xylene	6	7	5	7	6	6	6	14	56	260	555	1325	1644	1992	2161	2760
o+p-xylene	7	8	6	7	7	7	7	12	61	294	596	1428	1781	2152	2316	2936
BTEX	55	57	41	50	52	211	284	464	1622	8749	7844	18646	21104	22930	24540	35243

Permeated BTEX mass in pipe joint (μg)

Time (Day)	7	14	21	28	35	43	50	57	66	77	84	91	99	106	119	133
Benzene	21	19	12	13	25	258	350	470	1391	7046	4215	9733	10096	9797	10913	16935
Toluene	55	58	41	51	45	109	151	346	1402	8172	7999	19244	21987	24077	25305	36713
Ethyl benzene	4	4	3	4	4	4	8	8	36	188	368	902	1154	1444	1500	1901
m-xylene	11	12	10	12	12	12	12	26	105	489	1043	2491	3091	3745	4063	5189
o+p-xylene	13	14	11	14	13	13	13	23	115	553	1120	2685	3348	4046	4354	5520
BTEX	104	107	77	95	98	396	535	872	3049	16448	14747	35054	39676	43108	46135	66257

Cumulative mass of BTEX permeated (mg)

Time (Day)	7	14	21	28	35	43	50	57	66	77	84	91	99	106	119	133
Benzene	0.0	0.0	0.1	0.1	0.1	0.3	0.7	1.2	2.6	9.6	13.8	23.6	33.6	43.4	54.4	71.3
Toluene	0.1	0.1	0.2	0.2	0.2	0.4	0.5	0.9	2.3	10.4	18.4	37.7	59.7	83.7	109.0	145.8
Ethyl benzene	0.0	0.0	0.0	0.0	0.0	0.0	0.0	0.0	0.1	0.3	0.6	1.5	2.7	4.1	5.6	7.5
m-xylene	0.0	0.0	0.0	0.0	0.1	0.1	0.1	0.1	0.2	0.7	1.7	4.2	7.3	11.1	15.1	20.3
o+p-xylene	0.0	0.0	0.0	0.1	0.1	0.1	0.1	0.1	0.2	0.8	1.9	4.6	7.9	12.0	16.3	21.9
BTEX	0.1	0.2	0.3	0.4	0.5	0.9	1.4	2.3	5.3	21.8	36.5	71.6	111.3	154.4	200.5	266.8

EPDM

Concentration of BTEX in pipe joint (μg/L)

Time (Day)	7	14	21	28	35	43	50	57	66	77	84	91	99	106	119	133
Benzene	8	18	8	17	344	2091	4950	2708	4536	8629	4900	3370	4133	4372	4997	7864
Toluene	20	21	20	12	103	113	3490	1897	4364	11282	9945	7344	9302	10371	11458	21461
Ethyl benzene	2	3	2	1	2	9	32	18	55	214	307	221	436	537	649	1216
m-xylene	6	6	6	3	5	20	72	50	137	534	760	571	1054	1334	1622	2944
o+p-xylene	7	7	7	4	5	23	84	59	158	623	875	655	1170	1474	1743	3144
BTEX	42	54	43	37	459	2256	8628	4732	9250	21282	16787	12161	16095	18088	20469	36629

Permeated BTEX mass in pipe joint (μg)

Time (Day)	7	14	21	28	35	43	50	57	66	77	84	91	99	106	119	133
Benzene	15	33	15	32	647	3931	9306	5091	8528	16223	9212	6336	7770	8219	9394	14784
Toluene	37	39	37	23	194	213	6561	3566	8204	21210	18697	13807	17488	19497	21541	40347
Ethyl benzene	3	5	4	2	3	17	60	34	103	402	577	415	820	1010	1220	2286
m-xylene	10	12	12	6	9	37	135	94	258	1004	1429	1073	1982	2508	3049	5535
o+p-xylene	12	13	14	8	10	44	158	111	297	1171	1645	1231	2200	2771	3277	5911
BTEX	78	102	81	70	863	4242	16221	8896	17390	40010	31560	22863	30259	34005	38482	68863

Cumulative mass of BTEX permeated (mg)

Time (Day)	7	14	21	28	35	43	50	57	66	77	84	91	99	106	119	133
Benzene	0.0	0.0	0.1	0.1	0.7	4.7	14.0	19.1	27.6	43.8	53.0	59.4	67.1	75.4	84.8	99.5
Toluene	0.0	0.1	0.1	0.1	0.3	0.5	7.1	10.7	18.9	40.1	58.8	72.6	90.1	109.6	131.1	171.5
Ethyl benzene	0.0	0.0	0.0	0.0	0.0	0.0	0.1	0.1	0.2	0.6	1.2	1.6	2.4	3.5	4.7	7.0
m-xylene	0.0	0.0	0.0	0.0	0.0	0.1	0.2	0.3	0.6	1.6	3.0	4.1	6.1	8.6	11.6	17.2
o+p-xylene	0.0	0.0	0.0	0.0	0.1	0.1	0.3	0.4	0.7	1.8	3.5	4.7	6.9	9.7	13.0	18.9
BTEX	0.1	0.2	0.3	0.3	1.2	5.4	21.7	30.6	47.9	88.0	119.5	142.4	172.6	206.6	245.1	314.0

Data for Ch3_Figure 4 (continued)

FKM

Concentration of BTEX in pipe joint (µg/L)

Time (Day)	7	14	21	28	36	43	50	59	70	77	84	92	99	112	126	141	154
Benzene	4	29	67	55	96	139	101	94	315	201	176	301	443	946	1140	1159	1902
Toluene	9	35	55	54	114	151	125	104	372	323	309	467	718	1435	1881	2004	3910
Ethyl benzene	1	2	2	2	4	6	5	3	11	10	10	20	30	73	91	64	182
m-xylene	2	5	6	6	10	13	11	8	23	27	21	38	59	144	179	147	461
o+p-xylene	2	6	7	6	11	14	12	8	26	33	21	42	65	155	196	167	507
BTEX	17	76	136	123	236	321	253	218	746	594	537	866	1316	2753	3487	3541	6962

Permeated BTEX mass in pipe joint (µg)

Time (Day)	7	14	21	28	36	43	50	59	70	77	84	92	99	112	126	141	154
Benzene	8	54	126	103	180	261	190	177	592	378	331	565	833	1778	2143	2179	3576
Toluene	17	65	103	101	214	283	235	196	699	607	581	878	1350	2698	3536	3768	7351
Ethyl benzene	1	3	4	4	8	10	8	6	20	19	19	37	57	137	171	120	342
m-xylene	3	10	11	11	20	24	20	14	43	51	39	71	112	271	337	276	867
o+p-xylene	4	10	12	11	21	26	22	16	48	62	39	78	123	291	368	314	953
BTEX	33	142	256	230	443	604	476	409	1403	1117	1010	1629	2475	5176	6556	6657	13089

Cumulative mass of BTEX permeated (mg)

Time (Day)	7	14	21	28	36	43	50	59	70	77	84	92	99	112	126	141	154
Benzene	0.0	0.1	0.2	0.3	0.5	0.7	0.9	1.1	1.7	2.1	2.4	3.0	3.8	5.6	7.7	9.9	13.5
Toluene	0.0	0.1	0.2	0.3	0.5	0.8	1.0	1.2	1.9	2.5	3.1	4.0	5.3	8.0	11.6	15.3	22.7
Ethyl benzene	0.0	0.0	0.0	0.0	0.0	0.0	0.0	0.0	0.1	0.1	0.1	0.1	0.2	0.3	0.5	0.6	1.0
m-xylene	0.0	0.0	0.0	0.0	0.1	0.1	0.1	0.1	0.2	0.2	0.2	0.3	0.4	0.7	1.0	1.3	2.2
o+p-xylene	0.0	0.0	0.0	0.0	0.1	0.1	0.1	0.1	0.2	0.2	0.3	0.4	0.5	0.8	1.1	1.4	2.4
BTEX	0.0	0.2	0.4	0.7	1.1	1.7	2.2	2.6	4.0	5.1	6.1	7.8	10.2	15.4	22.0	28.6	41.7

CR

Concentration of BTEX in pipe joint (µg/L)

Time (Day)	7	14	21	28	35	43	50	57	63	77	84	91	99	106	119	133
Benzene	2	2	0	1	6	6	306	816	3381	5170	3258	8259	7736	4725	8465	13129
Toluene	8	9	1	4	13	12	120	422	2228	4390	3628	10823	10625	8736	12937	19642
Ethyl benzene	1	1	0	1	1	1	7	17	33	69	58	234	317	308	483	716
m-xylene	4	5	0	3	4	3	16	41	74	172	142	573	785	734	1156	1670
o+p-xylene	5	6	0	4	5	4	17	45	86	196	166	657	885	815	1289	1861
BTEX	19	23	2	13	29	26	466	1341	5802	9997	7252	20546	20348	15318	24330	37018

Permeated BTEX mass in pipe joint (µg)

Time (Day)	7	14	21	28	36	43	50	59	70	77	84	92	99	112	126	141
Benzene	3	3	1	2	11	12	575	1534	6356	9720	6125	15527	14544	8883	15914	24683
Toluene	15	16	1	8	25	23	226	793	4189	8253	6821	20347	19975	16424	24322	36927
Ethyl benzene	2	3	0	2	2	2	13	32	62	130	109	440	596	579	908	1346
m-xylene	7	10	1	6	7	6	30	77	139	323	267	1077	1476	1380	2173	3140
o+p-xylene	9	12	1	7	8	7	32	85	162	368	312	1235	1664	1532	2423	3499
BTEX	36	43	3	24	54	50	876	2521	10908	18794	13634	38626	38254	28798	45740	69594

Cumulative mass of BTEX permeated (mg)

Time (Day)	7	14	21	28	36	43	50	59	70	77	84	92	99	112	126	141
Benzene	0.0	0.1	0.2	0.3	0.5	0.7	0.9	1.1	1.7	2.1	2.4	3.0	3.8	5.6	7.7	9.9
Toluene	0.0	0.1	0.2	0.3	0.5	0.8	1.0	1.2	1.9	2.5	3.1	4.0	5.3	8.0	11.6	15.3
Ethyl benzene	0.0	0.0	0.0	0.0	0.0	0.0	0.0	0.0	0.1	0.1	0.1	0.1	0.2	0.3	0.5	0.6
m-xylene	0.0	0.0	0.0	0.0	0.1	0.1	0.1	0.1	0.2	0.2	0.2	0.3	0.4	0.7	1.0	1.3
o+p-xylene	0.0	0.0	0.0	0.0	0.1	0.1	0.1	0.1	0.2	0.2	0.3	0.4	0.5	0.8	1.1	1.4
BTEX	0.0	0.2	0.4	0.7	1.1	1.7	2.2	2.6	4.0	5.1	6.1	7.8	10.2	15.4	22.0	28.6

Data for Ch3_Figure 4 (continued)

NBR

Concentration of BTEX in pipe joint (µg/L)

Time (Day)	6	13	20	27	35	41	48	56	63	70	98	111	118	124	132	139	146
Benzene	8	0	1	0	1	2	0	0	1	2	21	151	107	190	172	385	561
Toluene	9	1	0	1	1	2	1	1	4	1	3	42	45	59	53	124	216
Ethyl benzene	1	2	0	0	0	0	0	0	0	0	0	1	1	0	2	1	4
m-xylene	1	0	0	0	0	0	0	0	0	0	0	0	1	1	3	2	10
o+p-xylene	1	0	0	0	0	0	1	0	0	0	0	0	1	1	3	2	1
BTEX	18	3	2	1	2	6	2	2	5	4	25	195	156	250	233	515	792

Time (Day)	153	160	167	175	182	189	198	209	216	223	231	238	251	293
Benzene	477	274	524	733	1940	1139	985	806	583	532	563	435	757	6638
Toluene	202	147	259	363	1193	686	642	621	543	518	497	400	556	4837
Ethyl benzene	3	1	4	3	11	17	8	8	11	15	15	12	28	147
m-xylene	5	4	6	7	25	33	17	18	27	25	39	31	54	337
o+p-xylene	1	3	5	8	28	34	20	21	30	23	40	32	59	365
BTEX	688	429	798	1115	3198	1909	1671	1474	1194	1113	1154	910	1454	12324

Permeated BTEX mass in pipe joint (µg)

Time (Day)	6	13	20	27	35	41	48	56	63	70	98	111	118	124	132	139	146
Benzene	14	0	2	0	1	4	1	1	2	4	39	285	200	357	324	724	1055
Toluene	17	1	1	1	2	5	2	2	8	3	6	80	85	110	99	233	406
Ethyl benzene	1	3	0	0	0	0	0	0	1	0	0	1	2	1	5	2	8
m-xylene	1	1	1	1	1	1	1	0	0	0	1	1	2	2	5	4	19
o+p-xylene	1	1	1	1	1	1	2	0	0	0	1	1	2	2	5	5	2
BTEX	34	6	4	3	4	10	5	3	10	7	46	367	292	470	438	968	1489

Time (Day)	153	160	167	175	182	189	198	209	216	223	231	238	251	293
Benzene	897	515	985	1378	3647	2141	1851	1515	1096	1000	1058	818	1423	12479
Toluene	380	276	487	682	2244	1290	1207	1167	1021	974	934	752	1045	9094
Ethyl benzene	6	2	8	6	21	32	15	15	21	28	28	23	53	276
m-xylene	9	8	11	14	47	62	33	34	51	47	73	58	102	634
o+p-xylene	2	6	9	16	53	64	37	39	56	43	75	60	111	686
BTEX	1293	807	1500	2096	6011	3589	3142	2771	2245	2092	2170	1711	2734	23169

Cumulative mass of BTEX permeated (mg)

Time (Day)	6	13	20	27	35	41	48	56	63	70	98	111	118	124	132	139	146
Benzene	0.0	0.0	0.0	0.0	0.0	0.0	0.0	0.0	0.0	0.0	0.1	0.4	0.6	0.9	1.2	2.0	3.0
Toluene	0.0	0.0	0.0	0.0	0.0	0.0	0.0	0.0	0.0	0.0	0.0	0.1	0.2	0.3	0.4	0.7	1.1
Ethyl benzene	0.0	0.0	0.0	0.0	0.0	0.0	0.0	0.0	0.0	0.0	0.0	0.0	0.0	0.0	0.0	0.0	0.0
m-xylene	0.0	0.0	0.0	0.0	0.0	0.0	0.0	0.0	0.0	0.0	0.0	0.0	0.0	0.0	0.0	0.0	0.0
o+p-xylene	0.0	0.0	0.0	0.0	0.0	0.0	0.0	0.0	0.0	0.0	0.0	0.0	0.0	0.0	0.0	0.0	0.0
BTEX	0.0	0.0	0.0	0.0	0.1	0.1	0.1	0.1	0.1	0.1	0.1	0.5	0.8	1.3	1.7	2.7	4.2

Time (Day)	153	160	167	175	182	189	198	209	216	223	231	238	251	293
Benzene	3.9	4.4	5.4	6.8	10.4	12.6	14.4	15.9	17.0	18.0	19.1	19.9	21.3	33.8
Toluene	1.4	1.7	2.2	2.9	5.1	6.4	7.6	8.8	9.8	10.8	11.7	12.5	13.5	22.6
Ethyl benzene	0.0	0.0	0.0	0.0	0.1	0.1	0.1	0.1	0.1	0.2	0.2	0.2	0.3	0.6
m-xylene	0.0	0.1	0.1	0.1	0.1	0.2	0.2	0.3	0.3	0.4	0.4	0.5	0.6	1.2
o+p-xylene	0.0	0.0	0.0	0.1	0.1	0.2	0.2	0.2	0.3	0.3	0.4	0.5	0.6	1.3
BTEX	5.5	6.3	7.8	9.9	15.9	19.5	22.6	25.4	27.6	29.7	31.9	33.6	36.3	59.5

Data for Ch3_Figure 5

NBR exposed to aqueous gasoline solution of 100% saturation

Water volume of pipe joint=1.88 L

Cumulative mass of BTEX permeated (μg)

Time (Day)	6	14	20	27	40	42	49	77	90	97	103	124	146	174	202
Benzene	1	2	2	2	3	4	4	5	5	6	7	8	8	9	9
Toluene	7	10	10	13	13	13	15	18	23	25	26	27	27	27	29
Ethyl benzene	2	2	2	3	3	3	4	5	6	8	8	8	9	9	9
m-xylene	2	2	3	4	4	4	5	6	8	9	10	11	11	11	13
o+p-xylene	2	2	3	4	4	4	5	6	8	10	11	11	12	12	13
BTEX	14	18	20	25	27	28	33	41	50	59	62	65	67	68	74

Time (Day)	217	230	244	272	346	370	384	398	412	441	472	501	531	564
Benzene	11	14	14	15	16	17	18	19	24	26	27	29	31	36
Toluene	31	36	37	38	39	40	40	42	51	51	52	53	54	58
Ethyl benzene	11	15	16	16	17	17	17	18	26	26	26	27	27	30
m-xylene	16	20	21	21	22	22	23	24	32	32	33	33	34	36
o+p-xylene	16	20	21	22	22	22	22	24	31	31	32	32	33	35
BTEX	84	106	108	112	116	119	120	126	163	166	170	174	179	194

NBR exposed to aqueous gasoline solution of 50% saturation

Cumulative mass of BTEX permeated (μg)

Time (Day)	6	14	20	27	40	42	49	77	90	97	103	124	146	174	230
Benzene	0	1	1	2	2	5	5	6	6	7	9	10	10	11	11
Toluene	2	4	5	7	9	17	19	25	32	34	36	36	37	37	38
Ethyl benzene	0	1	1	1	2	2	2	3	4	5	6	6	6	6	7
m-xylene	1	1	2	2	3	6	6	7	8	9	10	10	10	10	11
o+p-xylene	1	1	2	2	2	5	6	7	8	9	10	10	11	11	11
BTEX	4	7	11	15	18	34	38	48	58	65	70	72	74	75	80

Time (Day)	244	272	352	370	384	398	412	441	472	501	531	564
Benzene	12	13	14	15	15	19	21	23	25	28	34	43
Toluene	41	42	43	43	44	50	53	53	54	54	61	67
Ethyl benzene	9	10	11	11	12	12	14	14	15	15	21	26
m-xylene	13	14	14	15	15	20	22	22	23	23	29	33
o+p-xylene	13	14	14	14	14	19	20	21	22	22	27	31
BTEX	88	93	96	99	100	121	130	134	138	142	171	199

NBR exposed to aqueous gasoline solution of 20% saturation

Cumulative mass of BTEX permeated (μg)

Time (Day)	6	14	20	27	42	90	97	103	124	146	174	230	244	272	352
Benzene	1	1	1	2	3	3	4	4	5	6	7	8	8	8	11
Toluene	2	3	4	5	16	38	39	40	40	41	41	41	42	43	44
Ethyl benzene	0	0	1	1	1	2	2	2	2	3	4	4	4	5	5
m-xylene	1	1	2	2	4	4	5	5	5	5	7	7	7	8	8
o+p-xylene	1	1	2	2	3	4	4	5	5	5	6	7	7	8	8
BTEX	4	6	9	12	27	51	54	56	58	59	64	67	68	72	77

Time (Day)	370	384	398	412	441	472	501	531	564
Benzene	13	14	15	17	21	26	30	37	45
Toluene	46	46	47	48	48	49	49	52	53
Ethyl benzene	7	8	8	8	8	9	9	11	11
m-xylene	10	10	11	11	12	12	13	14	15
o+p-xylene	10	10	10	11	11	12	12	14	14
BTEX	86	88	90	94	100	107	112	127	138

NBR exposed to aqueous gasoline solution of 5% saturation

Cumulative mass of BTEX permeated (μg)

Time (Day)	3	7	20	35	83	90	96	117	139	167	223	237	265	345	363
Benzene	0	1	2	3	5	5	6	7	7	8	9	9	10	12	15
Toluene	1	2	4	14	33	34	34	35	35	35	36	36	38	39	40
Ethyl benzene	0	0	1	2	5	6	7	7	7	8	8	8	9	10	11
m-xylene	1	1	2	2	5	6	6	7	7	8	8	9	9	10	11
o+p-xylene	1	1	2	2	5	6	6	6	7	8	8	9	9	10	11
BTEX	2	6	10	23	53	57	59	61	62	67	70	72	76	80	87

Time (Day)	377	391	405	434	465	494	524	557
Benzene	16	17	19	22	30	37	46	56
Toluene	40	41	41	41	43	44	47	49
Ethyl benzene	11	12	12	12	13	13	13	14
m-xylene	11	11	12	12	13	13	14	14
o+p-xylene	11	11	11	12	13	13	14	14
BTEX	89	92	95	100	111	121	134	146

Data for Ch3_Figure 5 (continued)

SBR exposed to aqueous gasoline solution of 100% saturation

Cumulative mass of BTEX permeated (μg)

Time (Day)	13	20	33	35	42	70	83	90	96	117	139	167	195	203	210
Benzene	1	1	2	2	3	4	4	5	6	8	10	19	124	283	434
Toluene	4	8	10	12	15	19	26	28	29	30	31	32	58	134	232
Ethyl benzene	0	2	2	2	2	3	4	4	5	5	5	6	11	11	13
m-xylene	1	2	2	2	3	3	4	5	5	6	6	7	8	10	13
o+p-xylene	1	2	2	2	2	3	5	5	6	7	7	7	8	11	14
BTEX	6	15	18	22	25	32	42	48	50	56	60	71	208	449	705

Time (Day)	223	237	265	363	377	391	405	434	465	494	524
Benzene	555	702	1084	8094	9865	10403	10975	11635	12187	12999	13767
Toluene	303	387	561	11181	16043	18681	21484	22162	23185	24574	25628
Ethyl benzene	15	16	19	440	677	837	1007	1032	1146	1268	1350
m-xylene	16	18	22	943	1438	1778	2227	2295	2541	2859	3056
o+p-xylene	17	19	24	915	1393	1720	2142	2210	2441	2738	2929
BTEX	905	1142	1710	21575	29416	33419	37835	39334	41501	44439	46731

SBR exposed to aqueous gasoline solution of 50% saturation

Cumulative mass of BTEX permeated (μg)

Time (Day)	13	20	33	35	42	70	83	90	96	117	139	167	203	210	223
Benzene	0	1	1	2	2	4	5	7	11	18	39	40	168	210	278
Toluene	5	10	14	19	23	40	47	48	51	53	55	55	72	83	97
Ethyl benzene	0	1	1	1	1	2	2	2	5	5	5	5	6	6	6
m-xylene	1	1	1	2	2	3	3	4	7	7	8	8	8	9	9
o+p-xylene	1	1	1	2	2	3	4	4	7	8	8	8	9	9	10
BTEX	7	13	18	25	30	51	61	65	81	90	115	117	263	317	400

Time (Day)	237	265	345	363	377	391	405	434	465	494	524
Benzene	342	467	538	942	1389	1781	2083	3154	4030	4974	5792
Toluene	110	148	160	264	350	463	560	883	1161	1480	1852
Ethyl benzene	7	7	8	8	14	14	16	18	20	23	32
m-xylene	10	11	12	13	30	31	33	36	39	43	62
o+p-xylene	11	12	13	14	27	28	30	33	36	41	65
BTEX	479	646	730	1240	1810	2317	2722	4125	5287	6562	7804

SBR exposed to aqueous gasoline solution of 20% saturation

Cumulative mass of BTEX permeated (μg)

Time (Day)	10	17	32	80	87	93	114	136	164	220	234	262	342	360	374
Benzene	0	1	2	2	2	3	4	5	7	16	21	21	79	111	134
Toluene	4	7	14	19	19	20	21	21	22	23	24	25	33	40	45
Ethyl benzene	0	0	1	1	2	2	3	3	3	3	4	4	5	5	5
m-xylene	1	1	1	2	2	4	4	4	4	4	5	5	5	6	6
o+p-xylene	1	1	1	2	2	3	4	4	4	4	4	5	5	5	6
BTEX	6	11	19	25	27	33	35	37	40	51	57	60	126	167	196

Time (Day)	388	402	431	462	491	521	554	589
Benzene	150	163	222	266	304	355	416	500
Toluene	49	52	64	72	80	93	107	131
Ethyl benzene	5	5	6	6	6	7	7	7
m-xylene	6	7	7	8	8	9	9	10
o+p-xylene	6	6	7	8	8	8	9	10
BTEX	217	233	306	360	406	472	549	656

SBR exposed to aqueous gasoline solution of 5% saturation

Cumulative mass of BTEX permeated (μg)

Time (Day)	10	17	32	80	87	93	114	136	164	220	234	262	342	360	374
Benzene	1	2	2	3	5	6	7	7	8	10	11	11	23	30	34
Toluene	2	4	8	17	22	23	23	24	24	25	25	26	28	30	31
Ethyl benzene	0	0	1	1	4	5	5	5	5	5	5	6	6	6	7
m-xylene	1	1	2	2	5	5	5	6	6	6	6	7	7	8	8
o+p-xylene	1	1	1	2	5	5	5	6	6	6	7	7	7	8	8
BTEX	5	9	14	25	40	43	45	47	49	52	54	57	72	81	87

Time (Day)	388	402	431	462	491	521	554	589
Benzene	39	42	50	60	71	91	115	138
Toluene	32	33	34	36	38	43	50	56
Ethyl benzene	7	7	7	8	8	8	8	9
m-xylene	8	8	9	10	10	11	11	11
o+p-xylene	8	8	9	9	10	10	11	11
BTEX	94	99	109	123	137	164	194	224

Data for Ch3_Figure 5 (continued)

FKM exposed to aqueous gasoline solution of 100% saturation

Cumulative mass of BTEX permeated (μg)

Time (Day)	10	17	32	39	67	80	87	93	114	136	164	207	220	234	262
Benzene	15	16	16	17	17	18	23	24	25	25	26	27	28	30	31
Toluene	18	19	19	22	23	25	39	39	40	40	41	42	45	48	50
Ethyl benzene	1	1	1	1	2	2	2	3	3	3	3	4	6	8	8
m-xylene	2	2	2	2	3	4	5	6	6	6	7	7	8	10	11
o+p-xylene	2	2	2	3	3	4	6	6	6	7	7	7	9	11	12
BTEX	37	40	41	45	49	53	75	78	80	82	83	86	97	108	113

Time (Day)	342	360	374	388	402	431	462	491	521	554	589
Benzene	33	33	33	34	34	35	35	36	36	37	38
Toluene	51	52	52	52	53	53	54	55	55	56	57
Ethyl benzene	9	10	10	10	10	11	11	11	12	12	12
m-xylene	11	11	12	12	12	13	14	14	14	15	15
o+p-xylene	13	13	13	13	14	14	15	15	16	16	16
BTEX	117	119	120	122	124	126	129	130	133	135	137

Data for Ch3_Figure 6

Gaskets (Heel portion)	Permeation rate (mg/joint/day)	weight gain (%)	Sorption rate (%/min$^{1/2}$)
EPDM	3.93	97.3	3.27
CR	4.23	57.1	2.06
SBR	5.2	61.6	2.09
NBR	0.36	26.9	0.38
FKM	0.49	0.81	0.0073

Data for Ch3_Figure 7

Flow rate needed to obtain benzene MCL (5 μg/L)

SBR gaskets exposed to gasoline

Size of DI pipe (inch)	20 feet long pipe (1 joint)	100 feet long pipe (5 joints)
	GPM (gallon per minute)	
4	0.24	1.20
6	0.34	1.69
8	0.37	1.87
10	0.42	2.11
12	0.50	2.49
14	0.68	3.39
16	0.77	3.84
18	0.86	4.29
20	0.95	4.74
24	1.13	5.63

SBR gaskets exposed to 100% saturated gasoline solution

Size of DI pipe (inch)	20 feet long pipe (1 joint)	100 feet long pipe (5 joints)
	GPM (gallon per minute)	
4	0.003	0.013
6	0.004	0.019
8	0.004	0.021
10	0.005	0.023
12	0.006	0.028
14	0.008	0.038
16	0.009	0.043
18	0.010	0.048
20	0.011	0.053
24	0.013	0.063

Data for Ch3_Figure 8

NBR gaskets exposed to gasoline

Size of DI pipe (inch)	20 feet long pipe (1 joint)	100 feet long pipe (5 joints)
	GPM (gallon per minute)	
4	0.006	0.029
6	0.008	0.041
8	0.009	0.045
10	0.010	0.051
12	0.012	0.060
14	0.016	0.082
16	0.019	0.093
18	0.021	0.104
20	0.023	0.115
24	0.027	0.137

Data for Ch3_Figure 9

Benzene concentrations after 8 hours of stagnation (100 feet long pipe, 5 joints)

Size of DI pipe (inch)	SBR exposed to gasoline	NBR exposed to gasoline	SBR exposed to 100% saturation gasoline solution
	Concentration in pipe (µg/L)		
4	30.7	0.745	0.342
6	20.9	0.506	0.232
8	13.4	0.325	0.149
10	10.1	0.244	0.112
12	8.4	0.204	0.094
14	8.5	0.207	0.095
16	7.5	0.181	0.083
18	6.6	0.161	0.074
20	6.0	0.145	0.067
24	5.0	0.121	0.055

A.2 Sorption and Diffusion Cell Experiment Data for Chapter 4

Data for Ch4_Figure 6

Sorption uptake of premium gasoline

SBR

Time			Weight	
hr	min	$min^{1/2}$	gain (g)	gain%
0	0	0	0	0
2	120	10.95	0.696	23.5
4	240	15.49	1.035	34.9
6	360	18.97	1.309	44.1
10	600	24.49	1.723	58.0
22	1320	36.33	2.313	77.9
46	2760	52.54	2.335	78.6
70	4200	64.81	2.275	76.6
94	5640	75.10	2.375	80.0
118	7080	84.14	2.345	79.0
142	8520	92.30	2.257	76.0
166	9960	99.80	2.257	76.0

EPDM

Time			Weight	
hr	min	$min^{1/2}$	gain (g)	gain%
0	0	0	0	0
2	120	10.95	1.052	35.9
4	240	15.49	1.543	52.7
10	600	24.49	2.541	86.9
22	1320	36.33	3.497	119.5
34	2040	45.17	3.715	127.0
46	2760	52.54	3.711	126.8
58	3480	58.99	3.662	125.2
82	4920	70.14	3.626	123.9
106	6360	79.75	3.595	122.9
130	7800	88.32	3.579	122.3
178	10680	103.34	3.591	122.8
226	13560	116.45	3.604	123.2

CR

Time			Weight	
hr	min	$min^{1/2}$	gain (g)	gain%
0	0	0	0	0
2	120	10.95	0.502	13.9
4	240	15.49	0.726	20.1
10	600	24.49	1.122	31.1
22	1320	36.33	1.505	41.7
34	2040	45.17	1.646	45.6
46	2760	52.54	1.692	46.9
58	3480	58.99	1.692	46.9
82	4920	70.14	1.660	46.0
106	6360	79.75	1.632	45.2
130	7800	88.32	1.619	44.9
178	10680	103.34	1.601	44.4
226	13560	116.45	1.591	44.1

FKM

Time			Weight	
hr	min	$min^{1/2}$	gain (g)	gain%
0	0	0	0	0
2	120	10.95	0.006	0.1
4	240	15.49	0.008	0.1
10	600	24.49	0.011	0.2
22	1320	36.33	0.014	0.2
34	2040	45.17	0.017	0.3
46	2760	52.54	0.020	0.3
58	3480	58.99	0.021	0.3
82	4920	70.14	0.026	0.4
106	6360	79.75	0.027	0.5
130	7800	88.32	0.030	0.5
178	10680	103.34	0.035	0.6
226	13560	116.45	0.039	0.7

Data for Ch4_Figure 6 (continued)

NBR

Time			Weight	
hr	min	$min^{1/2}$	gain (g)	gain%
0	0	0	0	0
1	60	7.75	0.089	4.3
3	180	13.42	0.152	7.3
5	300	17.32	0.195	9.4
7	420	20.49	0.228	11.0
9	540	23.24	0.255	12.3
11	660	25.69	0.277	13.3
13	780	27.93	0.299	14.4
25	1500	38.73	0.391	18.8
37	2220	47.12	0.456	22.0
49	2940	54.22	0.502	24.2
61	3660	60.50	0.531	25.6
73	4380	66.18	0.551	26.5
85	5100	71.41	0.562	27.1
97	5820	76.29	0.571	27.5
121	7260	85.21	0.575	27.7
145	8700	93.27	0.573	27.6
169	10140	100.70	0.568	27.4
217	13020	114.11	0.558	26.9

Data for Ch4_Figure 8

SBR Heel portion (3 mm) exposed to gasoline

	Cumulative mass of benzene permeated (µg)									
Time (Hour)	**1**	**2**	**4**	**6**	**8**	**12**	**24**	**36**	**48**	**72**
Benzene	0	0	6	37	86	211	579	1031	1460	2324
Toluene	0	0	6	37	84	204	559	1031	1502	2404
Ethyl benzene	0	0	0	6	9	14	21	44	69	118
m-xylene	0	0	1	9	15	27	62	127	199	331
o+p-xylene	0	0	1	9	15	28	65	132	208	347
BTEX	1	1	14	98	208	484	1286	2365	3438	5523

SBR Bulb portion (3 mm) exposed to gasoline

	Cumulative mass of benzene permeated (µg)								
Time (Hour)	**1**	**2**	**4**	**6**	**8**	**12**	**24**	**36**	**48**
Benzene	0	0	26	91	161	316	704	1098	1504
Toluene	0	0	27	98	182	360	785	1299	1801
Ethyl benzene	0	0	1	5	12	26	53	91	130
m-xylene	0	0	3	12	29	59	128	242	350
o+p-xylene	0	0	4	14	32	62	132	251	363
BTEX	0	0	61	220	416	823	1802	2981	4149

NBR Bulb portion (2 mm) exposed to gasoline

	Cumulative mass of benzene permeated (µg)											
Time (Hour)	**2**	**4**	**8**	**12**	**24**	**36**	**48**	**60**	**72**	**96**	**120**	**168**
Benzene	0	0	0	0	0	1	1	13	55	189	353	614
Toluene	0	1	1	1	1	1	1	14	67	235	440	771
Ethyl benzene	0	0	1	1	1	1	1	1	3	9	16	31
m-xylene	0	0	0	0	1	1	1	2	6	21	40	77
o+p-xylene	0	0	0	0	0	0	1	2	6	21	42	82
BTEX	1	3	3	3	3	3	4	31	138	475	891	1574

SBR Bulb portion (2 mm) exposed to 100% saturated gasoline solution

	Cumulative mass of benzene permeated (µg)									
Time (Hour)	**6**	**30**	**66**	**90**	**114**	**144**	**168**	**192**	**240**	**288**
Benzene	0	0	0	0	1	3	6	10	23	42
Toluene	0	0	0	0	1	5	10	17	37	68
Ethyl benzene	0	0	0	0	0	0	0	0	1	1
m-xylene	0	0	0	0	0	0	0	1	2	3
o+p-xylene	0	0	0	0	0	0	0	1	2	3
BTEX	0	0	0	1	2	8	17	29	63	117

Time (Hour)	**336**	**385**	**439**	**487**	**535**	**607**
Benzene	72	106	142	179	217	269
Toluene	126	193	269	343	418	520
Ethyl benzene	3	4	6	8	10	12
m-xylene	6	10	14	18	22	28
o+p-xylene	6	10	15	20	24	31
BTEX	214	323	446	567	691	860

Data for Ch4_Figure 8 (continued)

NBR Bulb portion (2 mm) exposed to 100% saturated gasoline solution

Cumulative mass of benzene permeated (µg)

Time (Hour)	**6**	**30**	**66**	**90**	**114**	**144**	**168**	**192**	**240**	**288**
Benzene	0	0	0	0	0	0	0	0	1	2
Toluene	0	0	0	0	0	0	0	0	1	3
Ethyl benzene	0	0	0	0	0	0	0	0	0	0
m-xylene	0	0	0	0	0	0	0	0	0	0
o+p-xylene	0	0	0	0	0	0	0	0	0	0
BTEX	0	0	0	1	1	1	1	1	2	6

Time (Hour)	**336**	**385**	**439**	**487**	**535**	**607**	**679**	**915**
Benzene	5	9	15	23	34	55	77	136
Toluene	8	16	27	42	65	111	162	321
Ethyl benzene	0	1	1	1	2	3	5	11
m-xylene	1	1	2	2	4	7	10	26
o+p-xylene	1	1	2	2	4	7	10	26
BTEX	14	28	45	71	109	182	264	520

Diffusion cell chamber volume=40 mL

Data for Ch4_Figure 9

SBR Heel (2 mm) exposed to gasoline

Time (hour)	Permeated benzene (μg)	Experimental benzene permeation (mg/m^2)	Modeled benzene permeation (mg/m^2)
0	0	0	0
1	1	4	4
2	1	6	91
4	101	796	679
6	212	1670	1611
8	369	2909	2702
12	544	4283	5063
24	1015	7991	12372
36	1635	12876	19703
48	2251	17722	27036

SBR Heel (3 mm) exposed to gasoline

Time (hour)	Permeated benzene (μg)	Experimental benzene permeation (mg/m^2)	Modeled benzene permeation (mg/m^2)
0	0	0	0
1	0	2	0
2	0	2	2
4	8	63	66
6	47	374	280
8	109	861	641
12	267	2099	1668
24	734	5776	5716
36	1306	10282	10092
48	1848	14551	14516
72	2942	23167	23373

SBR Heel (4 mm) exposed to gasoline

Time (hour)	Permeated benzene (μg)	Experimental benzene permeation (mg/m^2)	Modeled benzene permeation (mg/m^2)
0	0	0	0
1	0	1	0
2	0	1	0
4	0	1	1
6	0	2	25
8	0	2	102
12	32	255	468
24	500	3940	2833
36	827	6514	6061
48	1249	9831	9558
72	1998	15736	16754

SBR Heel (5 mm) exposed to gasoline

Time (hour)	Permeated benzene (μg)	Experimental benzene permeation (mg/m^2)	Modeled benzene permeation (mg/m^2)
0	0	0	0
1	0	1	0
2	0	1	0
4	0	1	0
6	0	1	1
8	0	1	11
12	0	1	93
24	143	1125	1089
36	374	2945	2970
48	672	5291	5316

Data for Ch4_Figure 10

SBR Bulb (3 mm) exposed to gasoline

Time (hour)	Permeated benzene (μg)	Experimental benzene permeation (mg/m^2)	Modeled benzene permeation (mg/m^2)
0	0	0	0
1	0	0	0
2	0	1	7
4	32	251	173
6	111	875	612
8	198	1556	1274
12	387	3049	2989
24	863	6792	9180
36	1346	10600	15665
48	1844	14516	22166

SBR Bulb (4 mm) exposed to gasoline

Time (hour)	Permeated benzene (μg)	Experimental benzene permeation (mg/m^2)	Modeled benzene permeation (mg/m^2)
0	0	0	0
2	0	1	0
4	0	1	11
8	4	118	253
12	60	1882	888
24	136	4258	4216
36	263	8209	8311
60	537	16776	16952

SBR Bulb (5 mm) exposed to gasoline

Time (hour)	Permeated benzene (μg)	Experimental benzene permeation (mg/m^2)	Modeled benzene permeation (mg/m^2)
0	0	0	0
2	0	0	0
4	0	0	0
6	0	0	8
8	0	1	40
12	9	70	238
24	262	2060	1981
36	626	4931	4795
48	1004	7903	8061

Data for Ch4_Figure 11

Bulb portion (2 mm) exposed to 100% saturated gasoline solution

SBR

Time (hour)	Permeated benzene (μg)	Experimental benzene permeation (mg/m^2)	Modeled benzene permeation (mg/m^2)
0	0	0	0
6	0	0	0
30	0	1	0
66	0	1	0
90	0	2	2
114	1	8	8
144	4	30	29
168	8	60	62
192	13	102	110
240	29	227	254
288	53	414	457
336	92	721	711
385	134	1054	1014
439	180	1416	1388
487	226	1783	1748
535	274	2159	2129
607	341	2681	2731

NBR

Time (hour)	Permeated benzene (μg)	Experimental benzene permeation (mg/m^2)	Modeled benzene permeation (mg/m^2)
0	0	0	0
6	0	0	0
30	0	1	0
66	0	1	0
90	0	1	0
114	0	1	0
144	0	2	1
168	0	2	1
192	0	3	2
240	1	6	8
288	3	20	27
336	6	47	60
385	12	92	112
439	19	147	189
487	29	226	275
535	43	338	375
607	70	550	552
679	98	769	755
915	172	1351	1560

A.3 Simulation Data for Chapter 5

Data for Ch5_Figure 12

Intact gasket exposed to gasoline_With hydrostatic pressure and changes in bulb portion

Time (day)	Permeated benzene (μg)	Experimental benzene permeation (mg/m^2)	Modeled benzene permeation (mg/m^2)						
			-30%	-20%	-10%	0%	10%	20%	30%
0	0	0	0	0	0	0	0	0	0
7	0	2	0	0	0	0	0	0	0
14	0	5	0	0	0	0	0	0	0
21	0	6	7	1	0	0	0	0	0
28	0	7	61	17	3	1	0	0	0
35	0	10	242	85	20	6	1	0	0
43	0	40	730	309	87	32	9	2	1
50	1	80	1506	716	227	95	29	9	2
57	1	134	2685	1393	485	223	77	27	7
66	3	293	4882	2763	1053	534	206	82	25
77	10	1100	8719	5342	2216	1231	526	234	81
84	14	1583	11859	7561	3277	1907	859	403	148
91	24	2697	15557	10258	4619	2797	1318	648	251
99	34	3854	20469	13946	6520	4107	2022	1042	426
106	43	4975	25366	17712	8525	5533	2817	1504	641
119	54	6225	35916	26050	13127	8931	4794	2704	1230
133	71	8165	49319	36961	19401	13757	7731	4577	2206